The effects of genes, antiepileptic drugs and risk of death on functional anatomy and cognitive networks in epilepsy

Britta Wandschneider
UCL Institute of Neurology
Department of Clinical and Experimental Epilepsy
Queen Square
London
WC1N 3BG

Thesis submitted to University College London

for the degree of Doctor of Philosophy

2016

Declaration

I, Britta Wandschneider, confirm that the work presented in this thesis is my own. Where information has been derived from other sources, I confirm this has been indicated in the thesis. All figures and illustrations in this thesis are my own.

The scientific studies presented here reflect collaborations with a team of researchers including other colleagues from the UCL Department of Clinical and Experimental Epilepsy. However, this thesis presents only studies in which I conducted most steps of data analysis. All results and data interpretation were presented by myself and were developed based on discussions at meetings with my colleagues and my scientific supervisors.

My individual contributions to the scientific studies included in this thesis are outlined below.

This thesis comprises three main projects:

1. The first project, imaging endophenotypes in Juvenile Myoclonic Epilepsy, builds on previous work of my colleague Christian Vollmar in a joint project of UCL and King's College London. I recruited all unaffected siblings from previously scanned index patients (n = 5) by Christian Vollmar, and also recruited additional JME index patients (n = 6) and their siblings. I acquired the neuroimaging data, including cognitive functional paradigms. I performed a standard out-of-scanner neuropsychometry assessment of all study participants, including a detailed frontal lobe test battery. I was responsible for transfer, conversion and processing of imaging data, as well as all data analyses.
2. The first part of the pharmaco-fMRI project, "The effect of Levetiracetam on fMRI working memory activations in temporal lobe epilepsy", included presurgical TLE patients who were scanned as part of an epilepsy presurgical imaging project at UCL. Functional MRI (fMRI) data

acquisition was done by my colleagues Meneka Sidhu and Jason Stretton. Clinical neuropsychological testing was performed by Pamela Thompson. Jason Stretton conducted the initial data processing, we were both responsible for the study design and I was responsible for the finalisation of imaging and behavioural data analysis and interpretation of results. For the retrospective pharmaco-fMRI project "The effect of Topiramate and Zonisamide on fMRI verbal fluency activations in refractory epilepsy" Jane Burdett had created a database of all clinical language fMRI scans and Lucy Townsend helped me to identify patients from this database who were relevant for the retrospective pharmaco-fMRI project. I was responsible for transfer, conversion and processing of imaging data. I was responsible for the study design, conducted all imaging data analyses and other statistical analyses, as well as interpretation of results.

3. For the retrospective project "Structural imaging biomarkers of sudden unexpected death in epilepsy", I searched clinical databases for appropriate patients and was responsible for transfer, conversion and processing of imaging data. Healthy control data were derived from an epilepsy presurgical TLE project at UCL. I was responsible for the study design and conducted all imaging data analyses and other statistical analyses, as well as interpretation of results.

18th October 2016

Abstract

Epilepsy is one of the most common neurological disorders. Apart from seizures, patients are also affected by epilepsy comorbidities, such as cognitive impairment, side effects of antiepileptic drugs, and an increased risk of dying from sudden death. Within epilepsy research, recent efforts have been made to identify reliable biomarkers to advance the understanding of disease-mechanisms, to individualize and optimize treatment and side-effect profiles and to enhance prediction of treatment success and disease progression. Biomarkers are objective measures of a normal or pathological biological process and, in the context of this PhD, neuroimaging biomarkers ideally enable *in vivo* measurements of (i) disease activity, (ii) treatment effects and (iii) risk of comorbidities and mortality. Employing functional and structural neuroimaging techniques, we studied potential neuroimaging biomarkers in three different domains of epilepsy.

In the first project, we explored fMRI endophenotypes in a prototype of a genetic generalised epilepsy syndrome, namely juvenile myoclonic epilepsy (JME). Endophenotypes are heritable traits, closer related to the genotype than the final phenotype and are found frequently in non-affected family members of patients. Our study revealed potential functional endophenotypes and support a genetically determined neurodevelopmental disease mechanism in JME.

The second project investigated fMRI markers of antiepileptic drug effects on cognitive networks in patients with refractory epilepsy. In two retrospective studies employing fMRI cognitive tasks, we isolated task- and medication-specific effects on working memory and language networks for Levetiracetam (study 1) and Topiramate and Zonisamide (study 2).

In the third project, we employed Voxel-Based-Morphometry in a retrospective analysis of structural imaging of patients who had died of sudden unexpected death in epilepsy (SUDEP) or were at high or low risk of SUDEP. We identified structural markers of high SUDEP risk, and discussed that these were at least partially specific, *i.e.* independent of disease progression and load.

Table of contents

List of figures

Chapter 8:

Chapter 9:

List of tables

List of abbreviations

5-HT	Serotonin
AED	Antiepileptic drugs
AMIPB	The Adult Memory and Information Processing Battery
BECTS	Benign Childhood Epilepsy with Centrotemporal Spikes
BOLD	Blood oxygen level dependent
BRIEF	Behavior Rating Inventory of Executive Function
CAE	childhood absence epilepsy
CBZ	Carbamazepine
CI	Confidence interval
CMCT	Central motor conduction time
COMT	Catechol-O-Methyltransferase
CS	Convulsive seizure
CSF	Cerebrospinal fluid
CSP	Cortical silent period
DARTEL	Diffeomorphic Anatomical Registration using Exponentiated Lie algebra
DFM	Default mode network
D-KEFS	Delis-Kaplan Executive Function System
DLPFC	Dorsolateral prefrontal cortex
DNET	Dysembryoplastic neuroepithelial tumor
DTI	Diffusion tensor imaging
EEG	Electroencephalography
EPI	Echo planar imaging
FA	Fractional anisotropy
FCD	Focal cortical dysplasia

FLAIR	Fluid-attenuated inversion recovery imaging
FLE	Frontal lobe epilepsy
FMHW	Full width at half maximum
fMRI	Functional Magnetic Resonance Imaging
FMRIB	Oxford Centre for Functional Magnetic Resonance Imaging of the Brain
FSL	FMRIB's software library
GM	Grey matter
GMV	Grey matter volume
GNT	Grades Naming Test
GSWD	Generalized spike and wave discharge
GWAS	Genome-wide association study
HRF	Haemodynamic response function
HRV	Heart rate variability
IFG	Inferior frontal gyrus
IGT	Iowa Gambling Task
ILAE	International League Against Epilepsy
ILS	Intermittent light stimulation
IQR	Interquartile range
JME	Juvenile myoclonic epilepsy
LEV	Levetiracetam
LQTS	Long QT-syndrome
LTG	Lamotrigine
MFG	Middle frontal gyrus
MNI	Montreal Neurological Institute
MRI	Magnetic Resonance Imaging
MRS	MR spectroscopy
NAA	N-acetyl aspartate

NART	National Adult Reading Test
OR	Odds ratio
PET	Positron Emission Tomography
PGES	Post-ictal generalised EEG suppression
PM	Prospective memory
PPR	Photoparoxysmal response
PVE	Partial Volume Estimation
rCBF	regional cerebral blood flow
rCBV	regional cerebral blood volume
SD	Standard deviation
SIDS	Sudden infant death syndrome
SMA	Supplementary motor area
SPM	Statistical Parametric Mapping
SSRI	Selective serotonin reuptake inhibitors
SUDC	Sudden unexplained death in childhood
SUDEP	Sudden unexpected death in epilepsy
TCI	transitory cognitive impairment
TLE	Temporal lobe epilepsy
TPM	Topiramate
VBM	Voxel based morphometry
VF	Verbal fluency
VPA	Valproate
WAIS	Wechsler Adult Intelligence Scale
WM	Working memory
ZNS	Zonisamide

List of publications

Original articles:

Wandschneider B, Hill A, Burdett J, Townsend L, Thompson P, Duncan JS, Koepp M. Effect of Topiramate and Zonisamide on functional MRI cognitive networks. *Under review* (Chapter 8)

Wandschneider B, Koepp M, Scott C, Micallef C, Balestrini S, Sisodiya SM, Thom M, Harper R, Sander JW, Vos SB, Duncan JS, Lhatoo S, Diehl B. Structural imaging biomarkers of sudden unexpected death in epilepsy. Brain 2015(Pt 10); 138:2907-19. (Chapter 9)

Wandschneider B, Centeno M, Vollmar C, Symms M, Thompson PJ, Duncan JS, Koepp MJ. Motor co-activation in siblings of patients with juvenile myoclonic epilepsy: an imaging endophenotype? Brain. 2014;137(Pt 9):2469-79. (Chapter 6)

Wandschneider B, Stretton J, Sidhu M, Centeno M, Kozák LR, Symms M, Thompson PJ, Duncan JS, Koepp MJ. Levetiracetam reduces abnormal network activations in temporal lobe epilepsy. Neurology. 2014;83(17):1508-12. (Chapter 7)

Wandschneider B, Centeno M, Vollmar C, Stretton J, O'Muircheartaigh J, Thompson PJ, Kumari V, Symms M, Barker GJ, Duncan JS, Richardson MP, Koepp MJ. Risk-taking behavior in juvenile myoclonic epilepsy. Epilepsia 2013;54(12):2158-65.

Co-authorship, original articles:

Balestrini S, Clayton LM, Bartmann AP, Chinthapalli K, Novy J, Coppola A, **Wandschneider B**, Stern WM, Acheson J, Bell GS, Sander JW, Sisodiya SM. Retinal nerve fibre layer thinning is associated with drug resistance in epilepsy. J Neurol Neurosurg Psychiatry. 2016; 87(4):396-401.

Reviews:

Wandschneider B, Koepp M. Pharmaco fMRI: determining the functional anatomy of the effects of medication. Neuroimage Clinical 2016; 12:691-697.

Koepp MJ, Thomas RH, **Wandschneider B**, Berkovic SF, Schmidt D. Concepts and controversies of juvenile myoclonic epilepsy: still an enigmatic epilepsy. Expert Rev Neurother. 2014; 14:819-31.

Wolf P, Yacubian EM, Avanzini G, Sander T, Schmitz B, **Wandschneider B**, Koepp M. Juvenile myoclonic epilepsy: A system disorder of the brain. Epilepsy Res. 2015;114:2-12.

Koepp M, Woermann F, Savic I, **Wandschneider B**. Juvenile myoclonic epilepsy - Neuroimaging findings. Epilepsy Behav. 2013;28 Suppl 1:S40-4.

Wandschneider B, Thompson P, Vollmar C, Koepp MJ. Frontal lobe function and structure in Juvenile Myoclonic Epilepsy: a comprehensive review of neuropsychological and imaging data. Epilepsia. 2012;53(12):2091-8.

Kasteleijn-Nolst Trenité DG, Schmitz B, Janz D, Delgado-Escueta AV, Thomas P, Hirsch E, Lerche H, Camfield C, Baykan B, Feucht M, Martínez-Juárez IE, Duron RM, Medina MT, Rubboli G, Jerney J, Hermann B, Yacubian E, Koutroumanidis M, Stephani U, Salas-Puig J, Reed RC, Woermann F, **Wandschneider B,** Bureau M, Gambardella A, Koepp MJ, Gelisse P, Gurses C, Crespel A, Nguyen-Michel VH, Ferlazzo E, Grisar T, Helbig I, Koeleman BP, Striano P, Trimble M, Buono R, Cossette P, Represa A, Dravet C, Serafini A, Berglund IS, Sisodiya SM, Yamakawa K, Genton P. Consensus on diagnosis and management of JME: From founder's observations to current trends. Epilepsy Behav. 2013 Jul;28 Suppl 1:S87-90

Book chapters:

Wandschneider B, Koepp M. Biomarkers of drug response. Book chapter *under review*.

Acknowledgements

This PhD and my years of research associated with it would not have been possible and as enjoyable without the great support of a number of people to whom I would like to express my deepest gratitude.

I am very grateful to my principal supervisor, Matthias Koepp, who was always available for discussion and guidance and who I greatly admire for his creative research approach and his ability to think translational and beyond boundaries of different research topics and diseases.

I would also like to thank my co-supervisor, Sanjay Sisodiya, for his continuous support, particularly with his great expertise in genetics.

Great thanks also goes to John Duncan, who was a continuous support both for my clinical and research career and always gave highly valuable advice on these topics, as well as additional directions on working in the UK, and great encouragement throughout my research at Chalfont.

I would also like to thank Beate Diehl, who guided me throughout the imaging project on SUDEP and without whose salary support my research life would have been very difficult at one stage!

Pam Thompson who was always supporting and encouraging and gave valuable advice on all neuropsychology matters.

My special thanks goes to all the people in Chalfont, who made my research experience so valuable and enjoyable on a daily basis, and gave me not only advice on MRI matters, but also on life in Britain, British cooking, Pubs and car matters! Thanks to the radiographers Jane Burdett, Philippa Bartlett, Andrea Hill and Elaine Williams, who were always flexible and helpful with patients scanning and handling.

Peter Gilford, who sorted out my IT and data storage issues and provided German plum cake to relieve homesickness once in a while.

I would also like to thank all my fellow research colleagues for all the hours of support, showing me the ropes, research discussions and helping out with various things, and for sharing challenges, worries, success and friendship. Research only works if you can brainstorm and exchange ideas with colleagues and Chalfont was a great place for that.

I am extremely grateful to all the patients and their siblings who came to Chalfont to participate in our research and spent hours, even on their weekends, to participate. This work would not have been possible without them.

I would like to thank the European Neurological Society and the German Research Foundation (Deutsche Forschungsgemeinschaft) for awarding me two personal fellowships to undertake this research, and the Wellcome Trust and Henry Smith Charity for providing project funding.

I am enormously grateful to my parents, sisters and friends for their support, encouragement and understanding for long working hours and sparse visits back home. Finally, I want to thank Lars Kremkow for everything.

Section 1: Introduction

Chapter 1: Epilepsy and its comorbidities

1.1 Definitions and Classifications

1.1.1 Definition of seizures and epilepsy

The International League Against Epilepsy (ILAE) defines a seizure as “a transient occurrence of signs and/or symptoms due to abnormal excessive or synchronous neuronal activity in the brain” (Fisher et al., 2005).

The most recent conceptual definition of epilepsy does not only relate to the occurrence of seizures, but characterizes epilepsy as “a disorder of the brain characterized by an enduring predisposition to generate epileptic seizures, and by the neurobiological, cognitive, psychological, and social consequences of this condition” (Fisher et al., 2005).

For the purpose of clinical diagnosis, an ILAE task force recently formulated an operational diagnosis in order to clarify the debate on seizure recurrence, as in the past epilepsy diagnosis required at least two unprovoked seizures. However, this may be inadequate in some patients, who e.g. acquired a brain lesion, such as a stroke, bearing a high risk of recurrence after the first seizure. (Fisher et al., 2014)

According to the operational definition, “epilepsy is a disease of the brain defined by any of the following conditions

1. At least two unprovoked (or reflex) seizures occurring >24 h apart

2. One unprovoked (or reflex) seizure and a probability of further seizures similar to the general recurrence risk (at least 60%) after two unprovoked seizures, occurring over the next 10 years

3. Diagnosis of an epilepsy syndrome.” (Fisher et al., 2014)

1.1.2 Epidemiology

Epilepsy is the most common neurological disease, affecting people of any age, race and different socioeconomic background. In industrialized countries, the incidence of epilepsy ranges from 40 to 70 per 100000/year (Sander, 2003). In European epidemiological studies, incidence rates of 43 to 47 per 100000 person years have been described in people of all ages (Forsgren et al., 2005). There is a disparity in epilepsy-burden and generally higher incidence rates in developing countries with 100 to 190 per 100000/year (Sander and Shorvon, 1996).

The prevalence rates of active epilepsy range in most studies from 4 to 7 per 1000 (Sander and Shorvon, 1996).

Premature death is 2 to 3fold higher in people with epilepsy than in the general population, and is highest in those who suffer from symptomatic epilepsy and persistent neurological deficits. Epilepsy related deaths include sudden unexpected death in epilepsy (SUDEP), status epilepticus, consequences from seizures, including accidents, drowning, burns, aspiration pneumonia, iatrogenic (drug toxicity and idiosyncratic) and suicide (Devinsky et al., 2015; Neligan et al., 2010). SUDEP will be addressed in more detail in chapter 1.4.

1.1.3 Classification of seizures and epilepsies

The classification of seizures and epilepsies is necessary both in a clinical and research setting. More importantly, it helps to find a more precise diagnosis and appropriate treatment choice.

The classification of seizures is based on the observable phenomenology. The ILAE established a standardised seizure classification in 1981, which is based on clinical manifestation and EEG findings only and has been revised in a 2010 proposal. (Berg et al., 2010; "Proposal for revised clinical and electroencephalographic classification of epileptic seizures. From the Commission on Classification and Terminology of the International League Against Epilepsy," 1981)

Both classifications are based on the conceptual dichotomy of focal and generalised seizures: Whereas generalised seizures originate and rapidly spread within neuronal networks of both hemispheres, focal seizures arise from a region in one hemisphere. Focal seizures can spread within the hemisphere and/or to the contralateral hemisphere.

The classification of epilepsies is based on information regarding seizure semiology, EEG findings, aetiology and associated conditions. Recognizing the heterogeneity of the epilepsies, the 1989 ILAE classification of the epilepsies and epileptic syndromes attempted to provide a syndromic classification. ("Proposal for revised classification of epilepsies and epileptic syndromes. Commission on Classification and Terminology of the International League Against Epilepsy," 1989) Over the last twenty years, epilepsy research had much advanced, particularly in the field of neuroimaging and genetics, and the new ILAE classification proposal from 2010 sought to take this into account.

The previous aetiological terminology, *idiopathic* (no cause, likely genetic), *symptomatic* (related to a structural or metabolic cause) and *cryptogenic* (presumed symptomatic but no identifiable lesion), was abandoned, as it was felt that these labels were not always used precisely and associated with certain expectations of prognosis and treatment response. Instead, the terms *genetic, structural/metabolic* or *unknown* were proposed for classification of aetiology.

1.2 Pharmacological treatment and chronic epilepsy

1.2.1 Initiation of treatment and pharmaco-resistance

When starting anticonvulsant treatment, the antiepileptic drugs (AED) are chosen according to the type of epilepsy and tailored to the individual, e.g. the comorbidity profile of the patient. In addition, issues such as teratogenicity and drug interactions with contraception in women of childbearing age have to be considered.

The majority of patients (60 to 70%) remain seizure free on antiepileptic medication. In about 80% of those, this is achieved with a single anticonvulsant, and in 10 to 15% with two agents. Approximately 30% develop treatment resistance, which is defined as persistence of seizures despite treatment with at least two tolerated anticonvulsants of appropriate choice and dosage. (Kwan and Brodie, 2000)

Apart from treatment efficacy, drug tolerability becomes a major concern particularly in refractory epilepsy treatment. The SANAD (Standard and New Antiepileptic Drug) study compared carbamazepine with lamotrigine, topiramate, gabapentin and oxcarbazepine in focal epilepsies, and valproate with topiramate and lamotrigine in mainly generalised epilepsies. Though newer AED were not as effective, some of them, *i.e.* oxcarbazepine and lamotrigine, were better tolerated than older AED, in this case carbamazepine. (Marson et al., 2007a, 2007b) A follow-up study investigating overall available newer AED, such as levetiracetam and zonisamide, is under way.

1.2.2 Effects of AED on cognition

There is a substantial body of literature on the cognitive effects of anticonvulsants and it is generally accepted that AED contribute to cognitive impairment in patients. Cognitive side effects are more likely to occur with rapid titration, high dosage and serum levels, and polytherapy (Mula and Trimble, 2009). Data with respect to differences between individual AED are limited and controversial. In addition, the interplay of several AED may be relevant and a recent study reported a higher inverse correlation of performance in executive functions with the total number of AED than with the overall daily dose (Witt et al., 2015). Cognitive impairment is likely multifactorial in nature and contributing factors are e.g. seizure frequency and disease onset during neurodevelopment. On the contrary, AED treatment may also “improve” cognition in the sense of preventing further deterioration through seizure control. (Pohlmann-Eden et al., 2015)

In the following, specific AED relevant to this thesis will be discussed in more detail.

1.2.3 AED relevant for this PhD

1.2.3.1 Levetiracetam

Levetiracetam is a broad-spectrum AED with efficacy in focal, generalised tonic-clonic and myoclonic seizures. Its main anti-seizure mechanism is attributed to its binding to the ubiquitous synaptic vesicle protein SV2A. Further modes of action include reduction of high voltage activated calcium currents, inhibition of intracellular calcium release and AMPA inhibition. (Abou-Khalil, 2016; Kaminski et al., 2014)

Effect on cognitive function

Most studies attribute a favourable cognitive profile to Levetiracetam. In a non-controlled surveillance study of 401 patients before and 3 and 6 months after starting Levetiracetam, subjective improvement on cognitive scores was apparent in almost a third of patients, taking a mean dose of 1500 mg at both time points. Better baseline scores, late onset epilepsy, fewer initial AED and seizure control were predictive of cognitive outcomes. (Helmstaedter and Witt 2008) In a comparison study of patients on Carbamazepine or Levetiracetam monotherapy, almost all cognitive measures, including verbal memory and executive functions, improved with Levetiracetam but not Carbamazepine irrespective of seizure control, suggestive of a mild superior outcome with Levetiracetam (Helmstaedter and Witt, 2010). In children and adolescents with focal epilepsy, Levetiracetam treatment has been associated with long-term stability in seizure control and cognitive functions (Schiemann-Delgado et al., 2012).

1.2.3.2 Topiramate

Topiramate, initially approved for treatment of pharmaco-resistant focal epilepsies, is a broad-spectrum AED with efficacy in genetic generalised epilepsies and tonic-atonic seizures in Lennox Gastaut Syndrome. It is further approved for migraine prophylaxis. Its modes of action include blockade of voltage-gated calcium channels and reduction of activation frequency of voltage-sensitive sodium channels, antagonism of alpha-amino-3-hydroxy-5-methylisoxazole-4-proprionic acid (AMPA)/kainate subtypes of glutamate receptors and increase of GABA activity via interaction with the $GABA_A$ receptors. Like acetazolamide, it contains a sulfamate moiety, which likely contributes to its carbonic anhydrase inhibitor mechanism. (Abou-Khalil, 2016; Mula, 2012)

Effect on cognitive function

Cognitive dysfunction has been described in patients with epilepsy, migraine and healthy controls characterised by reduced attention, psychomotor speed, short-term memory and more specifically, impairment of expressive language and working memory. These deficits are noted even after single-dose administration and on steady-dose in mono- or combination therapy, irrespective of seizure control. Psychometric measures consistently improve after significant dose reduction or discontinuation. (Bootsma et al., 2008; Martin et al., 1999; Meador et al., 2005; Mula and Trimble, 2009; Thompson et al., 2000) Topiramate has been reported inferior with regards to its effect on cognition in comparison to gabapentin, lamotrigine, and valproate (Aldenkamp et al., 2000; Blum et al., 2006; Gomer et al., 2007; Martin et al., 1999; Meador et al., 2005).

1.2.3.3 Zonisamide

Similar to Topiramate, Zonisamide is a broad spectrum AED with efficacy in focal and idiopathic generalized epilepsies. Its mechanisms of action include modulation of T-type calcium and voltage-sensitive sodium channels, augmentation of presynaptic GABA release, reduction of presynaptic glutamate release, down-regulation of GABA removing transporters and up-regulation of glutamate transporter 1 removal from the synaptic cleft. Like Topiramate, it contains a sulfamate moiety responsible for its weak carbonic anhydrase inhibitor mechanism. (Abou-Khalil, 2016; Schulze-Bonhage, 2015)

Effect on cognitive function

Zonisamide treatment leads to similar, probably less pronounced neurocognitive impairment (Mula and Trimble, 2009; Ojemann et al., 2001).

Underlying mechanisms of cognitive impairment patterns in patients on Zonisamide or Topiramate are poorly understood. As both contain a sulfamate moiety and language impairment has been described in other sufamate-compound medication, i.e. sulthiame (Dodrill, 1975), it has been suggested that the carbonic anhydrase inhibition mechanism shared by these AED may contribute to the cognitive impairment pattern, with a possible specific sensitivity of the expressive language areas to sulfa-compounds (Burns et al., 2009; Mula, 2012; Ojemann et al., 2001; Yasuda et al., 2013).

1.3 Juvenile myoclonic epilepsy

1.3.1 Diagnostic criteria and clinical picture

Juvenile myoclonic epilepsy (JME) is the most common genetic generalised epilepsy (GGE) syndrome affecting up to 12 % of all epilepsies with a high genetic predisposition (Berg et al., 2010; Delgado-Escueta et al., 2013; Zifkin et al., 2005). Patients present with symmetric, myoclonic jerks, mostly affecting upper limbs, generalized tonic clonic seizures and more rarely absence seizures. Myoclonic jerks without loss of awareness, occurring predominantly upon awakening, have been described as the hallmark of JME. Apart from this typical chrono-dependency, seizures can also occur from sudden awakening after a nap or from night sleep. Disease onset peaks between the age of 12 and 18 years, with a range of 6 to 25 years. The EEG typically shows a normal background and ictal generalized polyspikes (and waves) with myoclonic jerks. (Janz, 1985) The diagnostic criteria of the syndrome were recently refined. (Kasteleijn-Nolst Trenité et al., 2013)

1.3.2 Seizure provocation and reflex traits

Common reflex traits include photosensitivity, eye closure sensitivity, orofacial reflex myoclonus and praxis induction.

Photosensitivity is the most frequent reflex trait in epilepsy in general and is genetically determined. A photoparoxysmal response (PPR), i.e. spike and wave discharge provoked by intermittent light stimulation (ILS), occurs in up to 50% of JME patients, and even in up to 90% with prolonged ILS (Appleton et al., 2000).

Eye closure sensitivity occurs in 15–20% of JME cases and is defined as occurrence of spike-wave discharge within 2 s after slow eye closure (*i.e.* not

blinking). Clinically, patients will have eyelid myoclonus, sometimes accompanied by absence seizures. (Beniczky et al., 2012)

Orofacial reflex myocloni are precipitated by language-related activities, such as reading and talking. They usually occur in primary reading epilepsy but are present in 25-30% of JME patients (Mayer et al., 2006; Wolf et al., 2015).

Praxis induction describes seizure precipitation by cognitive tasks including a complex motor component. Clinically, patients will have myoclonic jerks in the active hand. Praxis induction is highly associated with JME, occurring in 24 to 47% of patients (Guaranha et al., 2009; Matsuoka et al., 2000).

1.3.3 Aetiology and histopathology

Clinical MRI scans are non-lesional. However, early histopathological studies in patients with GGE report subtle grey and white matter abnormalities, suggestive of microdysgenesis (Meencke and Janz, 1984, 1985). These findings could not be replicated in a controlled and blinded study (Opeskin et al., 2000). Recent histopathological studies in epileptic baboons, a natural animal model of JME, report a reduction of cortical neurons, most pronounced in the primary motor cortex of the hand area and less so in the somatosensory cortex (Young et al., 2013).

1.3.4 Clinical genetics of JME

The heritability in JME is high (0.7, (Nair and Thomas, 2004)) and a complex polygenetic inheritance is suspected in most cases, though Mendelian inheritance also exists in JME (Delgado-Escueta et al., 2013; Zifkin et al., 2005). Large epidemiological studies in unselected epilepsy populations report a high prevalence of first-degree relatives with epilepsy (Bianchi et al., 2003). Amongst

those, GGE had the highest prevalence with on average 5%. For first-degree relatives of JME, particularly siblings and offspring, there is an even higher risk for epilepsy with up to 6.2% and syndrome concordance is more pronounced than in other GGE syndromes, with 30% of affected first degree relatives also suffering from JME (Marini et al., 2004; Winawer et al., 2005). Twin studies show very high monozygous concordances with almost always identical syndromes within concordant pairs. (Koepp et al., 2014; Vijai et al., 2003)

1.3.5 Treatment and prognosis

Patients are advised to avoid major seizure precipitants, such as sleep deprivation and relative alcohol withdrawal as caused by binge drinking. Antiepileptic medication, particularly after occurrence of the first generalised tonic clonic seizure, is initiated in the majority of patients. Valproate with its anti-myoclonic effect is particularly effective in JME, though preferred in male given its teratogenicity. First-line choices in women are Lamotrigine and Levetiracetam. (Kasteleijn-Nolst Trenité et al., 2013)

Remission on antiepileptic treatment occurs in approximately two-thirds of new onset JME cases. Long-term remission is described in up to 30%, though most patients in these long-term follow-up cohorts still remain on AED treatment, making it difficult to evaluate true remission rates. (Geithner et al., 2012; Koepp et al., 2014; Senf et al., 2013)

1.3.6 Psychiatric comorbidities

In the initial syndrome description, Janz (1985) anecdotally reported immature

and impulsive behavior in JME patients, contributing to poor seizure control and social adaption. Two studies corroborated increased impulsivity and risk-taking behaviour in patients with poor seizure control (Wandschneider et al., 2013; Zamarian et al., 2013).

Psychiatric disorders have been reported in up to 47% of patients, particularly mood, anxiety and cluster B personality disorders (de Araujo Filho and Yacubian, 2013). One study identified an association of comorbid cluster B personality disorders, moderate-to-severe degrees of anxiety traits and prevalence of seizures triggered by praxis-induction or speech with poor seizure control (Guaranha et al., 2011) .

1.3.7 Frontal lobe dysfunction – behavioural and imaging studies

Though JME patients have average intellectual abilities, even long-term seizure-free patients present 'real-world problems' (Thomas et al., 2014), leading to poorer socioeconomic outcomes, such as higher unemployment rates (Camfield and Camfield, 2009). There is increasing evidence that dysfunction within thalamo-frontocortical networks leads to impairment of higher frontal lobe functions, such as working memory (WM), planning and risk-taking behaviour (Wandschneider et al., 2013; Zamarian et al., 2013). Other cognitive functions, e.g. hippocampal-related episodic memory, are relatively preserved, although there have been reports on more widespread cognitive impairment (Lin et al., 2013).

1.3.7.1 Working memory in JME

The first study of WM performance in JME (Swartz et al., 1994) investigated visual WM in patients with frontal lobe epilepsy (FLE) and used JME patients as a patient control group. Surprisingly, JME patients had similarly impaired WM function as FLE patients when compared to healthy controls. A subsequent ^{18}FDG-PET study employing the same cognitive task showed widespread decreased ^{18}FDG-uptake in the ventral premotor cortex, caudate and dorsolateral prefrontal cortex at resting state (Swartz et al., 1996). This was consistent with the poor performance on the WM task. More recent fMRI WM studies reported varying results: Roebling and colleagues (2009) employed the Sternberg Item Recognition Test, a visual-spatial WM task, and found no differences in performance and activation patterns between JME patients (n = 19) and controls. Vollmar and colleagues (2011) investigated a larger (n = 30) JME patient population with a more challenging visual spatial n-back WM task. Though performance again did not differ between groups, patients displayed abnormal motor cortex co-activation with fronto-parietal WM networks during increasing cognitive demand. Subsequent combined functional and structural connectivity analyses showed decreased connectivity between prefrontal and fronto-polar regions, possibly accounting for dysfunction of cognitive frontal lobe functions, and increased connectivity between the motor and prefrontal cortex. These observations may help to explain the mechanism of praxis-induction, or cognitively triggered myoclonic jerks, in JME (Vollmar et al., 2012).

1.3.7.2 Executive function and risk-taking behaviour in JME

Behavioural studies on executive functions, such as planning, response inhibition, cognitive flexibility and verbal fluency describe varying degrees of impairment. Amongst these, verbal fluency is most consistently affected (Devinsky et al., 1997; Pascalicchio et al., 2007; Piazzini et al., 2008; Sonmez et al., 2004; Thomas et al., 2014; Wandschneider et al., 2012).

Few studies relate executive functions to findings on structural, functional and metabolic imaging. In a quantitative MR spectroscopy (MRS) study, Savic and colleagues (2004) compared patients with either JME or GGE with generalized tonic clonic seizures (GTCS) to a group of healthy controls. N-acetyl aspartate (NAA) is a neuron specific metabolite. Reduced levels can be associated with neuronal dysfunction or damage (Savic et al., 2000). Within the frontal lobes, NAA concentrations were reduced in the JME group in relation to both healthy controls and GTCS patients. In addition, JME patients with low frontal NAA concentrations showed frontal lobe dysfunction on a brief neuropsychological assessment. In contrast, frontal lobe functions were spared in JME patients with normal NAA concentrations, GTCS patients and controls. Hence, although a prefrontal neuronal lesion may be present in some JME patients, JME seems to be a heterogeneous condition. Low NAA levels did not correlate with any other clinical parameter, such as current seizure frequency or seizure number over lifetime.

Pulsipher et al. (2009) aimed to investigate the integrity of thalamo-frontocortical networks in relation to executive function in recent onset JME. Twenty JME patients within 12 months of diagnosis were compared to an epilepsy control group of 12 patients with recent onset Benign Childhood Epilepsy with Centrotemporal Spikes (BECTS) and 51 healthy controls. Participants were assessed with three subtests of the Delis-Kaplan Executive Function System (D-

KEFS) and a questionnaire for parents, the Behavior Rating Inventory of Executive Function (BRIEF). JME patients performed less well than controls on D-KEFS Inhibition. Behavioral Regulation and Metacognition scores of the BRIEF were also significantly lower in the JME group. Quantitative MRI measurements revealed smaller thalamic volumes and greater frontal CSF in JME patients than in healthy controls and BECTS-patients. Thalamic and frontal volumes predicted D-KEFS performance only for the JME group.

In a resting FDG-PET study (McDonald et al., 2006), regional cerebral rates of glucose uptake values (rCMRGlc) were regressed on various executive function test scores in patients with frontal lobe epilepsy, JME and healthy controls. In the JME group, frontal hypometabolic values predicted impairment on measures of figural fluency and cognitive flexibility.

O'Muircheartaigh and colleagues (2011) reported subtle dysfunctions in verbal fluency, comprehension and expression, mental flexibility and response inhibition in a cohort of 28 JME patients. In a structural and diffusion tensor MRI (DTI) study, voxel-based morphometry revealed reductions in grey matter volume in the supplementary motor area and posterior cingulate cortex. Fractional anisotropy (FA) in the supplementary motor area predicted performance in tasks of word naming and expression. Grey matter volumes of the posterior cingulate cortex and FA correlated with scores on the mental flexibility task. The authors describe their JME cohort as relatively high functioning but with neuropsychological evaluation revealing subtle cognitive impairments.

Another frontal lobe function, engaging working memory networks, the orbitofrontal cortex and SMA, is decision making. Impaired experienced-related learning and impulsive decision-making have been described in a behavioural study in JME patients (Zamarian et al., 2013). A recent fMRI study investigated

impulsivity in JME using the Iowa Gambling Task (IGT), which is a measure of decision-making under ambiguity, and correlated IGT performance with activation patterns during a working memory task (Wandschneider et al., 2013) (Figure 1.1). Subjects are instructed to choose from four decks of cards, which award virtual monetary gains and losses. Card deck choices are indicative of either advantageous or disadvantageous long-term choices, however participants are not informed about the IGT's contingencies. Apart from overall advantageous or disadvantageous decision-making, learning from previous card choices can be assessed. The authors report overall no differences in card-choices and both groups, JME patients and healthy controls learned throughout the task. However, post hoc analysis revealed a greater proportion of patients with seizures than seizure-free patients having difficulties in advantageous decision-making and learn less from previous experience than both seizure-free patients and controls. Overall poor IGT performance was associated with increased activation within the dorsolateral prefrontal cortex (DLPFC). Impaired learning and ongoing seizures were associated with bilateral mesial prefrontal cortex and SMA, right superior frontal gyrus and left DLPFC activation. Findings suggest a dysfunction within macroscopically "normal" working memory networks, which implicates decision-making particularly in patients with poor seizure control.

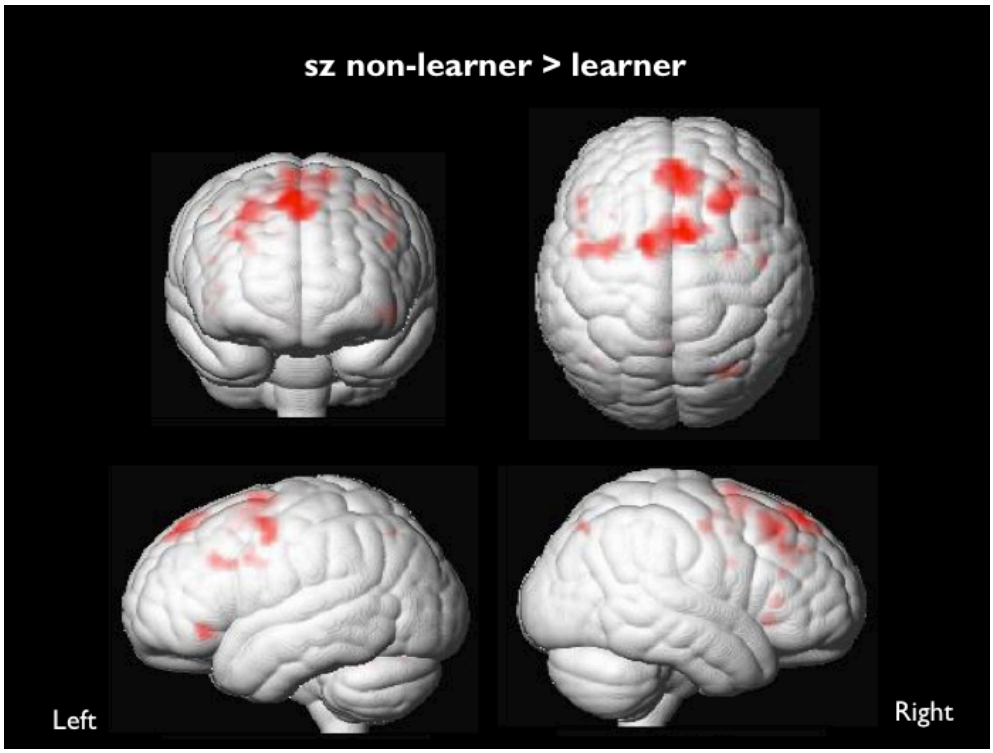

Figure 1.1 (Wandschneider et al., 2013). **Association of working memory network activation with learning in patients.** A subgroup analysis in patients with ongoing seizures showed a bilateral medial prefrontal cortex and pre-SMA, a left dorsolateral prefrontal cortex (DLPFC), and right superior frontal gyrus activation in nonlearners compared to learners. ($p < 0.005$ unc.) (sz, seizures).

1.3.7.3 Possible confounds of cognitive function

Cognitive abilities of patients with epilepsy in general can be modulated by disease activity, subclinical epileptiform discharges, and medication. Evidence for GGE and JME in particular is outlined.

Disease activity

Parameters of disease activity include seizure frequency and disease duration. Pascalicchio and colleagues (2007) reported a positive correlation of disease duration and the risk of cognitive impairment in JME. Vollmar and colleagues

(2011) observed abnormal motor-cortex co-activation in an fMRI working memory task, which was more prominent in patients with a more active disease and shorter seizure-free interval.

Subclinical epileptiform discharges

The phenomenon of transitory cognitive impairment (TCI) during subclinical epileptiform discharges has been reported in up to 50% of epilepsy patients (Binnie, 2003). Associated deficits were reported to be site and material specific, *i.e.* impairment occurs in the cognitive domain related to the area where subclinical discharges occur.

However, the distinction between subclinical and clinically evident discharges is challenging, as illustrated by Porter et al. (1973). They applied a paroxysm-triggered method to measure reaction time as an indicator of responsiveness at specific time points during spike-wave discharges of absence seizures. Fifty-four percent of reaction times were reported abnormal at the onset of spike-wave discharges. The relationship of generalized spike-wave discharges and cognitive functions have been mostly studied in patients with absence seizures (Blumenfeld, 2005). The level and nature of cognitive impairment are highly variable and depend on tests applied (Binnie, 2003). Impairments have been especially observed in tasks requiring a response to verbal questions, decision-making, complex motor performance and short-term memory. Deficits were more subtle when discharges occurred without any obvious clinical manifestation (Binnie, 2003; Blumenfeld, 2005). Greater discharge generalization and amplitude, as well as longer duration and fronto-central distribution, have been associated with worse performance in some studies (Blumenfeld, 2005).

In JME, Lavandier and colleagues (2002; cited by (Hommet et al., 2006)) investigated performance on cognitive tasks in relation to subclinical EEG

discharges. Executive function tasks were administered during continuous EEG and video monitoring. In view of the circadian seizure distribution in JME, the assessment was always performed in the morning. Patients who presented epileptiform discharges during rest were significantly more impaired on tests of abstract reasoning, concept formation and mental flexibility than patients without paroxysmal EEG changes. There was no increase of EEG abnormalities during the cognitive tasks.

Antiepileptic medication

Several studies attribute adverse effects of antiepileptic medication on cognition (for overview see e.g. Hermann et al., 2010). Processing speed and sustained attention are among the domains most vulnerable. In the studies reviewed here, antiepileptic medication was varied and the study samples were relatively small, rendering the statistical analysis of the impact of specific antiepileptic drugs difficult. Swartz and colleagues (1994) divided patients into groups with sedative (phenobarbital, primidone, and/or Dilantin) and non-sedative (carbamazepine and/or valproic acid) medications. They found no association between the type of medication and the performance variables correct responses and reaction time. Roebling and colleagues (2009) compared patients on valproic acid (VPA) to untreated patients or patients on lamotrigine (LTG) monotherapy respectively. The VPA-group was significantly more impaired on the verbal memory test and the authors concluded that cognitive dysfunction in this cohort is at least partially caused by medication side effects. On the contrary, Vollmar et al. (2011) reported a beneficial VPA effect in JME. In their fMRI working memory study, abnormal left motor cortex co-activation correlated negatively with an increasing daily VPA dose, implying a “normalisation” of function through VPA, which may also reflect its beneficial effect in suppressing motor seizures.

1.3.8 Genetic imaging biomarkers: the endophenotype concept

Identifying culprit genes has proven difficult in complex inherited diseases, such as epilepsy. Given the strong link between genetic variations, neurodevelopment and function of brain regions (Bigos and Weinberger, 2010), advanced functional and structural imaging techniques can be used to improve phenotype characterization. This can ultimately help to understand effects of the genotype onto the phenotype and to increase the power of genetic analyses (Siniatchkin and Koepp, 2009). How highly heritable cognitive fMRI activation patterns are, has been shown in a twin study employing an n-back working memory paradigm (Blokland et al., 2011), a task similar to the one employed for projects of this thesis (see general methods section).

Intermediate biological phenotypes are also called endophenotypes.
Gottesman and Gould (Gottesman and Gould, 2003) define endophenotypes as follows:

” 1. The endophenotype is associated with illness in the population.
2. The endophenotype is heritable.
3. The endophenotype is primarily state-independent (manifests in an individual whether or not illness is active).
4. Within families, endophenotype and illness co-segregate.[...]
5. The endophenotype found in affected family members is found in non-affected family members at a higher rate than in the general population.“

As discussed in previous chapters, medication or disease activity represent confounds on cognitive networks; isolating a disease related causal component is therefore challenging (Meyer-Lindenberg, 2012). One approach to control for

such confounds is to study unaffected first-degree relatives in heritable neurodevelopmental conditions.

Spencer and colleagues (2012) employed the Embedded Figure Task in patients with autism, their unaffected siblings and healthy controls. Autism is a presumed neurodevelopmental condition with a high heritability and siblings of patients have a more than 20 times higher risk than the general population to develop the same condition. Both patients and healthy siblings showed atypical activation patterns with reduced activation in the visual association cortex and enhanced activation in fronto-temporal regions compared to controls.

In an fMRI working memory study, unaffected, cognitively intact siblings of patients with schizophrenia showed increased activation within the dorsolateral prefrontal cortex (DLPFC) when compared to controls (Callicott et al., 2003). The same "imaging trait" had been previously described in patients with schizophrenia (Spence et al., 1998; Weinberger et al., 1986). As abnormal activation patterns within the DLPFC in patients with schizophrenia or their siblings has been a robust finding in several studies (Cannon and Keller, 2006; Karlsgodt et al., 2007; Perlstein et al., 2001), it has been successfully used as a quantitative imaging trait in combination with candidate gene studies, e.g. COMT (Egan et al., 2001), and in genome-wide association studies (GWAS) (Potkin et al., 2009).

Though imaging studies in first-degree relatives of epilepsy patients are rare, behavioural and neurophysiological studies have identified potential endophenotypes in juvenile myoclonic epilepsy, the syndrome relevant for this thesis:

Neuropsychological studies

Levav et al. (2002) investigated 10 JME families, 25 with childhood absence epilepsy (CAE), 30 TLE and 16 healthy control families. One affected family

member defined epilepsy families. The test battery was age-group adapted and assessed sustained attention, encoding and verbal memory, executive and focused attention and attentional flexibility/regulation of impulsivity. Comparing all scores, relatives' performance tended to fall between those of the patients' group and controls'. Among the relatives, JME relatives acquired the lowest scores for sustained attention and mental flexibility.

Iqbal and colleagues (2015) assessed 22 pairs of JME patients and unaffected siblings during and without video-EEG monitoring. Performance was compared to a control group. The neuropsychological test battery included tests of intelligence, visual-spatial skills, language, memory, attention and reaction time, as well as executive functions. Patients were more impaired than controls on tests of semantic and phonemic fluency. Siblings held an intermediate position between patients and controls and significantly differed from controls on psychomotor speed and phonemic verbal fluency. In addition, patients more frequently reported behavioural traits associated with executive dysfunction (*i.e.* impulsivity) on a behaviour rating scale. Impaired cognitive performance appeared to be independent of subclinical EEG discharges, as no discharges were recorded during testing.

Wandschneider et al. (2010) investigated performance on a complex prospective memory (PM) paradigm in JME patients, their unaffected siblings and healthy controls. Prospective memory (PM) describes the ability to fulfil previously planned intentions (Ellis, 1996). Successful PM performance is indispensable for managing activities of daily living, for example, remembering to post a letter or to attend a doctor’s appointment.

The employed PM paradigm allowed the evaluation of different phases of prospective memory, namely intention formation, intention retention, intention initiation and execution. Patients and siblings developed less complex plans than controls during intention formation. During intention execution, both groups

presented significantly more rule breaks than controls. Patients additionally completed fewer tasks and presented impairment in some executive functions, *i.e.* verbal fluency and response inhibition. It is assumed that PM performance is highly dependent on executive functions (Kliegel et al., 2000). Hence, performance during each PM phase was correlated post-hoc with scores on executive function measures. As expected, planning abilities predicted overall performance during intention formation, and response inhibition and planning performance during intention execution. In a post-hoc subgroup analysis, there was only a significant correlation between intention formation and planning in the healthy control group. Surprisingly, patients and siblings were unimpaired on a specific measure for planning performance (Tower of London task). This may indicate that patients and siblings fail to use their planning abilities efficiently when they are needed in more cognitively demanding tasks, such as the PM paradigm.

Neurophysiological studies

Atakli and colleagues (1999) reported 27% asymptomatic siblings with EEG abnormalities. 10.4% had 4-6 Hz spike/polyspike and wave paroxysms, 10.4% slow wave paroxysms, and 6.25% focal spike and wave activity during hyperventilation.

A Transcranial Magnetic Stimulation (TMS) study (Akgun et al., 2009) showed a higher motor threshold (RMT), a longer CSP (cortical silent period) and a shorter central motor conduction (CMCT) time in JME patients. In unaffected siblings, CSP was also prolonged, suggesting a potential impairment of supraspinal or intracortical inhibitory mechanisms. Similarly, Badawy and colleagues (2013) employed TMS to measure motor threshold and paired pulse transcranial magnetic stimulation in patients with focal or genetic generalised epilepsy

syndromes and their unaffected siblings. In all siblings of epilepsy patients, cortical excitability was higher than in healthy controls; however, among siblings it was most prominent in siblings of JME patients. Only drug naïve new onset JME patients had a lower motor threshold (i.e. increased excitability) than their unaffected siblings.

1.3.9 Structural neuroimaging in JME

Clinical MRI in JME patients are normal, however volumetric studies of high-resolution MRI identified changes of the mesial frontal and orbitofrontal cortices (Alhusaini et al., 2013; O'Muircheartaigh et al., 2011; Woermann et al., 1999), and anterior cingulate (Cao et al., 2013). Imaging analysis of the micro-architecture in JME, employing DTI-based parcellation and tractography, revealed increased structural connectivity between central motor and prefrontal cognitive (pre-SMA) networks, but decreased connectivity within prefrontal cognitive networks (pre-SMA to orbitofrontal), providing an explanation for both cognitively triggered jerks and cognitive impairment in JME (Vollmar et al., 2012). Thalamic volume changes were identified within 12 months of disease onset, indicative of an early or neurodevelopmental disruption of the thalamo-fronto-cortical circuit (Pulsipher et al., 2009). This was corroborated by a longitudinal study describing altered cortical developmental trajectories in recent onset JME cases compared to their peers with attenuation of age-related decline in cortical volume, thickness, and surface area. These changes were mainly observed in higher-association fronto-parietal-temporal regions (Lin et al., 2014).

1.4 Sudden Unexpected Death in Epilepsy

1.4.1 Definitions and epidemiology

SUDEP (sudden unexpected death in epilepsy) refers to a sudden death, often occurring after a generalised convulsive seizure, in a person who suffers from epilepsy but is otherwise healthy. It is the most common cause of epilepsy related death. (Surges and Sander, 2012)

It has been defined as "sudden, unexpected, witnessed or unwitnessed, nontraumatic and non-drowning death in patients with epilepsy, with or without evidence for a seizure and excluding documented status epilepticus, in which postmortem examination does not reveal a toxicologic or anatomic cause of death." (Nashef, 1997; Nashef et al., 2012)

A recent revision of the SUDEP definition distinguishes *definite* SUDEP, where autopsy or direct observation of the terminal event exclude a concomitant condition as cause of death, from *probable* SUDEP, where autopsy was not carried out, and *possible* SUDEP, where a competing cause of death is present. (Nashef et al., 2012) In *Near*-SUDEP, an individual with epilepsy is successfully resuscitated from a cardiorespiratory arrest and investigations cannot identify a structural cause. (Nashef et al., 2012)

Patients with epilepsy have a 20-fold increased risk of sudden death compared to the general population (Ficker et al., 1998). SUDEP risk varies depending on the type of epilepsy population, with the highest incidence in patients with chronic refractory epilepsy (1.1 to 5.9 per 1000 person-years (Annegers et al., 2000; Timmings, 1993)), epilepsy surgery candidates and particularly in those who continue experiencing seizures after surgery (6.3 to 9.3 per 1000 person-years; Shorvon and Tomson, 2011). As it often occurs in relatively young adults, it is associated with a disproportionate number of potential years of life lost and

second only to stroke when compared to other frequent neurological conditions (Thurman et al., 2014).

1.4.2 Risk factors

A recent meta-analysis of four major case-control studies of SUDEP compared 289 SUDEP cases with 958 living epilepsy controls. The frequency of generalised tonic clonic seizures (GTCS) was identified as the major risk factor of SUDEP, with an odds ratio of 15.46 (95% confidence interval (CI) 9.92 – 24.10) for at least three GTCS per year (Hesdorffer et al., 2011). Further epilepsy related significant risk factors, but with an odds ratio < 2, were duration of epilepsy longer than 15 years (OR 1.95, 95% CI 1.45 – 2.63); disease onset below the age of 16 (OR 1.72, 95% CI 1.23 – 1.40) and polytherapy (OR 1.95, 95% CI 1.09 – 3.47). After adjusting for GTCS frequency, a further pooled analysis of three case-control studies concluded that neither the use of specific AEDs nor polytherapy were associated with increased SUDEP risk (Hesdorffer et al., 2012).

Most deaths occur unwitnessed, during night time and in sleep (Nashef et al., 1998; Nobili et al., 2011; Ryvlin et al., 2013). There is evidence that nocturnal seizures constitute an important independent risk factor for SUDEP (OR 3.9, 95% CI 2.5–6.0 when compared to living controls) (Lamberts et al., 2012), and nocturnal supervision leads to a significant decrease of SUDEP risk (Langan et al., 2005). Similarly to sudden infant death syndrome (SIDS), most deaths occurred in prone position (Liebenthal et al., 2015).

A meta-analysis of placebo-controlled randomised trials reports a more than 7-fold decrease of SUDEP incidence in those treated with efficacious AED doses compared to those receiving placebo (Ryvlin et al., 2011), stressing the

importance to revise treatment in patients with refractory epilepsy in order to reduce SUDEP risk.

1.4.3 Neuropathological findings

A recent audit of 154 post mortem reports from UK neuropathology centres (Thom et al., 2015) identified macroscopic brain abnormalities in 52% of cases, including malformations of cortical development (MCD), perinatal infarcts and low grade tumours. Mild brain swelling was reported in almost a third of cases.

Abnormalities of the hippocampus, including asymmetry, mal-rotation and volume-loss, were present in 28% of cases. Microscopic pathology (in 89% of cases) mainly identified malformations (MCD and vascular, 15%), tumours (7%) and hippocampal sclerosis (21%). Toxicological studies report reduced or non-detectable post-mortem AED levels in patients presumed to be on medication, though post-mortem AED levels may be unreliable (Tomson et al., 2016; Zhuo et al., 2012).

Post-mortem genetic analysis for common long QT-syndrome (LQTS) genes in an Australian SUDEP cohort revealed variants in *KCNH2* and *SCN5A* in 13% of cases, stressing the importance of post mortem testing for relevant ion channel genes (Tu et al., 2011).

1.4.4 Theories of SUDEP mechanisms

1.4.4.1 Respiratory mechanisms

As demonstrated in a retrospective study of 16 SUDEP cases while being monitored on video-telemetry units (MORTEMUS study (Ryvlin et al., 2013),

SUDEP usually occurs after a generalised tonic-clonic seizure followed by early centrally mediated fatal cardiorespiratory dysfunction. However, respiratory parameters other than respiratory rate were not monitored, and further factors, such as upper airway obstruction and prone position (14 of 16 cases), may well have contributed to hypoxemia apart from centrally driven apnoea.

Ictal hypoxemia has been described in one third of generalised and partial seizures and has been associated with temporal onset and contralateral seizure spread (Bateman et al., 2008). Central mechanisms of hypoventilation are supported by stimulation studies of mesial temporal and insular regions resulting in respiratory inhibition (Dlouhy et al., 2015; Kaada and Jasper, 1952).

Several animal models, including DBA/1, DBA/2 mice and Htr2c knockout mice, confirm seizure-induced respiratory arrest and death. In DBA/2 mice, it has been shown that seizures inhibit the ponto-medullary respiratory control network (Massey et al., 2014). Aiba and Noebels (2015) recently demonstrated that in mice carrying mutations in Kv1.1 potassium channels (−/−) and Scn1a sodium ion channels (+/R1407X) seizures lead to irreversible spreading depression in the dorsal medulla, preventing auto-resuscitation via these cardiorespiratory centres.

1.4.4.2 Cardiac mechanisms

Seizures are associated with a variety of cardiac abnormalities, including brady- and tachyarrhythmias, asystole and repolarization abnormalities, such as QT prolongation. Tachycardia is much more common during seizures (57% of all seizures) than bradycardia (2%) and asystole (0.5%), and is correlated with seizure generalisation. There is evidence that arrhythmias in some cases may be secondary to hyperkapnia and hypoxia. (Massey et al., 2014; Rugg-Gunn et al., 2016)

Heart rate variability (HRV) is a measure of autonomic nervous system control on cardiac activity and reduced HRV has been associated with an increased rate of cardiac death. In chronic refractory epilepsy, HRV is interictally and peri-ictally depressed, particularly in patients with temporal lobe epilepsy and at night (Massey et al., 2014; Tomson et al., 2016), and may normalise with successful epilepsy surgery in TLE (Hilz et al., 2002). A potential role of HRV in SUDEP pathomechanisms remains however unproven.

1.4.4.3 Central nervous system mechanisms and EEG markers

Postictal generalised EEG suppression (PGES) is frequently observed after generalised tonic-clonic seizures and has been reported in monitored SUDEP cases (Lhatoo et al., 2010; Seyal et al., 2012). It is linked with ictal respiratory dysfunction and duration of the tonic phase (Lhatoo et al., 2010). The mechanisms underlying PGES are unclear but it has been suggested to reflect central cerebral shut-down leading to inhibition of respiratory centres in the brainstem (Lhatoo et al., 2010). Later risk of SUDEP was associated with longer PGES in a case-control study of monitored patients, suggesting that PGES could be a predictor of SUDEP (Lhatoo et al., 2010). However, these findings have not been replicated so far (Surges et al., 2011).

1.4.4.4 The role of Serotonin

Serotonin (5-HT) plays an important role in respiratory control and its dysfunction may therefore increase the risk of SUDEP, as shown in several animal models.

5-HT neurons are mainly located in the raphe nuclei of the brainstem and project to and stimulate the respiratory neurons in the nucleus of the solitary tract (NTS), nucleus ambiguus, pre-Bötzinger complex and other nuclei in the brainstem. Serotonin neurons in the midbrain cause cortical arousal as response to hyperkapnia. Mice lacking the 5-HT_{2C} receptor present with seizures and associated rapid death due to respiratory arrest. (Richerson et al., 2016) Peri-ictal respiratory arrest in DBA/2 mice has been prevented by treatment with selective serotonin reuptake inhibitors (SSRI) and in humans with refractory epilepsy, SSRIs have been associated with less severe ictal hypoxaemia (Bateman et al., 2010; Massey et al., 2014). *Lmx1b*$^{f/f/p}$ mice, where 5-HT neurons are absent, present with apnoea, high mortality in the neonatal period and do not adequately arouse during sleep as response to hyperkapnia. They also have a decreased seizure threshold and are at risk of ictal respiratory arrest. (Hodges et al., 2009; Massey et al., 2014) 5HT dysfunction has also been reported in another sudden death entity, sudden infant death syndrome (Massey et al., 2014).

1.4.4.5 Adenosine theory

Adenosine is released as a response to high-energy consumption, e.g. caused by a seizure, to suppress neuronal activity and limit neuronal injury, hence acting as an endogenous anticonvulsant. However, adenosine is also involved in respiratory control in the brainstem and increased activation of adenosine receptors there will lead to suppression of respiratory and cardiovascular functions. Prolonged seizures can lead to impaired clearance of released adenosine, causing over-activation of adenosine receptors, which may trigger apnoea and cardiac arrest. (Shen et al., 2010)

1.4.5 Genetic studies

There is evidence of genetic susceptibility from genes that have been identified in individuals who died from SUDEP. These include genes of potentially fatal cardiac arrhythmias, such as LQTS and catecholaminergic polymorphic ventricular tachycardia (CPVT), and genes associated with specific epilepsy syndromes with frequent sudden death, most commonly Dravet syndrome. (Goldman, 2015)

Discovery of the cardiac voltage-gated sodium channel SCN5A in the brain has lead to the hypothesis that mutations in ion channels expressed both in the brain and heart may cause a combined neuro-cardiac phenotype (Goldman et al., 2016; Hartmann et al., 1999). In LQTS, which is most commonly caused by mutations in *KCNH2*, *KCNQ1* and *SCN5A,* a seizure phenotype (*i.e.* personal or family history of seizures) has been described in almost a third of patients (Massey et al., 2014). Mice with a point mutation in the LQTS gene *KCNQ1* accounting for 50 % of LQTS cases have cardiac arrhythmias, seizures and sudden death (Massey et al., 2014). Catecholaminergic polymorphic ventricular tachycardia is a dysrhythmia presenting with stress-induced syncope and is associated with a high mortality in young adults (Postma et al., 2005). It is caused by a defect in the ryanodine receptor (RYR2) and similar to LQTS, a combined phenotype of arrhythmias and seizures has been described in families affected by RYR2 mutations (Goldman et al., 2016).

Dravet syndrome is a severe refractory epilepsy syndrome with childhood onset after the first year of life. Many patients succumb to sudden death. The genetic cause is in 80% of cases a loss-of-function mutation in SCN1A, which is both expressed in brain and heart, facilitating potentially fatal cardiac arrhythmias. (Massey et al., 2014)

Two recent studies were carried out in 18 (Leu et al., 2015) and 61 SUDEP

(Bagnall et al., 2015) cases respectively. Leu and colleagues (2015) analysed rare, protein-changing variants from whole-exome sequences in the SUDEP cohort and identified a significantly increased genome-wide burden of deleterious variants, suggesting a polygenic SUDEP causation. Bagnall and colleagues (2015) identified candidate pathogenic variants in LQTS-associated genes in 7%, in dominant variant arrhythmia genes in 15% and in epilepsy genes in 25% of SUDEP cases. Mutations in epilepsy genes were most commonly found in *DEPDC5* (six cases).

1.4.6 Imaging studies

Imaging studies implicate areas of cortical and brainstem autonomic control in patients at risk of SUDEP.

Tang and colleagues (Tang et al., 2014) employed resting state functional MRI connectivity analysis of thirteen regions of interest, involved in cardiorespiratory control, in patients at high and low risk of SUDEP. High risk patients were defined as those with early onset (< 16 years of age) intractable epilepsy, frequent GTCS (>3/year) and polytherapy. Low risk patients did not have any of the above risk factors. The high risk patients showed a significant decrease in the resting-state functional connectivity between the pons and the right thalamus, the midbrain and the right thalamus, bilateral anterior cingulate cortex and the right thalamus, and between the left and right thalamus when compared to the low risk group.

Mueller and colleagues (2014) described volume loss in brainstem regions involved in autonomic control, predominantly in the region of the periaqueductal grey, colliculi raphe and reticular formation and extending into the diencephalon in patients with mesial temporal lobe epilepsy (TLE). This was more severe and even extending to the medulla oblongata in two cases of mesial TLE who later

died of SUDEP. In addition, graph analysis was indicative of impaired interaction between those regions in the SUDEP cases.

1.4.7 Commonalities with sudden death in infants and toddlers

Several similarities between SUDEP, sudden infant death syndrome (SIDS) and sudden unexplained death in childhood (SUDC) have been reported. SIDS is defined as sudden death of an infant below the age of 12 months, whereas SUDC occurs in toddlers. As in SUDEP, SIDS and SUDC remain unexplained by most mortem and death scene examination. Both more often occur unwitnessed, presumably in sleep and victims are found in prone position. (Krous et al., 2004, 2005) There has been an association with a family history of febrile seizures in SUDC and some authors argue that SIDS and SUDC may be caused by not yet diagnosed epilepsy and potentially autonomic seizures or seizures with apnoea only (Kinney et al., 2015; Watanabe et al., 1982). Neuropathological studies in SIDS report brainstem abnormalities, *i.e.* brainstem gliosis and abnormalities of medullary nuclei containing 5-HT neurons (Paine et al., 2014; Richerson et al., 2016). Similar to SUDEP, SIDS has been linked to 5-HT dysfunction leading to respiratory and arousal deficits (Kinney et al., 2009b).

Dentate gyrus abnormalities in the hippocampus were reported in a large subset of 153 sudden infant death syndrome cases, and may reflect defective neuronal migration and proliferation (Kinney et al., 2015). Hippocampal and temporal lobe anomalies were also described in 62% of sudden unexplained death in childhood cases (Kinney et al., 2009a), creating a potential link between hippocampal/temporal lobe maldevelopment, susceptibility to seizures, and sudden death. Microdysgenetic features of the hippocampal formation included

dentate gyrus and subicular anomalies, granular nodular heterotopia, subventricular neuroblasts and hamartia, all indicative of aberrant neurodevelopment.

Chapter 2: Neuroimaging in epilepsy

2.1 Structural MRI

2.1.1 Clinical MRI sequences

Structural brain imaging is part of the diagnostic work-up in epilepsy and of particular importance if epilepsy surgery is considered, since identification of an epileptogenic lesion will give the patient a higher chance of becoming seizure-free after surgery (Duncan et al., 2016). The basic imaging protocol as established by the ILAE includes whole-brain T1-weighted and T2-weighted imaging acquired with the minimum slice thickness possible in two orthogonal planes, and a volumetric T1-weighted acquisition for three-dimensional reconstruction ("Recommendations for neuroimaging of patients with epilepsy. Commission on Neuroimaging of the International League Against Epilepsy," 1997).

After a review of presurgical MRI data in the epilepsy centre in Bonn, Germany, most epilepsy centres use an optimized MRI-protocol for all epilepsy patients as follows (Saini et al., 2009; Wellmer et al., 2013):

A three-dimensional volumetric T1-weighted imaging with 1 mm isotropic voxels, providing excellent grey-white matter contrast to identify e.g. malformations of cortical development (MCD); T2-weighted imaging (axial and coronal) to assess hippocampal architecture and cystic tissue components of other lesions; fluid-attenuated inversion recovery imaging (FLAIR; axial and coronal) to identify hippocampal sclerosis, inflammation, tumours and MCDs; and T2* gradient echo or susceptibility-weighted imaging (axial) for vascular and calcified lesions, such as cavernomas and arteriovenous malformations.

Imaging diagnostics in epilepsy have greatly advanced in the last decades, mainly due to improvement of scanners, acquisition protocols and imaging

processing (Duncan et al., 2016). Despite this, no lesions are identified with visual evaluation of conventional MR imaging in up to 30% of patients with presumed focal epilepsies.

However, in those cryptogenic or MRI-negative cases undergoing surgery, histo-pathological examination of the resected specimens often reveals subtle epileptogenic lesions, in most cases MCDs (Bernasconi et al., 2011).

This has led to increased application of imaging post-processing techniques, mainly employed on three-dimensional T1 volume scans, with the goal to improve the detection of subtle abnormalities of brain tissue overlapping with the epileptogenic zone, undetectable on visual inspection.

The field of computational neuroanatomy, or morphometry, has much advanced and to date, several fully automated post-processing imaging tools are available to capture and quantify regional differences of brain structure through mathematical models of tissue characteristics and cortical features, such as cortical thickness, surface area and folding complexity. (Bernasconi et al., 2011)

Beyond their application in individual patients in a clinical setting, these techniques have been broadly used to identify general patterns of structural abnormalities in groups of different epilepsy syndromes. Identification of patterns of structural pathology reaching beyond the presumed epileptogenic focus in “focal” epilepsy syndromes, and, vice versa, detection of regional structural abnormalities in presumed genetic “generalised” epilepsies has challenged the traditional dichotomy of focal versus generalised epilepsy syndromes.

In the following, automated post-processing tools relevant to this thesis will be discussed.

2.1.2 Automated post-processing tools

2.1.2.1 Voxel-based morphometry

Voxel-based morphometry (VBM) is a fully automated, objective image-processing framework to assess regional differences in tissue volume at a voxel level and is one of the most popular computational anatomy tools. Usually, grey matter is examined but it can also be used to assess white matter changes, though with decreased sensitivity. (Ashburner and Friston, 2000)

The software package Statistical Parametric Mapping (SPM), which has been designed for the analysis of brain imaging data trough the assessment of spatially extended statistical processes, offers one option to analyse VBM data.

Preprocessing

There are three basic preprocessing steps, including tissue classification, normalisation to a common space and spatial smoothing.

Tissue classification

Prior to tissue segmentation, non-brain parts are removed via skull-stripping. Inhomogeneities of the magnetic field will cause intensity nonuniformities, resulting in different intensities for the same tissue class in different regions. This is corrected for by using bias correction prior to applying tissue segmentation. The tissue is then segmented into grey matter, white matter and cerebrospinal fluid (CSF). Additional probability maps can be used to guide the segmentation process, *i.e.* the segmentation process is restricted and driven by a map for each tissue class that indicates how probable it is to be present at a certain voxel in the image. These tissue probability maps are problematic in cohorts that may deviate from these maps, e.g. children.

Normalisation

Images are normalised to a standard space to enable voxel-wise comparisons across subjects. There are two main normalisation methods available in Statistical Parametric Mapping (SPM): a low-dimensional SPM default normalisation, which uses pre-existing symmetric tissue probability maps as a reference atlas, and a high-dimensional DARTEL (Diffeomorphic Anatomical Registration using Exponentiated Lie algebra) normalisation, which creates a study specific reference atlas (Ashburner, 2007). In DARTEL normalisation, registration starts by creating a mean of all images. This is then used as initial template; the images are registered to this template and subsequently averaged again. This procedure is repeated several times and eventually results in a highly accurate mean template and deformation fields, describing how local structures were adjusted to match the mean template. Deformations are finally used to warp the initial images into standard space.

Voxel-wise volume changes due to normalisation can be derived from the deformation fields as Jacobian determinants. This information can be used to apply modulation, which means that the normalised grey matter segments are multiplied with the Jacobian determinants to correct for volume changes due to normalisation. Hence original local volumes will be preserved even in standard space.

Spatial smoothing

The normalised tissue segments are then convolved with a Gaussian function, which is referred to as smoothing. Since statistical analysis will be done with parametric tests, smoothing is done to ensure that random errors have a Gaussian distribution. In addition, smoothing compensates for small registration errors and renders the analysis sensitive to effects that approximately match the

size of the smoothing kernel. Usually, a smoothing kernel of full width at half maximum of 4-12 mm is recommended. After smoothing, each voxel represents a weighted mean of its own and neighbouring voxels' values.

SPM8 toolbox

The SPM8 toolbox is an extension of the "classical" VBM8 method, but uses a different segmentation approach.

Firstly, the segmentation approach is based on an adaptive Maximum A Posterior (MAP) technique without the need for a priori information about tissue probabilities. The Tissue Probability Maps are only used for spatial normalisation. The resulting MAP estimation is adaptive, as local parameter variations (*i.e.* means and variance) are modelled as slowly varying spatial functions (Rajapakse et al., 1997), accounting for intensity inhomogeneities and other local variations of intensity.

Secondly, a Partial Volume Estimation (PVE) with a mixed model of at most two tissue types is used during segmentation. Images are initially segmented into grey matter (GM), white matter (WM), and cerebrospinal fluid (CSF) based on the MAP estimation. This is followed by a PVE of two additional mixed classes, namely GM-WM and GM-CSF. As single voxels may contain more than one tissue type, this will result in an estimation of the fraction of each tissue type present in each voxel.

Thirdly, two denoising methods are applied: A spatially adaptive nonlocal means (SANLM) denoising filter (Manjón et al., 2010) that will remove noise while preserving edges; and a classical Markov Random Field (MRF) approach to include spatial prior information of adjacent voxels into the segmentation estimation (Rajapakse et al., 1997).

Finally, for DARTEL normalisation an already existing DARTEL template in Montreal Neurological Institute (MNI) space is used, which was derived from 550 healthy control subjects of the IXI-database (http://www.braindevelopment.org) and is provided in MNI space for six different iteration steps of DARTEL normalisation.
(http://dbm.neuro.uni-jena.de/vbm8/VBM8-Manual.pdf)

Statistical analysis

Parametric statistical testing is usually applied in a mass-univariate approach, *i.e.* the same test is applied to each voxel simultaneously. The general linear model and Gaussian random field theory to account for multiple comparisons are employed as described for fMRI in chapter 2.2.4.

2.2 Functional MRI

2.2.1 Principles of functional MRI

Functional MRI is a non-invasive imaging technique that utilizes regional haemodynamic changes as a surrogate marker of neuronal activity. It relies on the principle that regional cortical increase of neural activity causes a local increase in cerebral blood flow (rCBF) and volume (rCBV). Resulting changes of the magnetic properties of blood can then be imaged with fMRI.

Functional imaging techniques measure signal changes caused by the blood-oxygen-level-dependent (BOLD) contrast, which describes the susceptibility changes of oxygenated and deoxygenated blood.

The change in regional blood flow exceeds the additional metabolic demand so that there is a relative increase of oxygenated arterial blood to deoxygenated venous blood at the capillary level and hence a decrease of deoxyhaemoglobin concentration. While oxyhaemoglobin has diamagnetic properties, deoxyhaemoglobin is paramagnetic and leads to local inhomogeneities of the magnetic field and a shortened effective spin–spin relaxation time T2*. As cortical activation is associated with a reduction of deoxyhaemoglobin concentration, it results in a local prolongation of the T2* time. Magnetic resonance sequences, such as echo planar imaging (EPI), are highly sensitive to local T2* changes and can hence measure the signal increase in activated brain regions.

As the signal increase is only about 2% and regional changes in rCBF and rCBV last for seconds, data sampling must be sufficiently long and usually implies repeated scanning of the brain region of interest with a repetition time (TR) of several seconds to collect a few hundred data volumes over time. (Logothetis, 2008)

2.2.2 Preprocessing of fMRI data

2.2.2.1 Realignment

During this first step of preprocessing, the imaging time series are realigned to the same space to correct for subject's head motion during the scanning.

This step is important for data interpretation, as head movement even by a few mm will result in different positions of every volume in the acquired time series. Hence it is not warranted that each voxel within the time series represents the same anatomical region throughout the whole fMRI task.

2.2.2.2 Normalisation

To enable group analyses and comparisons, each subject's data have to be transformed into a standard anatomical space to ensure a voxel-wise comparability. This process is called spatial normalisation and entails creating a mean image from the realigned time series to provide a better signal to noise ratio than a single volume. With a combination of linear and non-linear transformations, the mean image is then normalised to a template image in common space and resulting transformation parameters are applied to the whole time series of images.

As the data is in standard anatomical space, results can then be reported in standardized coordinate systems. (Ashburner et al., 2000)

2.2.2.3 Smoothing

Spatial smoothing creates an average of each voxel value and its neighbouring voxels, resulting in a blurring of the brain image. Smoothing increases the signal-to-noise ratio and as most fMRI acquisitions contain a significant amount of

noise, smoothing helps to achieve more consistent regional image intensities. Smoothing is also advised prior to statistical analysis in SPM, as parametric tests are based on the assumption that the data follow Gaussian distribution, which is satisfied by smoothing.

A Gaussian kernel of known width is applied to each voxel. The width of the Gaussian is described as the width of the kernel, at half of the maximum of its height - the Full Width at Half Maximum (FWHM). The FWHM usually has 4-16 mm and approximately a FWHM of twice the voxel size results in appropriate smoothness to carry out statistical analysis. (Friston et al., 2000)

2.2.3 Statistical analysis

Statistical parametric mapping is utilized for statistical analysis of functional mapping, *i.e.* fMRI studies. Statistical parametric maps (SPMs) are also known as T- or F-maps, which refers to the concept that under the null-hypothesis their distribution of voxel values is usually according to the F or student's T distribution (Friston, 2005). SPMs analyse spatially extended data by constructing complex statistical processes to test hypotheses about regionally specific effects. To achieve this, statistical parametric mapping mainly utilizes

1. the general linear model (GLM) to explain spatially continuous data and
2. the Gaussian random field theory to account for the problem of multiple comparisons when analysing brain volumes by adjusting *p* values to control for false positive rates.

2.2.3.1 The general linear model

The general linear model is described by the equation

$$y = X\beta + \varepsilon$$

where the measured signal *y* is a linear combination of explanatory variables in the matrix *X* and a residual error term ε. The contribution of each explanatory variable to the total signal is unknown, which is expressed by the unknown scaling factor *β* for each variable.

In the design matrix of the fMRI model, each row corresponds to an observation (*i.e.* each scan) and each column to a model parameter, which may correspond to designed effects or confounds, and the residual error column. The design matrix is displayed graphically by SPM.

The relative contribution of each of these columns to the observed effect is controlled by the parameters *β*, which can be estimated using standard least squares. Some of these parameters may be of interest, and the remaining of no interest and are hence treated as nuisance variables. The null hypothesis (*i.e.* no relationship between the experimental model and the voxel data) can be tested by calculating T statistics for a particular linear combination, or contrast. T-statistics are obtained by dividing the contrast of parameter estimates by the standard error of that contrast.

Usually, a mass-univariate approach is used, in which every voxel location across images is tested for effects by employing a general linear model. Variance is firstly analysed at each voxel. T-statistics of these results are then created, followed by a Z score equivalent for the T-statistic before creating a statistical parametric map, or T-map.

False positives are accounted for by correcting the significance value for multiple comparisons. An inference is then drawn from this statistical parametric map and voxels in which an effect is reliably present are located.

Prior to the statistical analysis, fMRI time series are temporally filtered in order to remove low-frequency noise. Regressors are then convolved with the haemodynamic response function (HRF) of the BOLD effect to account for its

delayed response. The scans cannot be treated as independent observations since one scan is usually correlated to the following. This is accounted for by a temporal smoothing function of the time-series.

2.2.3.2 Movement parameters

The magnetic field of an MRI scanner contains regional inhomogeneities and the T2* weighted acquisitions used for fMRI are particularly susceptible to these effects, causing a signal change of up to 10%. If a study participant moves his head during the experiment in one of these zones of regional intensity changes, the acquired voxels will have a higher value, which requires further correction beyond the realignment during the preprocessing procedure. Hence realignment parameters resulting from the preprocessing steps are included as covariates into the design matrix. Including movement parameters into the model also helps to control for the impact this movement may have had on cognitive performance at that time (e.g. the subject is coughing during the experiment and hence cannot fully concentrate on the task).

Chapter 3: Imaging biomarkers of epilepsy

3.1 Concept of biomarkers in epilepsy

Biomarkers are objectively measurable characteristics of a normal or pathological biological process (Trusheim et al., 2007). Within epilepsy research, recent efforts have been made to identify reliable biomarkers to advance the understanding of disease-mechanisms, or epileptogenesis, to individualize and optimize treatment and enhance treatment prediction (Engel, 2011). Ideally, biomarkers can be a direct measure of disease activity and treatment effects, an indicator of how well a patient functions, and hence may substitute clinically meaningful endpoints to increase the yield of clinical trials (Koepp, 2016; Pitkänen et al., 2016).

This is particularly necessary since

1. the diagnosis of epilepsy relies on seizure occurrence, although it is now known that epilepsy encompasses far more than seizures, e.g. cognitive impairment and psychiatric comorbidities, which can even precede seizure onset and progress beyond seizure control (e.g. (Camfield and Camfield, 2009; Jennum et al., 2011)). In presumed genetically determined epilepsies, few neuro-imaging studies so far suggest that functional and structural alterations in neural circuits are already present at disease onset (Lin et al., 2014; Pulsipher et al., 2009) but these cannot be fully related to epileptogenesis/neurodevelopment and separated from medication and seizure effects.
2. epilepsy is mainly treated with antiepileptic medication in a trial-and-error approach, as so far, treatment response and occurrence of side effects

cannot be predicted after the first seizure. Biomarkers are necessary to identify those likely to respond to treatment or experience side effects.

3. epilepsy is associated with a high morbidity and mortality, with SUDEP constituting one of its worst outcomes. Though risk factors for potentially fatal disease are known, biomarkers for early prediction of progressive and pharmacoresistant disease are necessary to tailor treatment early and to develop and evaluate the success of prevention strategies.

3.2 Imaging biomarkers in epilepsy

Advances in imaging techniques and the recent advent of meta-analytic techniques have helped to understand commonalties in imaging findings. For example in fMRI, reproducible patterns of activation or deactivation elicited by cognitive tasks could be identified, such as the default mode network, a set of brain regions, which are commonly deactivated during goal-directed tasks (Bullmore, 2012; Raichle et al., 2001). Several "imaging traits" have so far been identified in complex neuropsychiatric diseases, such as schizophrenia or autism (Ecker et al., 2010; Spence et al., 1998; Weinberger et al., 1986), rendering neuroimaging an attractive tool to analogously identify reliable disease biomarkers in epilepsy.

3.2.1 Biomarkers of treatment response: pharmacological fMRI

3.2.1.1 Principles of pharmacological fMRI

Pharmacological fMRI (ph-MRI) is a promising emerging application of functional MRI to assess regional network effects of and treatment response to specific AED. However, ph-MRI studies in epilepsy are so far rare and usually of small sample sizes (Koepp, 2011), which may be due to several methodological difficulties:

The signal change in fMRI related to the drug is low; hence drug effects are generally studied as an interaction effect in task-related fMRI, *i.e.* task-related activation patterns for a drug are compared to those without the drug or placebo. Drugs can influence the BOLD signal both at a neuronal and vascular level complicating the interpretation of the effects observed. As the BOLD signal is contaminated by low-frequency noise, detection of slowly evolving medication

effects can be challenging (Mehta and O'Daly, 2011). A more epilepsy-specific problem is, that patients usually are already on AED treatment, therefore the study design has to control for effects of co-medication in addition to other confounders, such as disease activity, syndrome and comorbidities (Beltramini et al., 2015).

Nevertheless, ph-MRI has the major advantage that it can investigate effects of pharmacological agents at a network level and remotely from regions of highest target receptor densities, whereas PET and molecular studies can define target receptor occupancy and affinity without necessarily translating effects to large-scale networks (Mehta and O'Daly, 2011). Hence fMRI enables a system evaluation of networks underlying behavioural effects of a drug, independent of its biochemical mechanism of action. As AEDs often target several receptor sub-types with varying regional distribution and AED efficacy differs across these targets, fMRI can monitor the combined effect of these interactions across multiple brain regions (Borsook et al., 2006). A further advantage is that fMRI does not use ionizing radiation and has no known biological side effects.

So far, ph-MRI has been widely applied in affective disorders, addiction and schizophrenia (Nathan et al., 2014). Overall, these studies show that pharmacological agents with known clinical efficacy have consistent effects on disease relevant neural networks and modulation of brain activation at treatment baseline is a potential surrogate marker for long-term efficacy (Nathan et al., 2014).

3.2.1.2 Application with antiepileptic drugs

Carbamazepine and Oxcarbazepine

Jokeit and colleagues (2001) were the first to employ ph-MRI in an epilepsy group. They studied the relationship of mesio-temporal fMRI activation and

carbamazepine (CBZ) concentrations in 21 patients with refractory TLE. Most patients were on monotherapy and a visual-spatial memory retrieval task was employed. The extent of task and syndrome specific fMRI activation within the medial temporal lobe was negatively correlated with the CBZ serum levels. The effect was most marked with close to toxic drug levels.

Employing a graph theoretical approach and resting state fMRI in a TLE cohort treated with CBZ or Oxcarbazepine (OXC) and comparing to those who were on other AEDs, Haneef and colleagues (2015) report altered hubness in those on CBZ/OXC, which refers to less highly connected nodes linking distant parts of the brain. Whereas betweeness centrality, or hubness, was reduced within the limbic circuit and thalamus with CBZ/OXC use, it was increased in default mode regions, *i.e.* cingulate and posterior cingulate/precuneus.

Previous data in TLE suggests a "re-distribution" of hub regions with high betweeness centrality to mainly paralimbic and temporal association cortices (Bernhardt et al., 2011). It is therefore tempting to speculate that CBZ/OXC may have a region-specific effect on disease-related network changes.

Valproate

An EEG-fMRI study attributes VPA treatment response among patients with GGE to regional differences in generalized spike and wave discharge (GSWD) generators (Szaflarski et al., 2013). Spike-related activation in VPA-resistant patients was increased in the medial frontal cortex and anterior insular bilaterally when compared to VPA-responders. The effect remained apparent in the medial frontal cortex even after controlling for spike-counts, but there was no difference between groups in the thalamus. Hence in the VPA-resistant group, seizure generators may be more cortically distributed.

Levetiracetam

Functional MRI data from individuals with amnestic mild cognitive impairment, which is associated with a risk of Alzheimer's disease, demonstrated that dysfunctional, increased hippocampal activation in the dentate gyrus/CA3 was normalised by low-dose LEV treatment with improvement of memory performance (Bakker et al., 2012, 2015).

Topiramate

Five functional MRI studies employing an expressive language task in healthy subjects, epilepsy and migraine patients after a single dose or on steady-state Topiramate treatment report reduced activation in language relevant regions, *i.e.* dominant inferior and middle frontal gyri, superior temporal gyrus (De Ciantis et al., 2008; Jansen et al., 2006; Szaflarski and Allendorfer, 2012; Tang et al., 2016), and a failure to deactivate task-negative regions, including the default mode network (Szaflarski and Allendorfer, 2012; Tang et al., 2016; Yasuda et al., 2013).

Chapter 4: Overall aims of studies

The studies presented in this PhD thesis use advanced functional and structural neuroimaging techniques to investigate potential *imaging* biomarkers of epilepsy in three different, but inter-connected domains:

(1) Genetic fMRI phenotypes in juvenile myoclonic epilepsy; group comparisons will be performed between patients, their unaffected siblings and healthy controls, to identify functional alterations specific to the genetic underpinnings of the syndrome, in contrast to more disease-related changes.

(2) The effect of specific antiepileptic drugs on cognitive fMRI activation patterns in treatment-resistant focal epilepsy; group comparisons will be carried out in patients who are on Levetiracetam (LEV), a drug with a presumed normalizing effect on cognitive networks, and patients who are not on LEV. In a second study, patients on medication associated with a negative cognitive profile, namely Topiramate or Zonisamide, will be compared to those who are on LEV. The overall aim of these projects is to establish drug specific effects on cognitive networks.

(3) Structural imaging markers of sudden unexpected death in epilepsy; in a retrospective study, structural imaging data will be compared in patients who later died of SUDEP, living epilepsy controls at risk of SUDEP and healthy controls. The aim of this study is to identify regional brain changes associated with SUDEP risk and to identify *in vivo* biomarkers to assist determination of the pathophysiology of SUDEP.

All three domains share that studies are focused on at-risk populations, *i.e.* at-risk of (1) developing epilepsy, (2) developing side effects and

responding/non-responding to treatment and (3) dying from epilepsy. Thus, identifying imaging biomarkers can inform clinical decision-making and development of preventative or disease-modifying treatment in several aspects:

Imaging biomarkers can be “preventive” in a sense that they can help to identify those individuals at risk. They can be used as surrogate markers to measure treatment effects and they can help to measure risk severity, which could be particularly helpful in monitoring the success of risk reduction in SUDEP.

Section 2: Experimental studies

Chapter 5: Common methods

This chapter describes experimental methods that were used for more than one of the studies described in chapter 6 to 9. Methods specifically applied in one study only are described in the relevant chapters.

5.1 Ethical approval

All studies were approved by the Research Ethics Committee of the University College London Institute of Neurology and University College London Hospitals. For prospectively acquired data, written informed consent was obtained from all study participants.

5.2 Subjects

Patients were recruited from outpatient clinics at the National Hospital for Neurology and Neurosurgery, London, and the Epilepsy Society, Chalfont St Peter. Healthy control data was taken from previous control cohorts acquired for functional and structural MRI studies (Stretton et al., 2012; Vollmar et al., 2011) on the same GE Excite HDx 3T scanner (General Electric, Wakashua, Milwaukee, WI, USA) at the MRI Unit of the Epilepsy Society, Chalfont St Peter. They were initially recruited from hospital staff, students and friends or carers of recruited patients. Healthy controls had no history of neurological disease and no family history of epilepsy and had a normal neurological examination.

5.3 MRI

MRI scans were acquired on a GE Excite HDx 3T scanner (General Electric, Wakashua, Milwaukee, WI, USA) at the Epilepsy Society MRI Unit, Chalfont St Peter, UK.

Standard imaging gradients were used with a maximum strength of 40 mT/m and slew rate of 150 T/m/s. All images were acquired with an 8-channel phased array head-coil for reception and the body coil for transmission.

5.4 functional MRI

Gradient-echo planar T2*-weighted images were acquired, providing blood oxygenation level dependent (BOLD) contrast. The acquisition consisted of 50 axial slices in AC-PC orientation with 2.4 mm thickness and 0.1 mm gap, providing full brain coverage. Slices had a 64 x 64 in plane matrix with 3.75 x 3.75 mm voxel size. Repetition time was 2500 ms and echo time 20 ms. Accelerated parallel imaging with a Sense factor of two was used. All fMRI acquisitions were preceded with four excitations to ensure steady magnetization before the paradigm started and data was recorded.

Images for the functional paradigms were acquired with the same sequence but of different total duration.

5.4.1 fMRI paradigms

All paradigms were explained in detail before the MRI scan, using printed instructions with screenshots of the paradigm presentation. Paradigms were presented by in-house software and presentations were synchronized to the MRI scanner via a TTL trigger signal. The paradigm presentation was projected on a semi-transparent screen in front of the MRI scanner, which could be seen by the subjects via a mirror system attached to the head-coil.

Appropriate vision was tested for every subject before the fMRI acquisition. MRI compatible frameless glasses were provided to subjects with impaired vision if needed.

A MRI compatible joystick was provided at the right hand side for responses during the Dot Back paradigm, which was positioned individually for comfortable use.

5.4.1.1 Dot Back paradigm

The Dot Back paradigm is an n-back task to assess visual-spatial working memory (Kumari et al., 2009; Figure 5.1). Yellow dots were presented every 2 seconds randomly in the four corners of a diamond shape on the screen. Participants were instructed to respond to the dots sequentially by using a joystick with their right hand. Participants monitored the locations of dots and were instructed to move the joystick to the position of the currently presented dot in the '0 Back' condition or to the position of the dot in the previous (1 Back) or two (2 Back) presentations earlier. The three conditions (0, 1 and 2 Back) lasted 30 seconds and were repeated five times in a pseudorandom order and alternated with rest blocks of 15 seconds. During the total duration of 11:15 minutes of the paradigm, 272 EPI volumes were acquired.

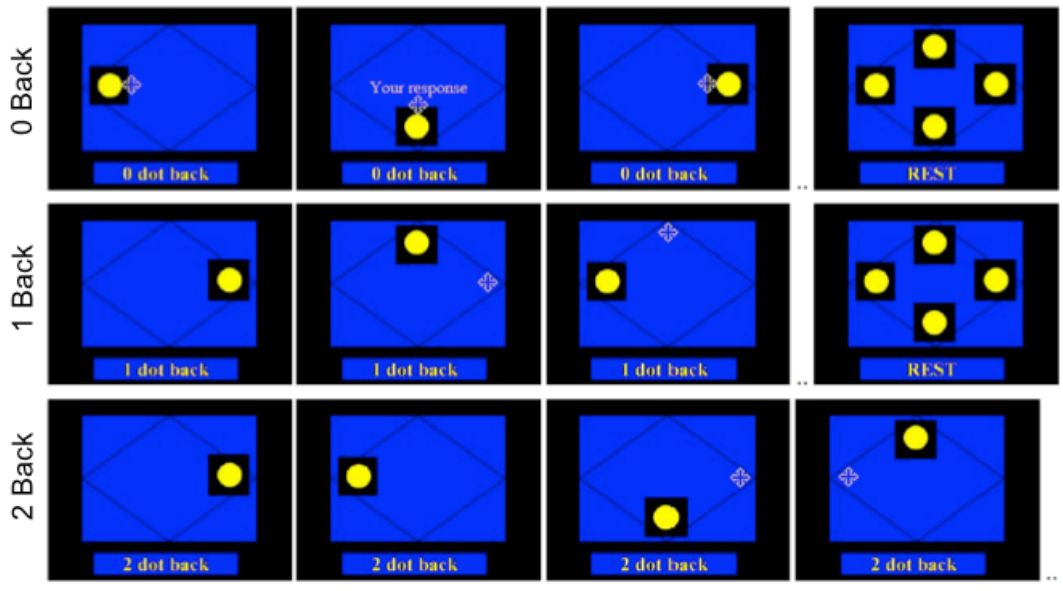

Figure 5.1. **Illustration of the n-back working memory task.** Participants monitor the locations of dots at a given delay of the original occurrence (0, 1, or 2 Back) and responded by moving a joystick corresponding to the location of the current or previously presented dot. The crosshair indicates the participant's response.

5.4.1.2 N-Back task

The N-Back task assessed verbal working memory. Single words were presented for 3 seconds each in 30 seconds blocks. In the control condition ("Is it bird?"), participants were instructed to respond with the joystick as soon as they read the word "bird". During the actual working memory condition, "Two back", subjects were asked to respond with the joystick when a word was repeated which they read two presentations earlier. As resting condition, 15 seconds of crosshair fixation were interleaved.

5.4.1.3 Verbal fluency paradigm

The verbal fluency is a covert task for language and executive function. Subjects were presented with single letters presented every 3 seconds in blocks of 30 seconds and were instructed to think of any word starting with the presented letter every time the letter is presented. These blocks alternated with 30-seconds rest blocks with presentation of an asterisk. The task lasted 5:10 minutes and 120 EPI volumes were acquired.

5.4.2 Functional MRI analysis

All fMRI analyses were performed with the SPM 8 software (www.fil.ion.ucl.ac.uk/spm/), including preprocessing, first level single subject analyses, group analyses and functional connectivity analyses.

5.4.2.1 Preprocessing

The preprocessing described in this section was applied identically to the data of all cognitive paradigms.

Realignment

Images were realigned for movement correction using the SPM realignment function. Realigned images were not resliced to avoid unnecessary interpolation, which could result in loss of image quality. The realignment parameters were stored in each image's header file and were taken into account before the next preprocessing step. A mean image was created from the realigned time series and saved.

Normalisation

A scanner and acquisition specific template in MNI space was used since the image contrast and spatial distortions from our acquisition differed considerably from the standard EPI template provided within SPM. This template had also been used in a previous, related fMRI study in JME, employing the same fMRI paradigms (Vollmar et al., 2011). Images of all subjects were normalised to this template.

Smoothing

Normalised images were smoothed with an 8 x 8 x 8 mm FWHM Gaussian kernel. All further statistical analyses were carried out on these realigned, normalised and smoothed images.

5.4.2.2 First level statistical analysis

Single subject statistical analysis was carried out applying a full factorial block design. Each task condition was modelled separately. Movement parameters were entered as regressors of no interest.

Dot Back paradigm

Task conditions were modelled separately as 30-s blocks and convolved with the SPM canonical haemodynamic response function. For each subject, contrasts were defined by comparing task conditions against rest or comparing cognitive task conditions ('1 Back' and '2 Back') against the control task (0 Back). Hence by controlling for motor response and visual attention, only cortical activation due to the working memory load was revealed.

N-Back paradigm

Task conditions were modelled separately as 30-s blocks and convolved with the SPM canonical haemodynamic response function. For each subject, contrasts were defined by comparing cognitive task conditions (Two Back) against the control task (Is it bird?).

Verbal fluency paradigm

The verbal fluency paradigm contained only one condition and only one contrast against the baseline, *i.e.* rest, was defined.

5.5 Standardized neuropsychological test battery

A battery of standardized tests assessing expressive language and verbal comprehension, verbal and non-verbal learning, as well as several frontal lobe functions was administered to all participants, who had cognitive fMRI. Administered tests and acquired scores are detailed in Table 5.1.

Table 5.1. Neuropsychological Test Battery

Cognitive ability	**Test**	**Score**
Verbal IQ	National Adult Reading Test (NART revised)	IQ points
Verbal Comprehension	Vocabulary and Similarities subscales of the Wechsler Adult Intelligence Scale (WAIS)	raw score
Expressive Language	McKenna Picture naming task	raw score
Verbal Learning	List Learning subtest of the Adult Memory and Information Processing Battery (AMIPB, Coughlan and Hollows, 1985)	sum of raw scores list 1-5
Nonverbal Learning	Design Leaning subtest of the AMIPB	sum of raw scores design 1-5
Psychomotor speed	Trail-Making Test form A (Reitan & Wolfson, 1985)	time (s)
Mental Flexibility	Trail-Making Test (form B-A) (Reitan & Wolfson, 1985)	time (s)
Verbal Fluency	Letter Fluency: “F”, “A”, “S” Category Fluency: “Animals”, “Fruits”, “Vegetables”	average of totalled number of words letter/ category in 1 minute
Working Memory	Digit Span and Arithmetic subtests of the WAIS	sum of raw scores

5.6 Statistical analysis of demographical and behavioural data

Data were analysed using SPSS Statistics Versions 17.0 and 20.0 (IBM).

Prior to statistical analysis, histograms were created to check whether datasets were normally distributed. In addition, Levene's test for homogeneity of variance was employed. Parametric or non-parametric tests were used accordingly. Chi-square tests were applied to categorical data. The level of significance was set at $p < 0.05$.

Chapter 6: fMRI endophenotypes in JME

6.1 Summary

Rationale: JME is a heritable genetic generalized epilepsy syndrome, characterized by myoclonic jerks that are frequently triggered by cognitive effort. Impairment of frontal lobe cognitive functions has been reported in patients with JME and their unaffected siblings. In a recent functional magnetic resonance imaging study we reported abnormal co-activation of the motor cortex and increased functional connectivity between the motor system and prefrontal cognitive networks during a working memory paradigm, providing an underlying mechanism for cognitively triggered jerks.

Methods: In this study, we used the same task in 15 unaffected siblings (10 female; age range 18–65 years, median 40) of 11 of those patients with JME (six female; age range 22–54 years, median 35) and compared functional magnetic resonance imaging activations with 20 age- and gender-matched healthy control subjects (12 female; age range 23–46 years, median 30.5).

Results: Unaffected siblings showed abnormal primary motor cortex and supplementary motor area co-activation with increasing cognitive load, as well as increased task-related functional connectivity between motor and prefrontal cognitive networks, with a similar pattern to patients ($p < 0.001$ uncorrected; 20-voxel threshold extent).

Conclusions: Findings in unaffected siblings suggest that altered motor system activation and functional connectivity is not medication- or seizure-related, but represents a potential underlying mechanism for impairment of frontal lobe functions in patients and siblings, and so constitutes an endophenotype of JME.

6.2 Introduction

Juvenile myoclonic epilepsy (JME) is a common genetic generalised epilepsy syndrome (Berg and Millichap, 2013; Zifkin et al., 2005), characterized by symmetric, myoclonic jerks, mostly affecting upper limbs, generalised tonic-clonic seizures and more rarely absence seizures (Janz, 1985; Kasteleijn-Nolst Trenité et al., 2013). A complex polygenetic aetiology is suspected in most cases (Delgado-Escueta et al., 2013) and clinical genetic studies support a high genetic predisposition: first degree relatives have an increased risk for epilepsy with up to six percent affected, mostly with genetic generalized epilepsy syndromes (Vijai et al., 2003). Reports on high syndrome concordance amongst first-degree relatives of 30% (Marini et al., 2004) and very high monozygous concordance reported by twin studies support a major heritable disease component (Corey et al., 2011; Vadlamudi et al., 2004).

Reflex-mechanisms of seizure precipitation are common in JME, including photic-stimulation but also cognitively triggered jerks by reading, decision-making or planned movement, leading to jerking of the body part, which is engaged in task execution, usually the hand (Guaranha et al., 2009; Koepp et al., 2016; Matsuoka et al., 2000, 2005).

Neuro-behavioural findings of impaired working memory and executive functions (Devinsky et al., 1997; Sonmez et al., 2004; Wandschneider et al., 2012) corroborated evidence from advanced imaging studies for subtle structural and functional changes within the dorsolateral prefrontal and medial frontal lobes and thalamo-fronto-cortical pathways (Koepp et al., 1997; O'Muircheartaigh et al., 2011, 2012; Pulsipher et al., 2009; Savic et al., 2000). In a previous study at our centre (Vollmar et al., 2011, 2012), the interaction of motor and cognitive networks in JME was investigated using an n-back functional MRI (fMRI) task, which assesses visual-spatial working memory with increasing cognitive demand

and also entails a complex motor component (Kumari et al., 2009). Patients with JME showed an abnormal motor-cortex co-activation with increasing task demand during the working memory task. In addition, both functional and structural connectivity were increased between cortical motor areas and dorsolateral prefrontal cognitive networks, and decreased within prefrontal cognitive networks (pre-supplementary motor area to fronto-polar regions), providing a potential underlying mechanism for both cognitively triggered jerks and cognitive impairment in juvenile myoclonic epilepsy. Although a "normalisation" of this altered co-activation with increasing doses of the anti-epileptic drug sodium valproate was observed, it could not be disentangled whether motor system hyperconnectivity to cognitive networks is a disease-underlying mechanism or a consequence of seizures and/or treatment.

Since JME has a high heritability and neuro-behavioural studies in unaffected siblings have described traits of its broader phenotype, such as frontal lobe cognitive impairment (Wandschneider et al., 2010), this study aimed to investigate whether motor system co-activation during a working memory task is an endophenotype of JME. Endophenotypes are manifest in an individual whether or not the condition is active, are heritable and are found more frequently in non-affected family members of diseased individuals than in the general population (Gottesman and Gould, 2003). Since the genetic risk for epilepsy is higher for siblings of JME patients than their offspring or parents and syndrome traits have also been more frequently reported in siblings than in other first-degree relatives, this study focused on investigating unaffected siblings (Jayalakshmi et al., 2006). Index patients and siblings are also more likely to be comparable for age, upbringing and socioeconomic background than patients and other first-degree relatives. The specific hypotheses of this study were, that unaffected siblings of JME patients will show

(1) abnormal fMRI activation patterns compared to healthy controls in previously defined region of interest in the motor cortex of JME patients, and

(2) increased functional connectivity between the motor system and fronto-parietal cognitive networks.

6.3 Methods

6.3.1 Study population

Fifteen unaffected siblings of 11 JME patients participated after contact with the consent of the related JME index patient. Juvenile myoclonic epilepsy patients were either identified from a previous functional MRI study (n = 5) (Vollmar et al., 2011) or recruited from University College London Hospitals epilepsy outpatient clinics (n = 6). Twenty healthy controls were also included (Siblings/patients/controls: 10/6/12 females; age: Siblings: median 40 (IQR: 21) years; patients: 35 (23); controls: 30.5 (7)). Siblings and controls were comparable for age (Mann-Whitney U = 98.500, p = 0.086), gender (Pearson Chi-square p = 0.686) and IQ (Table 6.1).

All index patients had a typical history of JME with myoclonic jerks, generalised tonic-clonic seizures and, in some, absence seizures. Disease onset was in adolescence, EEGs showed generalised polyspike wave complexes and clinical MRI were normal.

Three patients reported movement-related jerks in the active hand: one when playing the guitar and writing down musical notes simultaneously; one when playing the violin or touch-typing on a screen; one patient reported jerks during tasks requiring fine motor skills.

No sibling had ever experienced seizures; except for one who had suffered two clearly provoked (sleep deprivation) generalised tonic-clonic seizures, over 20 years prior to study participation, without any further seizures, and without antiepileptic medication.

In five JME families, other relatives apart from the index patient suffered from epilepsy. There was a family history of febrile convulsions in two cases.

Healthy controls had no history of epilepsy or other neurological disease and no family history of epilepsy.

6.3.2 MRI data acquisition

MRI data were acquired on a GE Excite HDx 3 Tesla scanner (General Electric Medical Systems, Milwaukee, WI, U.S.A) with a multichannel head coil. A 50 slice gradient echo planar imaging sequence was used in axial orientation with 2.4 mm thickness and 0.1 mm gap providing full brain coverage. Slices had a 64 x 64 matrix, voxel size was 3.75 x 3.75 mm. Repetition time was 2500 ms, echo time was 25 ms.

6.3.3 fMRI working memory paradigm

An adaptation of the visual-spatial n-back working memory task was employed (Kumari et al., 2009), as in the previous JME study at our centre (Vollmar et al., 2011). Dots were presented randomly in four possible locations on a screen. Participants responded by moving a joystick with their right hand. They monitored the locations of dots and had to move the joystick to the position of the currently presented dot in the '0 Back' condition or to the position of the dot in the previous presentation (1 Back) or two (2 Back) presentations earlier. Each condition lasted 30 seconds, was repeated five times in a pseudorandom order and alternated with rest blocks of 15 seconds. During the total duration of the paradigm (11 min 20 s), 272 echo planar imaging volumes were acquired.

6.3.4 fMRI processing and analysis

Functional MRI data were analysed with Statistical Parametric Mapping-8 (SPM8, www.fil.ion.ucl.ac.uk/spm). Images were realigned, normalised to an acquisition-specific echo planar imaging template in Montreal Neurological Institute space, resampled to isotropic 3 x 3 x 3 voxels and smoothed with an 8 x 8 x 8 mm kernel.

Single subject statistical analysis was carried out applying a full factorial block design. Movement parameters were entered as regressors of no interest. Task conditions were modelled separately as 30 seconds blocks and convoluted with the SPM canonical haemodynamic response function.

For each subject, contrasts were defined by comparing task conditions against rest and comparing task conditions with working memory load ('1 Back' and '2 Back') against the control task (0 Back). Hence by controlling for motor response and visual attention, only cortical activation due to the working memory load was revealed.

Subjects with fMRI activation of at least $p > 0.05$ uncorrected at single subject level for the relevant contrasts were included into the second level analyses.

At the second level, one sample t-tests were employed to explore group effects. Group comparisons were then carried out employing two-sample t-tests or a full factorial design. The level of significance was set at $p < 0.001$ uncorrected with an extent threshold with minimum cluster size of 20 voxels (Lieberman and Cunningham, 2009). Where appropriate, performance during the n-back task was entered as a regressor of no interest.

Functional MRI results were rendered on a 3D surface previously created from the Montreal Neurological Institute_152_T1 data set (Vollmar et al., 2011).

6.3.5 Independent component and functional connectivity analyses

An independent component analysis was carried out using MELODIC from the FMRIB software library (FSL, http://www.fmrib.ox.ac.uk/fsl/) to identify different network components.

A 4D file of the realigned, normalised and smoothed images was created for each subject. Image data were prefiltered with a high-pass filter with a cut-off at 100 s. The algorithm was restricted to identify 32 components common across all subjects. Motor and working memory components were visually identified at the group level. Individual timeseries for each component were extracted for each subject using Dual Regression (Filippini et al., 2009).

Subsequently, for each subject and each component, connectivity maps were generated by regressing the timeseries in a general linear model including movement parameters as regressor of no interest. Group comparisons were carried out employing two-sample t-tests or a full factorial design.

6.3.6 Behavioural data

All participants underwent a standardized neuropsychological assessment. The Nelson Adult Reading Test was used as an index of intellectual level (Nelson, 1982). The Vocabulary and Similarities subtests from the Wechsler Adult Intelligence Scale III were used to measure verbal comprehension and the Digit Span and Mental Arithmetic subtests from the same scale provided a measure of working memory. Expressive language functions were measured using the Graded Naming Test (McKenna and Warrington, 1983). The List Learning and Design Learning Subtests from the Adult Memory and Information Processing Battery measured verbal and visual learning respectively (Baxendale et al., 2008). The Trail Making Test provided a measure of psychomotor speed (Trail Making A) and mental flexibility (Trail Making B-A). Participants also completed measures of letter and category fluency.

6.3.7 Statistical analysis of clinical and behavioural data

Behavioural and clinical data were analysed using SPSS Statistics Version 20.0 (IBM). Mann-Whitney U Test was applied to non-parametric data and Chi-square tests to categorical data. The level of significance was set at $p < 0.05$.

6.4 Results

6.4.1 Dot-back task performance

Both, siblings and healthy controls performed equally well during the '0 Back' condition (success rate median (IQR) siblings: 95 (10)%; controls: 93 (11); Mann-Whitney U = 143.000, p = 0.831). However, siblings performed worse in the '1 Back' (Siblings: 77 (43), controls: 92.5 (11.75); Mann-Whitney U = 82.000 p = 0.023) and '2 Back' condition (Siblings: 55 (41), controls: 88 (31.5); Mann-Whitney U = 69.500, p = 0.006). Performance measures were therefore entered as regressors of no interest in the fMRI group comparisons.

6.4.2 Performance on standardised neuropsychometry

There were no significant group differences in performance on the neuropsychological test battery. The results are detailed below in Table 6.1.

Table 6.1. Neuropsychological test results

Cognitive measures	controls Median (IQR)	siblings Median (IQR)	Statistical analysis* U	*p*
IQ				
NART	110 (10)	107 (19)	71.500	0.574
WAIS-III (raw scores)				
Verbal Comprehension				
Vocabulary	50 (21)	49 (24)	73.000	0.935
Similarities	26.5 (12)	24 (5)	51.000	0.196
Working Memory				
Digit Span	17 (6)	20 (5)	43.000	0.080
Arithmetics	14 (10)	14 (7)	68.000	0.862
Expressive Language				
Graded Naming Test	23 (5)	23 (7)	64.500	0.567
Verbal Learning				
List Learning (AMIPB) (Trials 1-5)	56 (13)	56 (6)	46.000	0.215
Nonverbal Learning				
Design Learning (AMIPB) (Trials 1-5)	40 (11)	36 (11)	60.500	0.152
Psychomotor speed				
Trail Making Test A (seconds)	25 (15)	25 (13)	66.000	0.413
Mental flexibility				
Trail Making Test time B-A (seconds)	19 (13)	23 (18)	49.500	0.235
Verbal fluency				
categorical fluency	18 (3)	18 (5)	60.000	0.808
letter fluency	14 (5)	14 (4)	82.000	0.862

*The Mann-Whitney U Test was applied for behavioural measures. All variables are reported as raw items, except for Trail Making Test (time in seconds) and verbal IQ points. AMIPB: The Adult Memory and Information Processing Battery; NART: National Adult Reading Test; WAIS: Wechsler Adult Intelligence Scale

6.4.3 fMRI group effects siblings and controls

In the ‘0 Back’ condition, due to the right hand motor-response all subjects showed a left central and bilateral supplementary motor area activation (Figure 6.1 A). By controlling for motor response and subtracting ‘0 Back’ from ‘1 Back’ and ‘2 Back’, cortical activations due to working memory were isolated. All participants showed significant bilateral prefrontal and parietal working memory network activation (Figure 6.1 A-C).

6.4.4 fMRI group differences between siblings and controls

There were no group differences detectable during the ‘0 Back’ condition (Figure 6.1 D). However, in the ‘1 minus 0 Back’ contrast, there was a significant difference in activation patterns between siblings compared to controls within the region of interest, the motor cortex. The effect became more prominent and extended to the supplementary motor area with increasing cognitive demand in the ‘2 minus 0 Back’ contrast.

To disentangle whether the differences between siblings and controls observed were due to an increase of the task-positive network or an impaired deactivation of the task-negative network in siblings relative to controls, we masked the results either by group effects of the task-positive (‘2 minus 0 Back’) or task-negative network (‘0 minus 2 Back’) for controls (Figure 6.1 E, F). Areas of difference corresponded to the task-negative network in controls. Hence the effect observed in the motor system in siblings is due to impaired deactivation of this area with increasing working memory load. There were no areas of greater activation in controls compared to siblings.

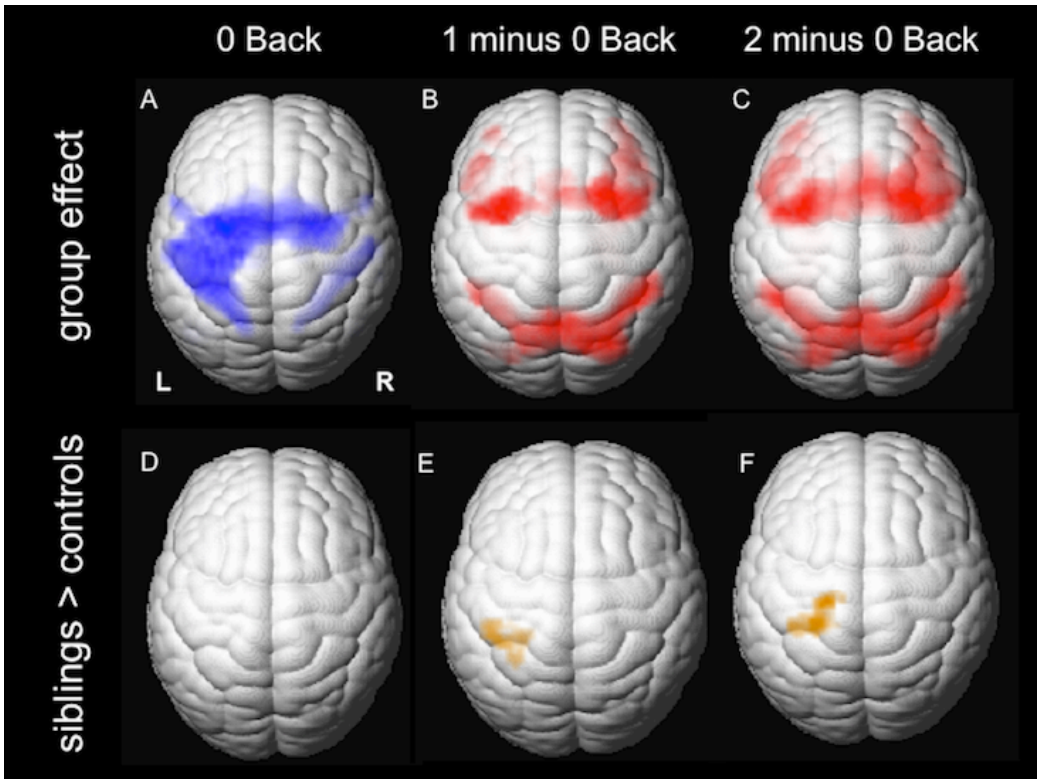

Figure 6.1. Group fMRI activation from working memory and group differences. Group fMRI activation maps from JME siblings and healthy controls (A-C) show cortical activation for the three different task conditions: motor cortex and supplementary motor area for '0 Back' (A), bilateral frontal and parietal activation for '1 minus 0 Back' and '2 minus 0 Back' (B, C).

Lower row (D-F), activation patterns in siblings compared to controls (inclusively masked for task-dependent deactivation maps of healthy controls (p < 0.001 uncorrected; 20 voxel threshold extent)): no difference for the '0 Back' condition (D), but attenuated deactivation in the motor cortex (E) and the supplementary motor area (F) with increasing task demand in the working memory contrasts was seen.

6.4.5 Areas of task-related deactivation in siblings and controls

To further explore group differences secondary to impaired deactivation in siblings, group maps of the task negative network are displayed in Figure 6.2. Whereas controls deactivate the primary motor cortices with increasing cognitive task demand, as well as areas in the default mode network, *i.e.* precuneus and

medial frontal and orbitofrontal areas, the group effect in siblings shows less deactivation in these areas.

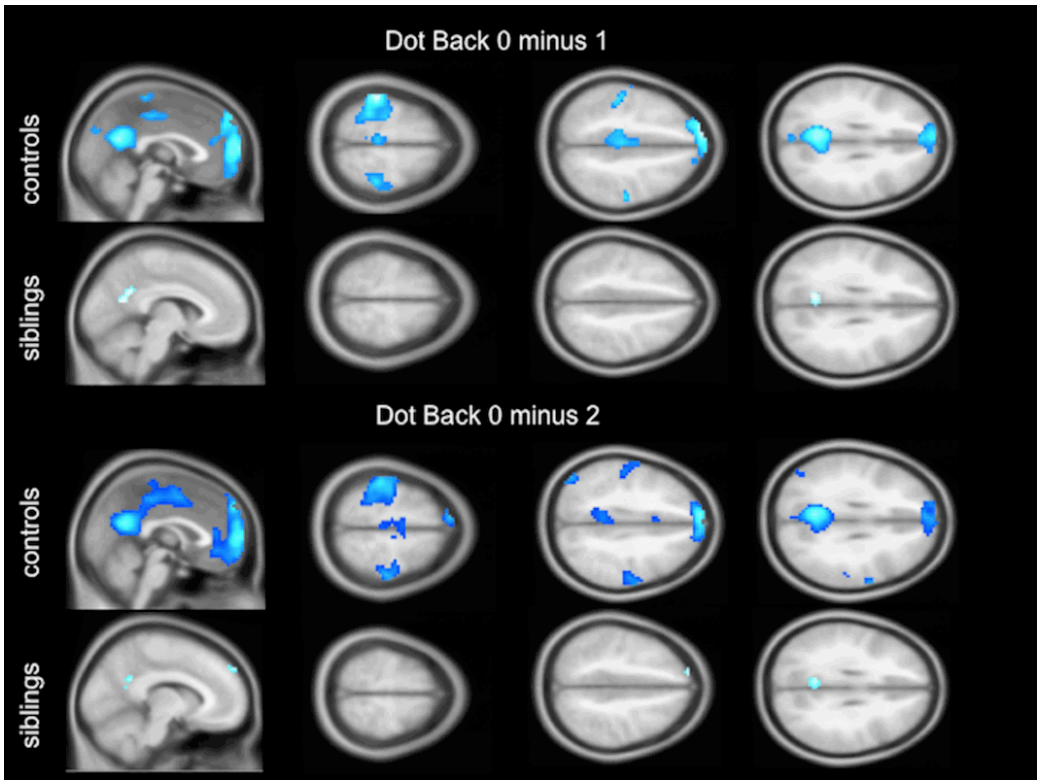

Figure 6.2. Group effect of task-dependent deactivation in controls and siblings for the two negative working memory contrasts ('Dot Back 0 minus 1', 'Dot Back 0 minus 2'). In controls, the task negative contrast shows bilateral deactivation of the motor cortex and supplementary motor area with increasing task demand, as well as deactivation of the precuneus and medial prefrontal areas (default mode network). Less group deactivation effects in these areas are observed in siblings ($p < 0.001$ uncorrected; 20 voxel threshold extent)

6.4.6 fMRI group differences and differences in task performance

To control for performance effects, in addition to treating performance as a confounder of no interest, a post-hoc group comparison between contrasts '1

minus 0 Back' in siblings and '2 minus 0 Back' in controls were performed, since controls' performance accuracy in the '2 Back' condition was comparable to siblings' accuracy in the '1 Back' condition (success rate median (IQR) siblings '1 Back': 77 (43) %; controls '2 Back': 88 (31.5); Mann-Whitney U = 121.000, p = 0.347), (Figure 6.3). As in the previous analysis, siblings show an attenuated deactivation of the motor areas and parts of the default mode network. There were no areas of greater activation in controls compared to siblings.

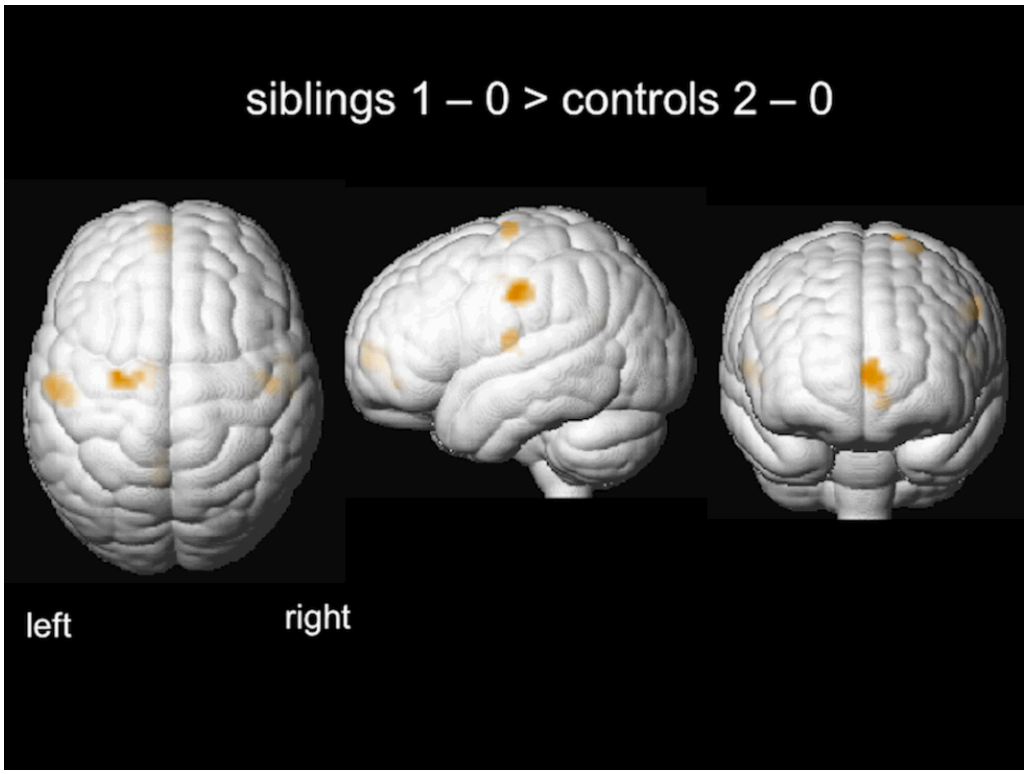

Figure 6.3. **Post hoc group comparisons of fMRI activation patterns during comparable working memory task performance**. Siblings' performance accuracy during the '1 Back' was comparable to controls' performance during '2 Back' condition. There was attenuated deactivation in the bilateral lateral primary motor cortex and left supplementary motor area, as well as in the left medial prefrontal cortex for '1 minus 0 Back' in siblings compared to '2 minus 0 Back' in controls (p < 0.005 uncorrected; 20 voxel threshold extent; inclusively masked for areas of task-related deactivation in controls). There were no areas of higher activation in controls.

6.4.7 fMRI group differences between patients, siblings and controls

Contrast images for '1 minus 0 Back' and '2 minus 0 Back' of siblings, controls and the 11 JME index patients were entered in a full-factorial design with group as factor.

Performance accuracy was different between the three groups for the '2 Back' performance (Kruskal-Wallis Test: '0 Back' $X^2 = 0.337$, $p = 0.845$; '1 Back' $X^2 = 5.757$, $p = 0.056$; '2 Back' $X^2 = 8.178$, $p = 0.017$). Post-hoc group comparisons showed that these performance differences were due to siblings performing worse than controls, with JME patients' performance accuracy being comparable to controls' and siblings' '2 Back' performance (patients vs. controls: Mann-Whitney U = 72.000, $p = 0.123$; patients vs. siblings: Mann-Whitney U = 56.500, $p = 0.180$).

Performance scores were entered as regressors of no interest. There were no differences in activations between JME patients and siblings for either working memory contrasts (not shown). In a conjunction analysis of areas activating in both JME patients and siblings more than controls, common areas of significant activations in the left primary motor cortex were identified (Figure 6.4).

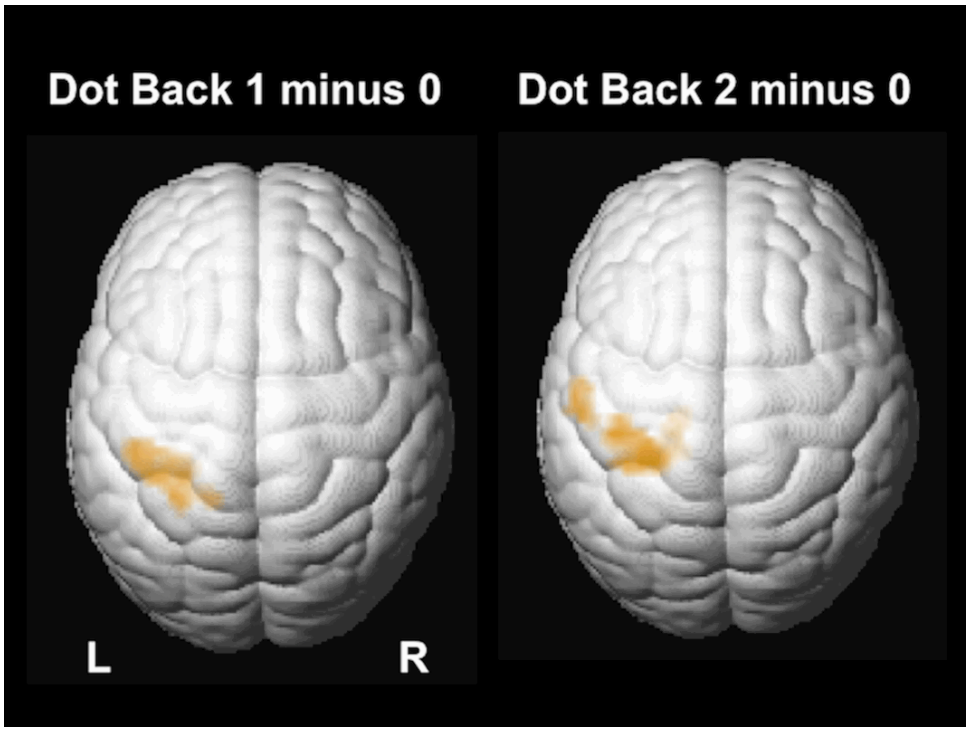

Figure 6.4. Conjunction analysis. In a conjunction analysis of patients greater than controls and siblings greater than controls for 'Dot Back 1 minus 0' and 'Dot Back 2 minus 0', patients and their siblings share significant areas of co-activation in the left motor cortex when compared to controls. (conjunction, $p < 0.005$ uncorrected; 20 voxels threshold extent)

To control for the effect of age, we performed a post-hoc group comparison and entered age as additional regressor of no interest, which did not change overall results (Figure 6.5). In subgroup analyses in patients and siblings, we correlated activation patterns during the '2 minus 0 Back' and '1 minus 0 Back' contrasts with age. This did not show an effect within the region of interest, the left primary motor cortex and supplementary motor area (data not shown).

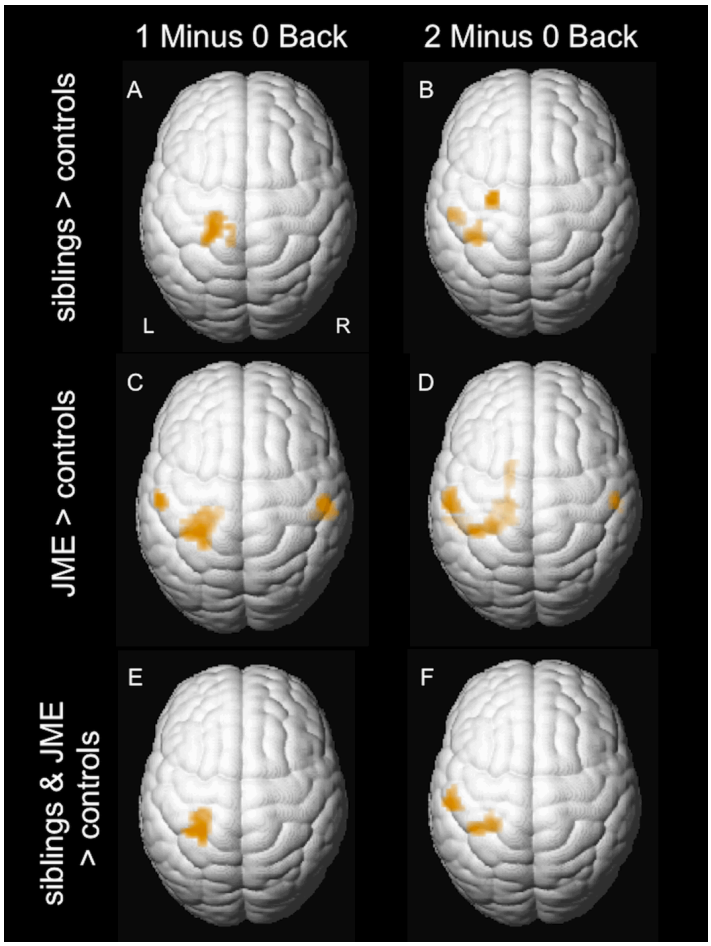

Figure 6.5. Post hoc group comparisons of fMRI activation patterns after correcting for age.

Age was entered as additional nuisance variable into the model. Siblings compared to controls (A, B) showed attenuated deactivation in the motor cortex and SMA with increasing task demand in the working memory contrasts ($p < 0.001$ uncorrected; 20 voxel threshold extent).

At a lower threshold ($p < 0.005$ uncorrected; 20 voxel threshold extent), attenuated deactivation is seen in similar regions in JME patients when compared to controls (C, D).

In a conjunction analysis of patients greater than controls and siblings greater than controls for the two working memory contrasts (E, F), patients and their siblings share significant areas of co-activation in the left motor cortex. (conjunction, $p < 0.005$ uncorrected; 20 voxels threshold extent)

Maps were inclusively masked for task-dependent deactivation maps of healthy controls.

6.4.8 Functional connectivity

From the 32 independent components identified by independent component analysis, two components of interest were chosen for further group comparisons (Figure 6.6): The component located in the left central region and representing the motor response (Figure 6.6 A) and the component comprising the bilateral prefrontal and parietal working memory network (Figure 6.6 C).

Compared to controls, JME siblings showed increased functional connectivity of the left motor cortex and supplementary motor area to the dorsolateral prefrontal and superior parietal cortex, which are part of the working memory network (Figure 6.6 B). Functional connectivity analysis of the working memory component showed increased connectivity to bilateral motor cortices in siblings than controls (Figure 6.6 D). There were no areas of higher connectivity in controls for these two components.

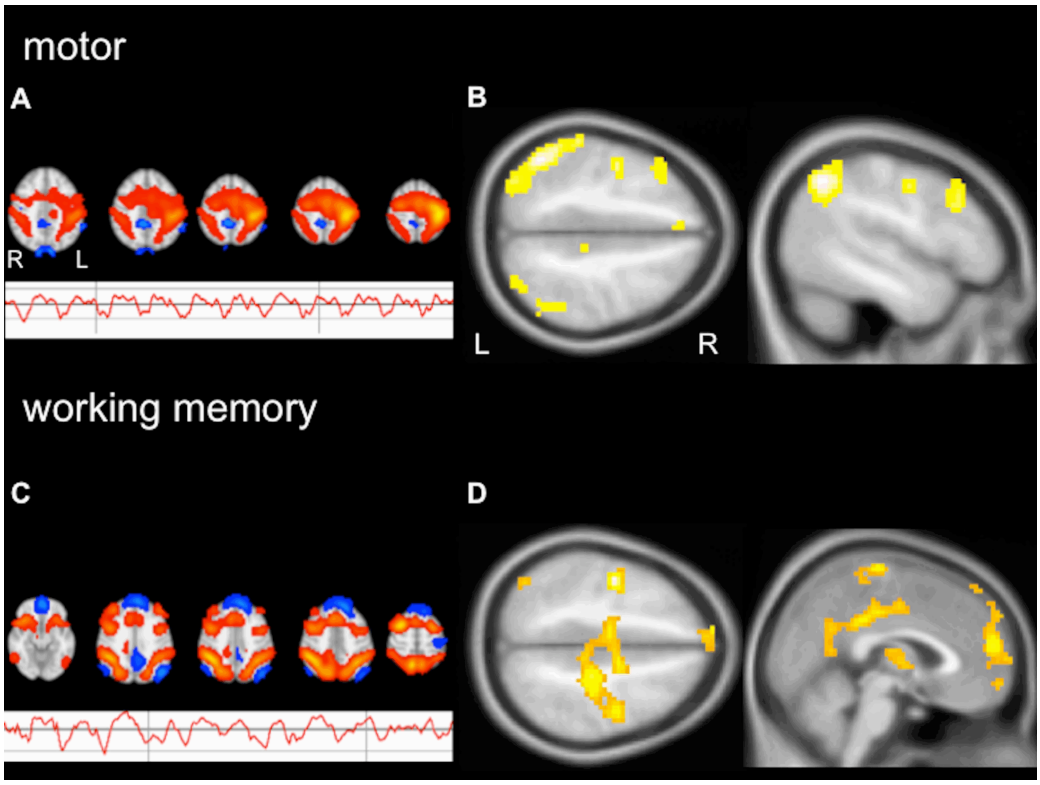

Figure 6.6. Group independent component analysis and functional connectivity in siblings compared to healthy controls. A: This figure shows the motor network component common to all subjects (FSL figure) and its corresponding group average signal time course during the experiment. The signal time course for the motor component shows constant response amplitude throughout the different task paradigms (0, 1 and 2 Back and rest). **B:** Group comparison of functional connectivity patterns in siblings and healthy controls are demonstrated for the motor component. Siblings show increased connectivity to fronto-parietal cognitive networks when compared to controls ($p < 0.005$; 20 voxels threshold extent). There were no areas of increased connectivity in controls. **C**: The working memory network component common to all subjects is demonstrated (FSL figure). Its corresponding group average signal time course is modulated by task demand and shows increased activation with higher cognitive demand during the actual working memory conditions (1 and 2 Back). **D**: Group comparison of functional connectivity patterns in siblings and healthy controls for the working memory component shows increased connectivity to central motor areas, as well as the medial prefrontal cortex as part of the default mode network (D; $p < 0.001$; 20 voxels threshold extent). There were no areas of increased connectivity in controls.

6.5 Discussion

This study showed co-activation of the primary motor cortex and supplementary motor area during a functional MRI working memory task in unaffected siblings of JME patients, similar to patterns seen in JME (Vollmar et al., 2011). In controls, we observed a relative attenuation of activations in the motor cortices with increasing task demand. In JME patients and siblings, motor areas remained co-activated with task-positive working memory networks, resulting in increased functional connectivity between the motor system and fronto-parietal cognitive networks.

6.5.1 Functional endophenotypes of JME

Using a conjunction analysis of working memory activation, we identified common areas of impaired attenuation of task-negative networks within the motor cortex for both patients and siblings. We conclude that motor cortex co-activation is not a consequence of seizures or medications. This supports the hypothesis that there is a heritable component of the disease, and represents an endophenotype of JME, defined as an intermediate phenotype that appears to be more frequently present in non-affected family members than in the general population. Since siblings do not suffer from seizures, this finding is clearly not solely an association with the full JME phenotype. However, in view of its regional specificity our finding is very likely to be related to pathomechanisms of the disease with its particular seizure type, *i.e.* motor seizures, and fronto-cortical cognitive dysfunction. This is corroborated by studies showing a modulation of motor cortex co-activation by disease severity and treatment (Vollmar et al., 2011). In a recent twin study (Blokland et al., 2011), fMRI activation patterns during the n-back working memory task have been shown to be significantly heritable and regions of interest identified here, *i.e.* the precentral gyrus and

supplementary motor area, have been among the regions with the highest heritability estimates. Thus, seizures and neuro-behavioural comorbidities may share this underlying functional mechanism. Longitudinal studies and imaging studies in recent onset genetic generalized epilepsies, as well as JME, identified subcortical and fronto-cortical abnormalities, which relate both to seizures and neuro-behavioural comorbidities (Pulsipher et al., 2009; Tosun et al., 2011). Some behavioural studies in genetic generalized epilepsies identified cognitive impairment even prior to disease onset (Hermann et al., 2012), suggesting that epilepsy and its comorbidities may reflect different degrees of disease with a shared underlying pathological condition, which may be a genetically determined neurodevelopmental dysfunction (Helmstaedter et al., 2014).

Previous imaging studies of unaffected siblings have been conducted mainly in schizophrenia and autism to control for the effect of disease severity and treatment and to identify potential imaging endophenotypes (Callicott et al., 2003; Spencer et al., 2012). Like JME, these are considered highly heritable, neurodevelopmental conditions with neuro-behavioural characteristics, which extend beyond the cardinal disease features and are frequently found in non-affected relatives. Such endophenotypes are intermediate biological phenotypes associated with the disease in the population, which are more closely related to the genotype than the final phenotype, increasing the yield for identifying susceptibility genes (Callicott et al., 2003). Studying the physiological mechanisms underlying neuro-behavioural impairments in unaffected siblings may help to understand biological effects of susceptibility genes (Callicott et al., 2003).

Statistical analyses of the blood oxygen level dependent contrast at single subject level do not directly reflect a quantitative measure of activation and findings at group level cannot be easily used to quantify activation at a single subject level. In the first instance, this would involve studying large cohorts to

establish quantitative normative data of task-related activation. Therefore, it is unlikely that one would be able to conclude from the scan data in one subject whether the trait is present or not in that individual. However in schizophrenia, results from functional MRI group analyses have been used successfully in a probabilistic approach for gene discovery in conjunction with genome-wide association (Potkin et al., 2009), whilst imaging studies in siblings of patients with epilepsy are rare (Scanlon et al., 2013). Analysis of a quantitative imaging trait in affected families, like motor cortex co-activation, may increase the yield of genetic studies for identifying culprit genes for JME, which so far has proven difficult.

A recent transcranial magnetic stimulation study in individuals with generalised and focal epilepsies and their asymptomatic siblings reported cortical hyper-excitability in the asymptomatic siblings compared to healthy controls, which was more prominent in generalised epilepsy syndromes. The cortical excitability profile in asymptomatic siblings was similar to those in patients. Only drug naïve new onset JME patients had a lower motor threshold, *i.e.* higher excitability, than their asymptomatic siblings. (Badawy et al., 2013)

To identify whether motor cortex co-activation is more prominent in patients with JME, we carried out a group comparison of JME patients and siblings, which did not show an effect. This may be a false negative finding due to the relatively small sample of 11 index patients. An alternative explanation for the lack of a difference could be that motor system co-activation “normalised” with high doses of Valproate (Vollmar et al., 2011) and was less prominent in our cohort of 11 patients: all were on medication with seven out of 11 on Valproate; six patients were seizure-free and none of the patients reported daily jerks.

To further investigate whether motor cortex co-activation is more prominent in patients than siblings, drug-naïve JME patients have to be studied (Badawy et al., 2013).

In a post-hoc analysis, our findings survived a further correction for age. Disease onset during adolescence coincides with an important phase of brain development. Normal cortical maturation involves thickening or thinning of grey matter during childhood and adolescence, following different developmental trajectories depending on the cortical region and neural system. Grey matter thinning may be associated with synaptic pruning, apoptosis and ongoing myelination, and has been correlated with cognitive and behavioural development. (Jernigan et al., 2011) Decrease in grey matter first involves primary sensorimotor cortices, then secondary and eventually multimodal cortices during late adolescence, such as the dorsolateral prefrontal cortex (Shaw et al., 2008). However, there is also evidence for continuous developmental changes in primary cortical areas during late adolescence (Giorgio et al., 2010). These crucial processes of cortical brain maturation and functional refinement may be implicated in JME. Mutations in one causative candidate gene, *EFHC1*, have recently been linked to alterations of several neural development steps, including migration, connection formation and apoptosis, the latter potentially leading to maintenance of hyperexcitable neurons (de Nijs et al., 2013). There is some evidence from longitudinal structural imaging studies in children with idiopathic epilepsy compared to controls describing disrupted patterns of brain development, mainly implicating prefrontal and parietal cortices (Tosun et al., 2011). Therefore, aberrant activation patterns may be more prominent in younger subjects. However, this effect was not seen in a subgroup correlation analysis (Figure 6.5). Considering that all our patients, and most of the siblings were older than adolescence (patients: age range 22 to 54 years; siblings: 18 to 65 years), this may be a false negative finding and a

potential age effect should be explored in future, preferably recent onset cohorts.

6.5.2 Abnormal fMRI activation patterns are markers of dysfunction

Motor system co-activation appears to be not only a disease marker, but is related to cortical network dysfunction. In our previous studies, we suggested that motor cortex co-activation with functional hyper-connectivity and increased microstructural connectivity between the prefrontal cognitive cortex (pre-supplementary motor area) and motor system is a potential underlying mechanism of cognitively triggered jerks and frontal lobe impairment in JME (Vollmar et al., 2011). Connectivity between the pre-supplementary motor area region and the fronto-polar cortex was reduced, providing an explanation for impaired frontal lobe functions in JME. In addition, thalamic inhibition of the supplementary motor area and premotor cortex has been shown to be decreased in association with reduced structural connectivity within thalamo-cortical motor control circuits which leads to alteration of task-modulated functional connectivity with subsequent impairment of frontal lobe functions (O'Muircheartaigh et al., 2012). The effect appeared more prominent in patients with persisting seizures. Likewise, impairment in experienced-related learning and impulsive decision making have been directly related to increased supplementary motor area activation in treatment refractory JME patients (Wandschneider et al., 2013).

Comparative studies of patients and controls however have failed to disentangle whether structural and functional changes are part of disease-underlying mechanisms or consequence of seizures and/or treatment. In our current study, we control for the impact of seizures and medication by studying unaffected

siblings. Similar findings in affected and unaffected family members support the contention that altered structural and functional cortico-cortical connectivity is part of the genetically determined disease-underlying mechanisms. To compare our current with previous findings in JME patients, task-related, but not resting-state functional connectivity was assessed. In a recent meta-analysis of over 7000 functional maps the main explicit activation networks were identified and compared to those identified in 36 subjects during resting state functional MRI (Smith et al., 2009). Major covarying network components of the task-related analysis were very similar to those in the resting brain (Laird et al., 2011). A task-related functional connectivity analysis approach appears appropriate in JME, since symptoms become more apparent during certain activities or with increasing cognitive demand.

As in patients, unaffected siblings show increased functional connectivity between working memory networks and motor systems and vice versa. Siblings demonstrate this imaging trait, but they do not experience seizures, which indicates that additional environmental and/or genetic factors are necessary to develop the full JME phenotype. On the other hand, motor cortex co-activation and hyper-connectivity may not only be a genetic marker but may be associated with disease traits in siblings. Previous studies have shown subtle frontal lobe impairment in unaffected JME siblings (Levav et al., 2002; Wandschneider et al., 2010), especially when performing a cognitively challenging task which required integration of several frontal lobe functions (Wandschneider et al., 2010). In the current study, siblings performed less well on the highly demanding fMRI working memory task, although they do equally well on the standardized neuropsychological test battery. Hence altered task-related functional connectivity between motor and cognitive networks demonstrated in this study

may be responsible for subtle cognitive impairments in siblings that are similar to those in patients.

6.5.3 Impaired task-related deactivation of motor systems

Motor cortex co-activation in siblings and patients compared to controls was due to attenuated deactivation of the motor systems. Group effects of task-related deactivations showed deactivation of areas of the motor cortex in controls, but to a lesser degree in siblings (Figure 6.2). In patients, an independent component analysis previously identified a “modulated motor” component during the n-back working memory task, which demonstrated that, similarly to the working memory component here (Figure 6.6), the motor component was modulated with increasing working memory task demand (Vollmar et al., 2011). In the current cohort, functional connectivity in siblings was increased between working memory networks and areas, which were deactivated in controls, *i.e.* motor cortices and the medial prefrontal cortex as part of the default mode network. Due to increased functional coupling of cognitive and motor networks in JME patients and their unaffected siblings, functional segregation of motor areas from task-active cognitive networks and their deactivation during a highly demanding working memory task may be impaired, which may account for the poorer performance in siblings during the fMRI working memory task in this study.

6.5.4 Limitations

Interictal epileptic discharges have been reported in up to 27% of unaffected siblings of JME patients (Atakli et al., 1999) and may therefore be also present in

our sibling cohort. A recent sibling study (Iqbal et al., 2009) controlling for interictal epileptic activity by performing video EEG recordings prior to and during neuropsychological assessment reported subtle cognitive impairment in siblings and patients independently of interictal epileptic discharges. Given the low sensitivity to detect interictal epileptic discharges routine EEGs were not performed in siblings for this study. We also postulate that fMRI is a far more sensitive tool to detect subtle neuronal dysfunction in clinically unaffected individuals and this has already been achieved in previous cognitive functional MRI studies despite the absence of impairment on routine neuropsychological tests (Spencer et al., 2012; Vollmar et al., 2011).

One of the siblings had experienced two seizures more than 20 years prior to study participation. However, these seizures were clearly provoked. There was no evidence of further unprovoked seizures and no antiepileptic medication had been taken. As affected participants were defined as individuals with recurrent unprovoked seizures, this participant was not excluded from the study. Excluding this dataset from the analysis did not alter the overall results.

6.5.5 Conclusion

Attenuated deactivation of the motor system and increased functional connectivity between fronto-parietal cognitive networks and the motor cortex occurred both in JME patients and their unaffected siblings during a functional MRI working memory task. Our findings most likely reflect an imaging endophenotype of JME, representing the shared underlying genetic risk of JME in both disease-affected and -unaffected siblings, and therefore providing a potential biomarker for future genetic imaging studies.

Chapter 7: The effect of Levetiracetam on fMRI working memory activations in temporal lobe epilepsy

7.1 Summary

Rationale: We used functional MRI and a left-lateralising verbal and a right-lateralising visual-spatial working memory (WM) paradigm to investigate the effects of Levetiracetam (LEV) on cognitive network activations in patients with drug-resistant temporal lobe epilepsy (TLE).

Methods: In a retrospective study, we compared task-related fMRI activations and deactivations in left (53) and right (54) TLE patients treated with or without LEV. In patients on LEV, activation patterns were correlated with the daily LEV dose.

Results: We isolated task- and syndrome-specific effects. Patients on LEV showed normalisation of functional network deactivations in the right temporal lobe in right TLE during the right-lateralising visual-spatial task and in the left temporal lobe in left TLE during the verbal task. In a post-hoc analysis, a significant dose-dependent effect was demonstrated in right TLE during the visual-spatial WM task: the lower the LEV dose, the greater was the abnormal right hippocampal activation. At a less stringent threshold ($p < 0.05$, uncorrected for multiple comparisons), a similar dose effect was observed in left TLE during the verbal task: both hippocampi were more abnormally activated in patients with lower doses, but more prominently on the left.

Conclusions: Our findings suggest that LEV is associated with restoration of normal activation patterns. Longitudinal studies are necessary to establish whether the neural patterns observed here translate to drug-response.

7.2 Introduction

Anti-epileptic drugs suppress seizures, but also cause cognitive and behavioural impairment. How AEDs affect specific epileptogenic and cognitive networks is poorly understood (Loring et al., 2011). In the first pharmacological fMRI study in epilepsy, a correlation between Carbamazepine (CBZ) levels and memory retrieval-related fMRI activations within the mesial temporal lobes was observed, which may explain the negative effect of CBZ on cognitive function (Jokeit et al., 2001). We showed recently that patients with temporal lobe epilepsy (TLE) due to unilateral hippocampal sclerosis failed to deactivate the diseased hippocampus with increasing cognitive demands during an n-back working memory task (Stretton et al., 2012). Failure to deactivate the hippocampus was associated with poor performance (Cousijn et al., 2012; Stretton et al., 2012). Using the same working memory paradigm, we observed a valproate (VPA) dose-dependent "normalisation" of impaired de-activation within the motor system in patients with juvenile myoclonic epilepsy (JME) (Vollmar et al., 2011).

Akin to VPA in genetic generalised epilepsies (GGE), Levetiracetam (LEV) is one of the most prescribed AEDs in focal epilepsies, and considered to be particularly efficacious with a positive cognitive side-effect profile (Helmstaedter and Witt, 2010; Schiemann-Delgado et al., 2012).

The aim of this retrospective study was to assess the effect of LEV on fMRI de-activation patterns during working memory tasks in TLE patients. We hypothesized that patients treated with LEV show greater de-activation within temporal lobe epileptogenic networks compared to those not on LEV.

7.3 Methods

7.3.1 Study population

A total of 107 patients with medically refractory TLE (53 left TLE, 59 on LEV) undergoing presurgical evaluation at the National Hospital for Neurology and Neurosurgery were included in this study. For further demographic and clinical characteristics see Table 7.1.

Fifty-nine patients (30 left TLE) were treated with LEV in combination with other AEDs, the most frequent being Carbamazepine (CBZ; Left TLE LEV +/- CBZ 11/11; right TLE 12/8) and Lamotrigine (LTG; left TLE LEV +/- LTG 8/10; right TLE 9/8).

Across groups, there was an equal distribution of Topiramate (TPM) and Zonisamide (ZNS) co-medication, which are known to have potential cognitive side effects (TPM: X^2=2.845, p=. 416; ZNS: X^2 = 3.009, p = 0.390). All patients had a structural 3T MRI and video-EEG to confirm side of seizure onset.

Hippocampal sclerosis (HS) was the most frequent pathology, in particular in left TLE patients on LEV (X^2=5.618, p = 0.019, see Table 7.2 for further details on pathologies).

7.3.2 MRI data acquisition and fMRI paradigms

MRI data were acquired on a GE Excite HDx 3T scanner with a multichannel head coil. A modified version of the n-back task was used for a visual-spatial and verbal WM paradigm. In the visual-spatial task, dots were presented randomly in four locations on a screen (Kumari et al., 2009). Participants monitor the locations of dots at a given delay of the original occurrence (0, 1, or 2 Back) and responded by moving a joystick corresponding to the location of the

current/previously presented dot. In the verbal n-back task, a sequence of words was randomly presented on a screen. During the control condition (“Is-it-bird?”), participants had to respond using a joystick whenever they read the word “bird”. During the actual working memory condition, participants had to indicate whenever a word had only been displayed two presentations earlier (“2 Back”). For more details see the Common Methods Chapter 5.4.1 and 5.4.2.

Table 7.1. Demographic and clinical parameters

	Left TLE		Right TLE		Analysis		
Clinical parameters	on LEV (n= 27)	no LEV (n= 26)	on LEV (n= 29)	no LEV (n= 25)	X^2	df	*p*
Gender female	14	14	23	17	6.35	3	.096
age in years	38 (19)	40 (20)	39 (15)	40 (22)	.648	3	.885
disease duration in years	17 (22)	16 (26)	16 (23)	17 (20)	1.737	3	.629
Seizure frequency							
SPS per month	0 (1.6)	0 (4)	0 (2.5)	0 (8)	1.086	3	.780
CPS per month	4 (7)	6 (14)	2.5 (11)	6 (9)	4.250	3	.236
GTCS per year	0 (1.75)	0 (0)	0 (0)	0 (0.5)	2.144	3	.543
Number of patients with mesial temporal seizure semiology	20	16	20	14	2.979	3	.395
number of current AEDs	2.5 (2.0)	3.0 (2.0)	3.0 (2.0)	3.0 (3.0)	6.240	3	.100

Number of previous AEDs	2 (2)	5 (4.5)	2 (3)	5 (4.5)	16.581	3	.001

All variables except gender are shown as median (IQR). Chi-Square test was employed for gender and seniology, and Kruskal-Wallis test for all other variables. AED = antiepileptic drug; CPS = complex partial seizure; GTCS = generalised tonic-clonic seizure; LEV = levetiracetam; SPS = simple partial seizure; $p < 0.05$

Post-hoc group comparisons revealed that the significant difference in number of previous AEDs is due to patients on LEV having had fewer previous AED than those without LEV (Mann-Whitney U = 706.000; $p < 0.001$).

Table 7.2. Distribution of pathologies

	Left TLE		Right TLE		Analysis		
Type of pathology	on LEV n = 30	no LEV n = 23	on LEV n = 29	no LEV n = 25	X^2	df	*p*
HS	23	11	13	9	11.978	3	.007
HS + cavernoma	0	0	1	0	3.271	3	.352
HS + FCD	0	0	0	1	2.680	3	.444
HS + DNET	1	0	0	0	2.680	3	.444
DNET	2	3	3	1	1.486	3	.686
FCD	0	2	0	0	7.356	3	.061
cavernoma	1	1	4	1	3.363	3	.339
other	2	2	4	6	3.965	3	.265
MRI negative	0	4	4	7	8.929	3	.030

DNET= dysembryoplastic neuroepithelial tumor; FCD= focal cortical dysplasia; HS= hippocampal sclerosis; LEV= levetiracetam; TLE= temporal lobe epilepsy $p < 0.05$

Post-hoc group comparisons revealed that a significant difference in number of patients with HS is caused by left TLE patients on LEV being more likely to have HS than all other groups (LTLE on LEV vs. RTLE on LEV: X^2=7.323, p = 0.007; LTLE on LEV vs. LTLE without LEV: X^2=5.618, p = 0.019; LTLE on LEV vs. RTLE without LEV: X^2=10.431, p = 0.001). The difference in MRI negative cases is mainly driven by the difference between patients with RTLE without LEV and LTLE on LEV (X^2=9.329, p = 0.003).

7.3.3 fMRI processing and analysis

A-priori models were chosen with regard to our experimental design. Models were estimated using a general linear model (GLM) implemented in SPM8 (www.fil.ion.ucl.ac.uk/spm). The GLM then estimated which voxels with greater change in blood oxygenation dependent (BOLD) signal fit which condition specified in the model, *i.e.* the BOLD signal was the outcome variable.

Both tasks were of a blocked design and modelled at a single-subject level using a box-car function for each of the conditions. We created contrast images for each subject to explore the patterns of activation and deactivation in both tasks. For the task-related activations, contrasts comparing the most difficult WM condition with the control task were generated (”2 minus 0 Back” and “2 Back minus Is-it-bird?”). For task-related deactivations, we used the opposite contrasts (”0 minus 2 Back” and “Is-it-bird? minus 2 Back”). We excluded nine patient data-sets due to lack of deactivation.

To explore task specific effects of LEV at a group level, a full-factorial design with group and LEV treatment as factors was built. All other AEDs, and presence or absence or HS, were entered as covariates of no-interest to control for interactions.

In a post-hoc analysis, task-related deactivation patterns were correlated with the daily LEV dose: Right TLE Median (IQR) 2500 (1000) mg, left TLE 2500 (1000) mg; Mann-Whitney U Test $p = 0.860$. All patients divided the daily dose into a morning (8-10 am) and an evening dose (6- 8 pm).

The level for significance was $p < 0.001$ uncorrected with a 20 voxels threshold extent (Lieberman and Cunningham, 2009).

7.3.4 Behavioural data

Standardized frontal lobe tests were administered to all participants (Table 7.3). As cognitive outcome variables we used verbal IQ; raw scores for category and verbal fluency, digit span backwards and Wisconsin Card Sorting Test categories. Performance accuracy on the fMRI WM tasks (2 Dot Back, 2 N-Back) was reported as a percentage.

7.3.5 Statistical analysis of clinical and behavioural data

We used SPSS Statistics Version 17.0 (SPSS Inc.,Chicago,IL,USA) for comparisons across all four groups (left/right TLE with/without LEV) and Pearson's Chi-Square tests for dichotomous data, i.e. gender, semiology, HS-frequency. Kruskal-Wallis tests were employed for all other data.

Table 7.3.Kruskal-Wallis test of cognitive performance measures in patients

	Left TLE		Right TLE		Analysis		
Cognitive Measures	on LEV Median (IQR)	without LEV Median (IQR)	on LEV Median (IQR)	without LEV Median (IQR)	X^2	df	*p*
Verbal IQ	93 (17)	94 (23.5)	93 (19)	99 (21.5)	2.552	3	.466
Letter fluency	12.5 (6.25)	11.5 (9)	14 (8)	15 (11)	3.680	3	.298
Category fluency	19 (10)	18 (7)	19 (8)	18 (8)	.490	3	.921
Digit Span bckw	4 (1)	4 (1)	4 (2)	3.5 (1.75)	.351	3	.950
WCST							
categories	6 (1)	6 (1)	6 (1)	6 (3)	1.404	3	.705
2-DB % correct	52 (31)	61 (33)	54 (33)	65 (40)	1.983	3	.576
2-NB % correct	93.5 (23.75)	98 (14)	97 (15.75)	97 (14)	1.573	3	.665

$p < 0.05$ bckw= backwards; DB= Dot Back; LEV= Levetiracetam; NB= N-Back; WCST= Wisconsin Card Sorting Test

7.4 Results

7.4.1 Performance during the fMRI working memory paradigms

Performance on the WM tasks was comparable for all groups (Table 7.3).

7.4.2 Performance on standardised neuropsychometry

There were no significant group differences (Table 7.3).

7.4.3 fMRI group effects

Group effects for task-positive and –negative networks during the highest working memory load condition are shown in Figure 7.1.

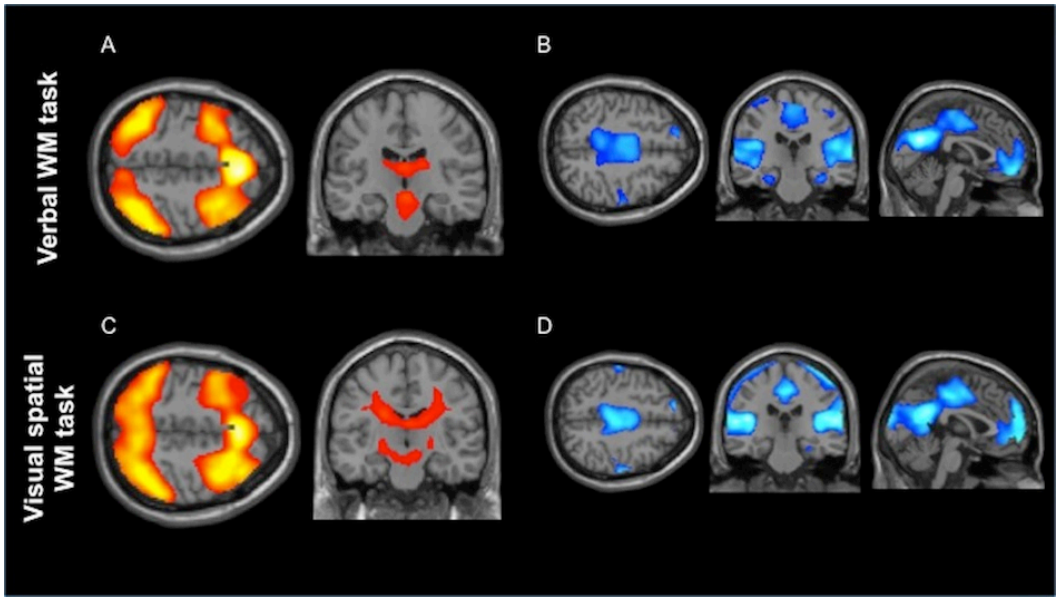

Figure 7.1. Group effects during the two fMRI working memory paradigms. Task-positive and –negative activation maps are demonstrated for the highest working memory load during the verbal (A, B) and visual-spatial (C, D) working memory task for all patients. All participants show activation of the task-relevant bilateral prefrontal and parietal areas of the working memory network during both the verbal and visual-spatial task (A, C). The task-negative contrast shows deactivation within the mesial and lateral parietal, mesial prefrontal and temporal structures, which are areas of the default mode network (B, D); $p < 0.001$, 20 voxels threshold extent

7.4.4 fMRI group differences

We isolated task and syndrome specific LEV effects on deactivation patterns (Figure 7.2). Patients on LEV and 28 healthy controls from a previous study (Stretton et al., 2012) showed similar patterns of deactivation. Compared to patients without LEV, those on LEV showed an augmentation of task-related deactivation in the "affected" temporal lobe, *i.e.* left mid-temporal gyrus in left TLE during the verbal, and right hippocampus in right TLE during the visual-spatial task (Figure 7.2 B). The reverse contrast (On LEV>No LEV) showed no effect for either working memory paradigm (not shown).

No LEV effect was observed in left TLE during the visual-spatial and in right TLE during the verbal working memory task.

We conducted the same analysis in patients treated with CBZ (22 left, 20 right TLE) or LTG (18/17) vs. those without CBZ (31/34) or LTG (35/37). No comparable effects were observed.

7.4.5 Post-hoc analysis in patients on LEV

In a post-hoc analysis, a significant dose-dependent LEV effect was demonstrated (Figure 7.2 C) in right TLE during the visual-spatial working memory task: the lower the LEV dose, the lesser the right hippocampal deactivation. At a less stringent threshold ($p < 0.05$, uncorrected for multiple comparisons) a similar dose effect was observed in left TLE during the verbal task (Figure 7.2 C).

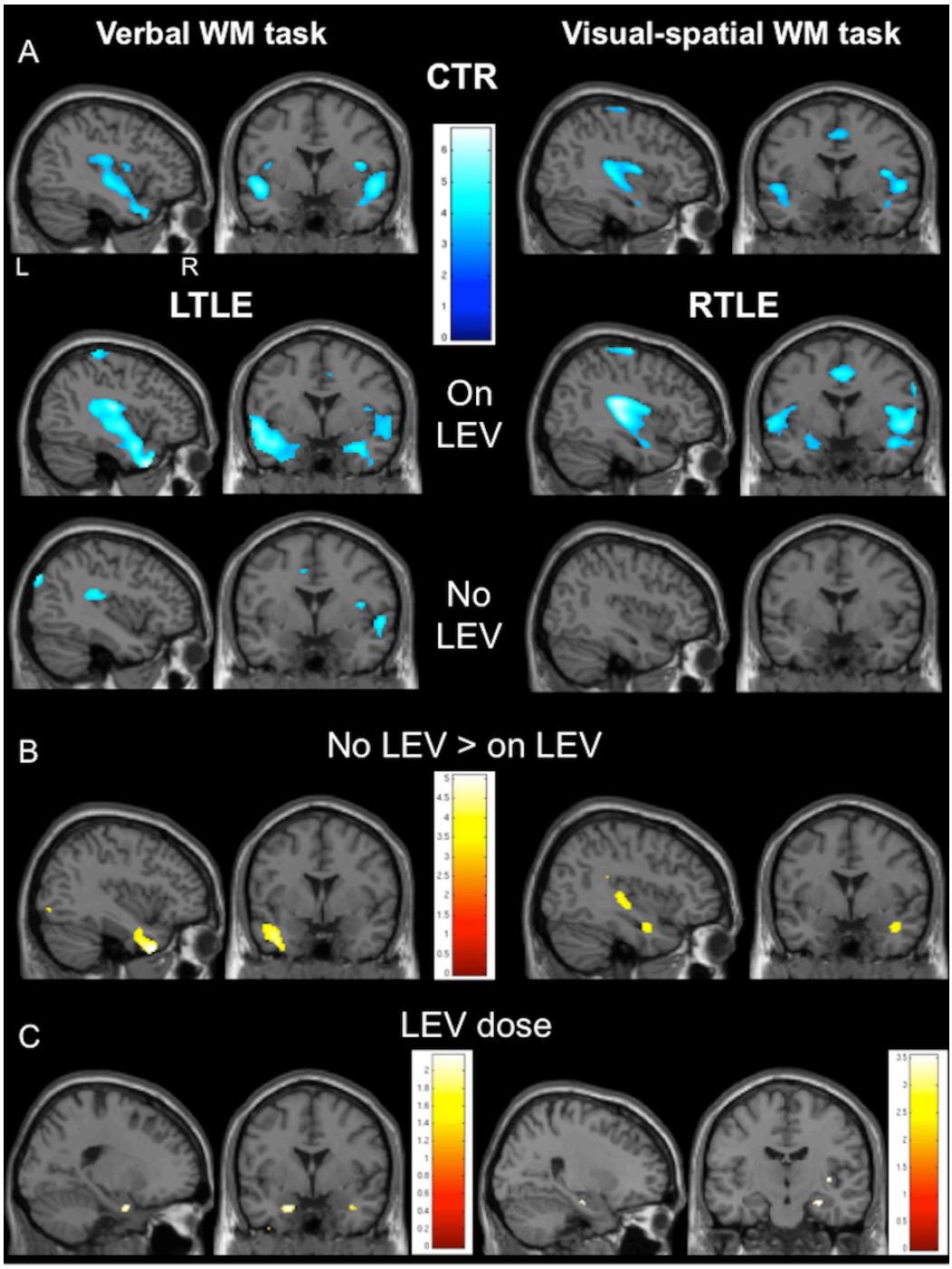

Figure 7.2. Group comparisons between patients with and without Levetiracetam (LEV) during the two working memory (WM) fMRI paradigms.

Group maps of areas of task-related deactivation networks in controls and all patients during the left- and right-lateralising task, are demonstrated. Whereas healthy controls and patients on LEV show similar patterns of deactivation, patients without LEV show less deactivation in the medial temporal lobe areas than both controls and patients on LEV in either lateralising task (Figure A). During the verbal WM task, left TLE patients without LEV significantly fail to deactivate the left mid-temporal gyrus (Figure B; left TLE

without LEV > left TLE with LEV, $p < 0.001$, 20 voxels threshold extent). During the right-lateralising visual-spatial task, patients with right TLE who are not treated with LEV fail to deactivate the right hippocampus (Figure B; right TLE without LEV > right TLE with LEV, $p < 0.001$, 20 voxels threshold extent).

A post-hoc analysis in patients treated with LEV demonstrated a dose-dependent effect of mesial temporal lobe deactivation through LEV. The lower the LEV dose, the lesser the right hippocampus is deactivated during the visual-spatial WM task (Figure C; $p < 0.001$, 20 voxels threshold extent). A similar dose effect is observed in left TLE patients during the verbal WM task at a lower level of significance (Figure C; $p < 0.05$, uncorrected): The left > right hippocampus becomes less strongly deactivated with lower LEV dose. Figure C was inclusively masked for task-related deactivation networks ($p < 0.05$).

CTR= healthy controls; LEV= Levetiracetam; LTLE= left temporal lobe epilepsy; RTLE= right temporal lobe epilepsy; WM= Working memory

7.5 Discussion

We demonstrate a dose-dependent, task-specific effect of LEV on functional network activations in TLE.

7.5.1 LEV effect on task-related deactivation

Progressive deactivation of mesial temporal structures during cognitive tasks has been associated with improved performance in healthy controls and patient cohorts (Bakker et al., 2012; Cousijn et al., 2012; Stretton et al., 2012). LEV's dose-dependent facilitation of the deactivation in this study suggests a beneficial drug-effect on cognitive networks in TLE. Since working memory performance was equal across groups, the observed effect was not influenced by performance.

Underlying hippocampal sclerosis was more frequent in left TLE patients on LEV than in all other groups, but hippocampal sclerosis distribution did not differ between right TLE patients on/without LEV (X^2 = 0.352, p = 0.352). We controlled for the effect of hippocampal sclerosis diagnosis, which ensures that our findings are not driven by the difference in hippocampal sclerosis frequencies.

Dose-dependency was more apparent in the more demanding non-verbal task. To ensure adequate performance in the 2-back condition of the Dot-back task, a greater task-related deactivation may be required. We did not find similar effects for CBZ or LTG, suggesting our findings are LEV-specific.

7.5.2 Limitations

Longitudinal data is lacking to determine whether LEV led to seizure reduction and/or improvement of cognitive functions. A further limitation is the number of

AED combinations, although distribution was equal for the most commonly prescribed other AEDs.

7.5.3 Conclusions

Our findings in TLE are consistent with previous findings in JME showing a Valproate dose dependent reduction of abnormal motor-system co-activation and enhanced working memory activations (Vollmar et al., 2011). These effects were not associated with better performance or seizure-control, but suggest that AEDs affect epileptogenic and cognitive networks differentially. Our sample included only drug-resistant patients, thus it would be an important to establish whether the neural patterns observed here translate to drug-responsive TLE patients in a longitudinal study.

Chapter 8: The effect of Topiramate and Zonisamide on fMRI verbal fluency activations in refractory epilepsy

8.1 Summary

Rationale: We used a functional MRI (fMRI) language task to investigate the effects of Topiramate (TPM), Zonisamide (ZNS) and Levetiracetam (LEV) on cognitive network activations in focal epilepsy patients.

Methods: In a retrospective, cross-sectional study, we identified patients from our clinical database of verbal fluency fMRI studies that were treated with either TPM (n=32) or ZNS (51). We matched 62 patients for clinical parameters who took LEV, but neither TPM nor ZNS. We entered antiepileptic co-medications as nuisance variables, and compared out-of-scanner psychometric parameters for verbal fluency and working memory between groups.

Results: Out-of-scanner psychometric data showed overall poorer performance for TPM compared to ZNS and LEV, and poorer working memory performance in ZNS-treated patients compared to LEV-treated patients. We found common fMRI effects in patients taking ZNS and TPM, with decreased activations in cognitive frontal and parietal lobe networks compared to those taking LEV. Impaired deactivation was only seen with TPM.

Conclusions: Our findings suggest that TPM and ZNS are associated with similar dysfunctions of frontal and parietal cognitive networks, which is associated with impaired performance. TPM is also associated with impaired attenuation of language-associated deactivation. These studies imply medication specific effects on the functional neuroanatomy of language and working memory networks.

8.2 Introduction

Amongst newer antiepileptic drugs (AED) highest rates of cognitive impairment have been reported for Topiramate (TPM; Topamax; Janssen-Cilag, Neuss, Germany) and Zonisamide (ZNS; Zonegran; EISAI, Tokyo, Japan) leading to early treatment discontinuation (Arif et al., 2009). For TPM, cognitive dysfunction is specifically characterised by impairment of expressive language and working memory. Zonisamide treatment leads to similar, less pronounced impairment (Mula and Trimble, 2009; Ojemann et al., 2001). The mechanisms of these specific impairment patterns are poorly understood. Five cognitive fMRI studies employed language tasks in two healthy participants, five to 16 epilepsy and ten migraine patients after a single dose or on steady-state TPM treatment. Taken together, the following patterns of dysfunctional activation emerge:

- decreased activation in task-positive regions, *i.e.* dominant inferior and middle frontal gyri (De Ciantis et al., 2008; Jansen et al., 2006; Szaflarski and Allendorfer, 2012)
- failure to deactivate task-negative regions, including the default mode network (Szaflarski and Allendorfer, 2012; Tang et al., 2016; Yasuda et al., 2013)

Only one study investigated potential pathomechanisms of cognitive impairment due to ZNS, describing decreased current-source density of high beta frequency in regions relevant to language and working memory during a verbal fluency task (Kwon and Park, 2013). All of the above studies are hampered by small sample sizes.

We therefore aimed to investigate in a larger group of patients than previous studies, how TPM and ZNS alter fMRI activation patterns, in order to early identify patients at risk of developing cognitive side effects. Based on previously observed beneficial effect of Levetiracetam (LEV; Keppra; UCB, Brussels,

Belgium) on cognitive networks in focal epilepsy (Wandschneider et al., 2014), we aimed to control for disease related effects by selecting patients on LEV as a comparison group.

8.3 Methods

8.3.1 Study population

In this cross-sectional study, we chose patients retrospectively from a clinical database of patients with drug refractory epilepsy, who had undergone clinical language fMRI scans at the UCL Chalfont Centre for Epilepsy (UK) between 03/2010 and 10/2015 as part of their presurgical evaluation. All patients were adults and seen at the adult epilepsy clinics of the National Hospital for Neurology and Neurosurgery (NHNN) and Chalfont Centre for Epilepsy. We included patients who were taking one of the following three AEDs, TPM, ZNS or LEV, either alone or with other AEDs as co-medications.

As requirements for patients' testability with the language fMRI paradigm, all patients had to be literate, proficient in English language and cognitively able to understand the simple task instructions (see paradigm description below). Our standard clinical language fMRI paradigm is conducted covertly, and hence we could not control for task compliance. For this reason, we excluded all patients without activations of language relevant regions (inferior and middle frontal gyri) from the analysis. We also excluded patients with data acquired post-operatively as well as those with large lesions or tumors (>2 cm) to avoid problems with imaging normalisation and further statistical analysis. Seventy-eight patients on LEV, 51 on ZNS and 32 on TPM were eligible. To create more balanced group sizes and ensure that TPM and ZNS groups were comparable in demographics and clinical characteristics to the LEV group, we employed propensity score matching. We started with the ZNS and TPM groups and to each group, looked for propensity-matched LEV patients for the variables of age at scan, age at disease onset, gender, language laterality index (middle and frontal gyri), total number of medications and lesion laterality using propensity scores in SPSS Version 21.0. We included 51 patients on ZNS, 32 on TPM and

62 on LEV in the final analysis. All patients suffered from refractory focal epilepsy and ictal EEG data was available in 86% of cases. See table 8.1 and 8.2 for further clinical details.

8.3.2 MRI data acquisition

Gradient-echo planar images were acquired for blood oxygen level dependent (BOLD) contrast on a 3T General Electric Excite HDx scanner (General Electric, Milwaukee, WI, U.S.A.).

Each volume comprised 50 contiguous oblique axial slices, providing full brain coverage, with 2.5 mm slice thickness, 64 × 64 matrix with a 24 cm field of view, 3.75 mm × 3.75 mm in-plane resolution, 25 ms echo time, 2.5 seconds repetition time.

8.3.3 fMRI verbal fluency paradigm

Patients performed a covert verbal fluency task lasting for 5.5 minutes. During the paradigm, 30 seconds blocks of task alternated with 30 seconds blocks of cross-hair fixation as a control condition. Patients were instructed to covertly generate words starting with a visually presented letter (A, D, E, S, W).

Table 8.1. Clinical parameters

	on LEV n=62	on ZNS n=51	on TPM n=32	df	*p*
age (Median, IQR), years	34 (26-42)	35 (29-42)	35 (28-47)	2	.804
male gender	27	28	14	2	.43
Handedness (right/left/ ambidextrous)	55/5/1	42/7/1	25/6/1	4	.631
age at onset (Median, IQR), years	14 (7-21)	13 (6-19)	11 (6-18)	2	.610
duration (Median, IQR), years	18 (12-26)	22 (13-31)	23 (10-30)	2	.362
ictal EEG available	52	45	28	2	.64
Lesion none/bilateral/left/right	25/2/19/16	26/0/15/10	15/3/6/8	6	.284
Dose (Median, IQR), mg	2000 (1250-3000)	225 (150-400)	312.5 (200-500)	2	N/A
number of AED (Median, IQR)	2 (2-3)	2 (2-3)	3 (2-3)	2	.245
patients on mono-vs. polytherapy	5/57	4/47	4/28	2	.730
laterality index (Median, IQR)	.75 (.53-.85)	.77 (.55-.92)	.72 (.23-.84)	2	.391
scanned on upgraded scanner	26	27	8	2	.041

Pearson's Chi-Square was employed for dichotomous variables and Kruskal-Wallis test was employed for all other variables.

$p < 0.05$; AED = antiepileptic drug; IQR = interquartile range between pair of quartiles; LEV = Levetiracetam; TPM = Topiramate; ZNS = Zonisamide

Table 8.2. Epilepsy syndromes

	LEV n= 55	ZNS n=51	TPM n=31
Non-localisable	5	6	7
Left/right hemispheric	1/6	6/6	3/4
Left/right/bi-temporal	16/11/4	9/7/2	3/5/1
Left/right/bi-frontal	3/0/1	5/4/1	2/2/0
Left/right/bilateral fronto-temporal	2/1/0	1/0/1	0/1/0
Left/right parietal	2/1	1/2	1/0
Left/right temporo-parietal	1/0	0	1/1

LEV = Levetiracetam; TPM = Topiramate; ZNS = Zonisamide

8.3.4 fMRI data analysis

Functional MRI analysis was performed using Statistical Parametric Mapping-8 (SPM8), version 4290 (http://www.fil.ion.ucl.ac.uk/spm/). Preprocessing included realignment, spatial normalisation to a template in Montreal Neurological Institute (MNI) Space, resampling to isotropic 3 x 3 x 3 voxels and smoothing with a Gaussian kernel of 8 mm full-width at half maximum (FWHM).

We performed the statistical fMRI analyses at single subject and then at group level. At single subject level, the task was modelled by convolving the vector of block onsets with a canonical haemodynamic response function (HRF) to create

regressors of interest. Movement parameters were included as confounds. Contrast images for each subject were created for task-relevant activation and deactivation.

At second level, we firstly explored activation and deactivation maps during the verbal fluency task in each patient group employing one-sample t-tests (Figure 8.1, Figure 8.2). For group comparisons, second level analysis was conducted entering the activation contrast of each patient into a full factorial design with group (LEV, ZNS, TPM) as factor. All other AEDs were entered as regressors of no interest. As the scanner was upgraded in 2013, this was entered as an additional covariate of no interest (scanned on upgraded scanner yes/no). An exploratory statistical threshold was set at $p < 0.005$ uncorrected with a 20 voxels minimum cluster size extent threshold (Lieberman and Cunningham, 2009). To be able to disentangle whether group differences were related to activation or deactivation, we masked the results with a binarized average task activation map of the patient controls, and subsequently with the binarized deactivation map to include the contrast relevant brain areas.

The interpretation of the results at the single subject and group level was not blinded, as resultant maps represent t-maps at a predefined statistical threshold. We anatomically objectified peak activations from group comparisons with coordinates in MNI (Montreal Neurological Institute)-space (Table 8.4).

8.3.5 Laterality index

To control for differences in language laterality, we matched the groups for laterality indices. These were calculated with the Bootstrap method in the SPM8

LI toolbox (Wilke and Lidzba, 2007) for the verbal fluency activation contrast for each subject in the inferior frontal and middle frontal gyri.

8.3.6 Behavioural data

In those patients who had standard clinical psychometric testing at the time of the scan, we carried out subgroup analyses of performances. We included tests measuring cognitive domains reported to be affected by TPM and ZNS: Letter and category fluency; the WAIS Digit Span measure of short term and working memory; the Graded Naming Test (GNT) measure of expressive language function. (Baxendale et al., 2008)

8.3.7 Statistical analysis of clinical and behavioural data

Statistical analysis of clinical and behavioural data was conducted using SPSS version 21.0 (IBM). Chi-square tests were applied to categorical data and the Kruskal-Wallis and/or Mann-Whitney U Test to all other parameters. The statistical significant threshold was set at $p < 0.05$.

8.4 Results

8.4.1 Performance on standardised neuropsychometry

There were significant group differences in cognitive test performance with the exception of the Graded Naming Test (see Table 8.3).

Post-hoc group comparisons revealed that for the digit span task, patients on LEV performed better than both those on ZNS and TPM (LEV vs. ZNS: U=451000, p = 0.002; LEV vs. TPM: U=120000, p < 0.001) (Mann-Whitney U Test), and those on ZNS performed better than patients on TPM (LEV vs. ZNS: U=205000, p = 0.007). TPM-treated patients performed less well than both LEV- and ZNS-treated for both fluency parameters (LEV vs. TPM: letter fluency U=177000, p < 0.001, category fluency U=149500, P < 0.001; ZNS vs. TPM: letter fluency U=237000, p = 0.047; category fluency U=145500, p < 0.001). There was no statistical difference between LEV- and ZNS-treated patients (letter fluency U=505500; p = 0.077; category fluency U=604500, p = 0.397).

Table 8.3. Cognitive performance

	LEV	ZNS	TPM	df	*p*
WAIS Digit Span	n=42	n=36	n=20		
(median, IQR)	9 (7.5-11)	7 (6-9)	5 (4.75-7)	2	<.001
letter fluency	n=38	n=35	n=20		
(median, IQR)	14.5 (10.25-17.75)	12 (8-15)	10 (8-11.5)	2	.003
categorical fluency	n=39	n=35	n=20		
(median, IQR)	18.5 (15-25.75)	17 (15-22)	12 (11-16)	2	<.001
naming (GNT)	n=34	n=28	n=15		
(median, IQR)	17 (13.45-21.25)	17 (14-20)	14 (10.5-17)	2	.391

Kruskal-Wallis test, $p < 0.05$

Scaled scores are presented for digit span and raw scores for all other cognitive parameters.

GNT = Grades Naming Test; IQR = interquartile range between pair of quartiles; LEV = Levetiracetam; TPM = Topiramate; ZNS = Zonisamide

8.4.2 fMRI group effects

As demonstrated by one sample t-tests of task-relevant activations and deactivations, each AED group activated frontal language areas including the inferior and middle frontal gyri (IFG, MFG), bilateral supplementary motor areas

(SMA), as well as the left lateral parietal region, and deactivated areas of the default mode network (DMN), i.e. bilateral precuneus, posterior cingulate, angular gyrus, medial prefrontal and lateral temporal cortices (Figure 8.1, 8.2).

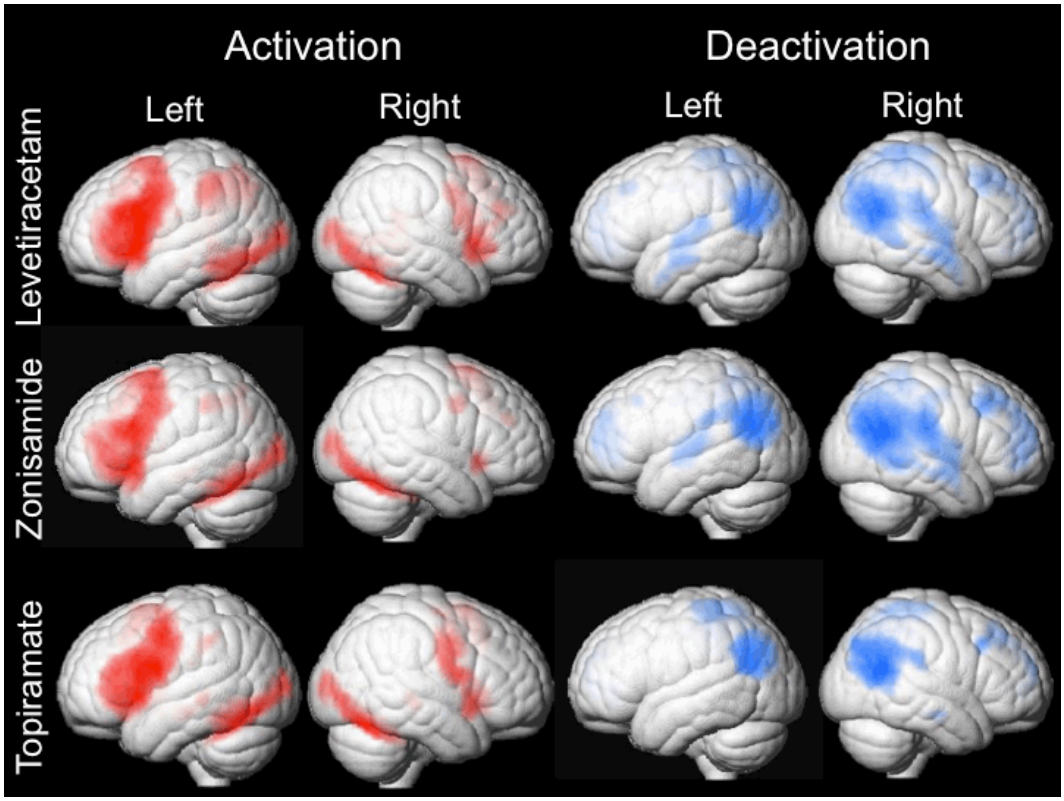

Figure 8.1. Group activation and deactivation maps during the verbal fluency task. One-sample t-tests of functional MRI activation and deactivation maps for the three different patient groups on Levetiracetam, Zonisamide and Topiramate are demonstrated on a surface rendered brain template. Task relevant regions (red) include bilateral inferior and middle frontal gyrus (left > right), bilateral supplementary motor area, and the left dorsolateral parietal region.

Areas of task-related deactivations (blue) include the bilateral precuneus, posterior cingulate, angular gyrus, medial prefrontal and lateral temporal cortex.

$p < 0.005$, 20 voxels threshold extent.

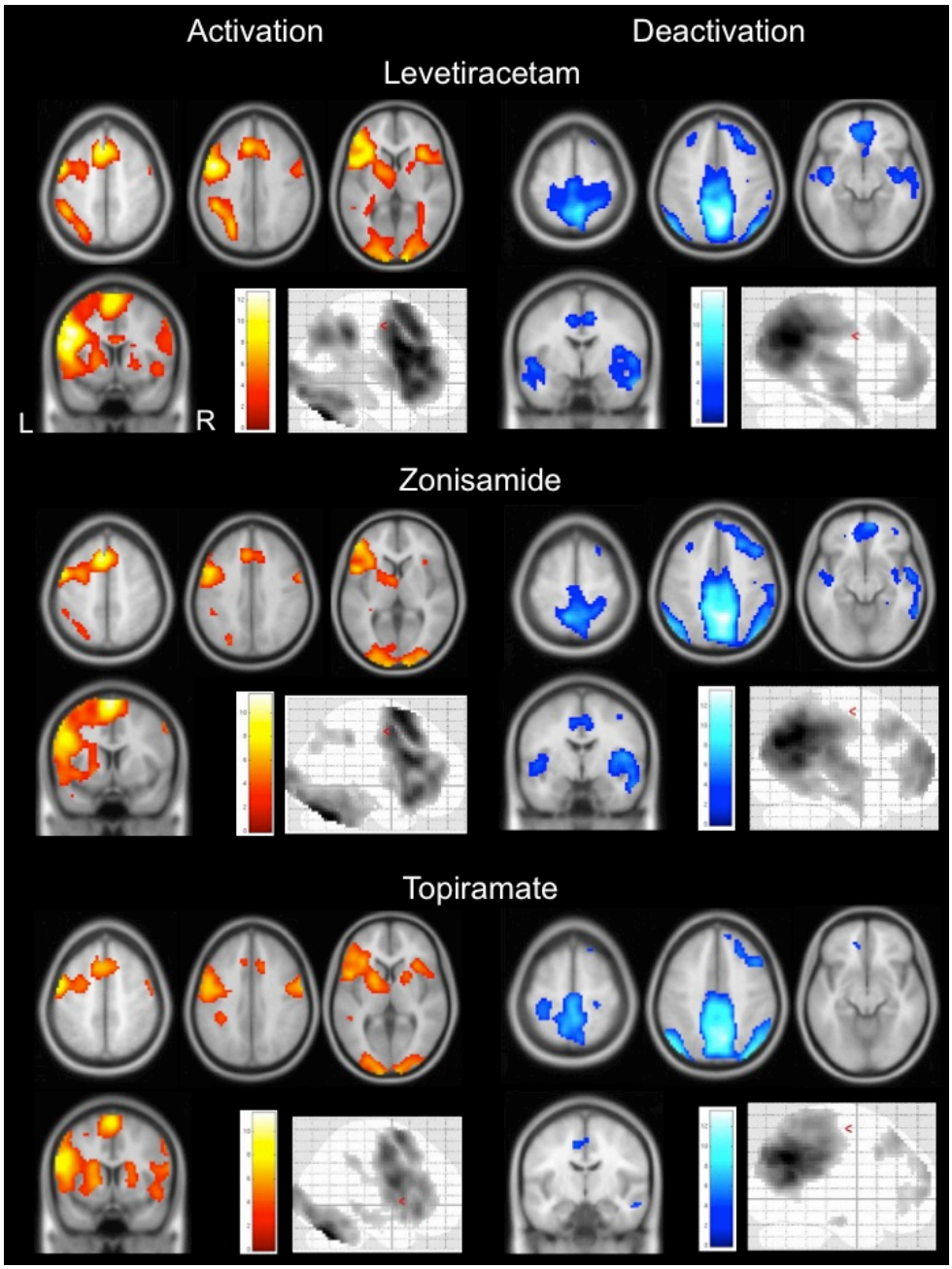

Figure 8.2. Group activation and deactivation maps during the verbal fluency tasks (slice view and glass brain). T-values are demonstrated as colour bars. Task relevant regions (orange-red) include bilateral inferior and middle frontal gyrus (left > right), bilateral supplementary motor area, and the left dorsolateral parietal region.

Areas of task-related deactivations (blue) include the bilateral precuneus, posterior cingulate, angular gyrus, medial prefrontal and lateral temporal cortex.

$p < 0.005$, 20 voxels threshold extent

L = left, R = right

8.4.3 fMRI group comparisons

Patients on TPM showed reduced activation in the left MFG and left dorsal parietal region compared to those taking LEV (Figure 8.3, 8.4). Similarly, those on ZNS had reduced activation in the bilateral MFG and IFG, as well as the left dorsal parietal region when compared to patients on LEV (Figure 8.3 B, 8.4 B). Compared to LEV patients, TPM-, but not ZNS-treated, patients showed less task-related deactivation in the temporal regions and the rolandic opercula bilaterally, and right inferior parietal lobule and supramarginal gyrus (Figure 8.3 C, 8.4 C).

Comparing TPM- and ZNS-treated patients directly revealed greater activation in the temporal regions and the rolandic opercula bilaterally and the insular cortex, inferior parietal lobule, supramarginal gyrus, superior temporal gyrus and rolandic operculum on the right in the TPM group (Figure 8.3 D, 8.4 D). Group differences on the right were mainly due to impaired deactivation in comparison to LEV and ZNS (masked inclusively for LEV and ZNS group deactivation maps; shown in blue in Figure 8.3 D). Left-sided changes were located within LEV group activation maps and were hence due to greater task-relevant activation in TPM (shown in red in Figure 8.3 D).

There were no regions of greater activation in ZNS-treated patients compared to those on TPM.

See Table 8.4 for a more detailed anatomical description of resultant regions from the individual group comparisons.

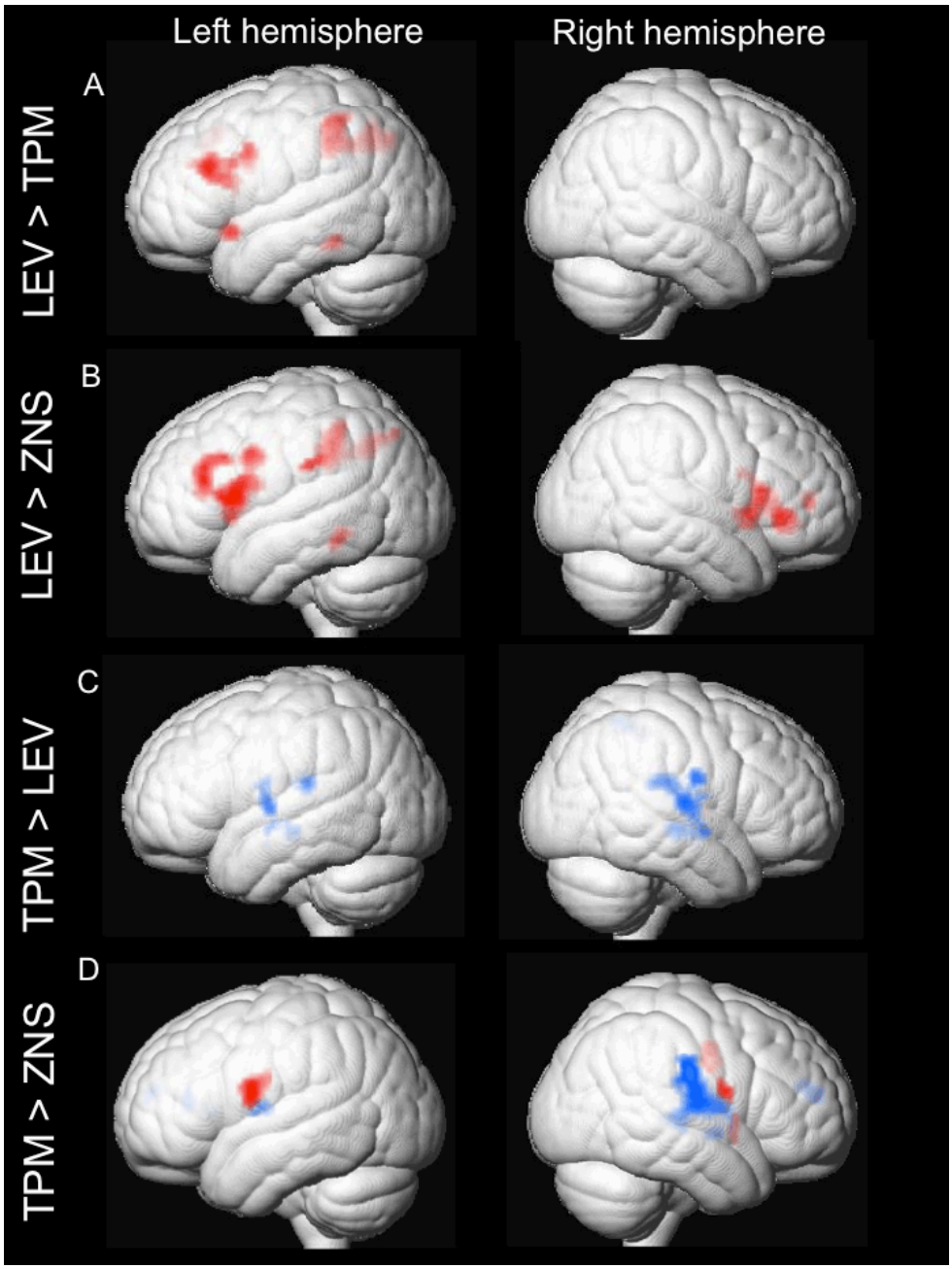

Figure 8.3. Group differences in fMRI activation maps during the verbal fluency task. Significant group differences between patients on Levetiracetam (LEV), Topiramate (TPM) and Zonisamide (ZNS) are demonstrated. Patients on TPM and ZNS have less activation in frontal and parietal cognitive networks than patients on LEV: In patients on TPM, activation is reduced in the left middle frontal gyrus (MFG) and left dorsal parietal region (A). In patients on ZNS, activation is reduced in the left MFG and bilateral inferior frontal gyrus (IFG), as well as the left dorsal parietal region (B).

Looking at task-relevant deactivation networks, bilateral lateral temporal regions and rolandic opercula, and the right inferior parietal lobule and supramarginal

gyrus are less deactivated (shown in blue) in patients on TPM when compared to those on LEV (C).

Compared to ZNS, TPM shows increased activation in the IFG, insular cortex and rolandic operculum on the left, and the insular cortex, inferior parietal lobule, supramarginal gyrus, superior temporal gyrus and rolandic operculum on the right. Differences in the left are mainly due to increased activation of task-relevant regions as shown in red (inclusively masked with LEV activation maps); on the right, activated regions mainly lie within task-negative areas, *i.e.* are due to impaired deactivation as shown in blue (inclusively masked with LEV and ZNS deactivation maps) (D).

$p < 0.005$, 20 voxels threshold extent

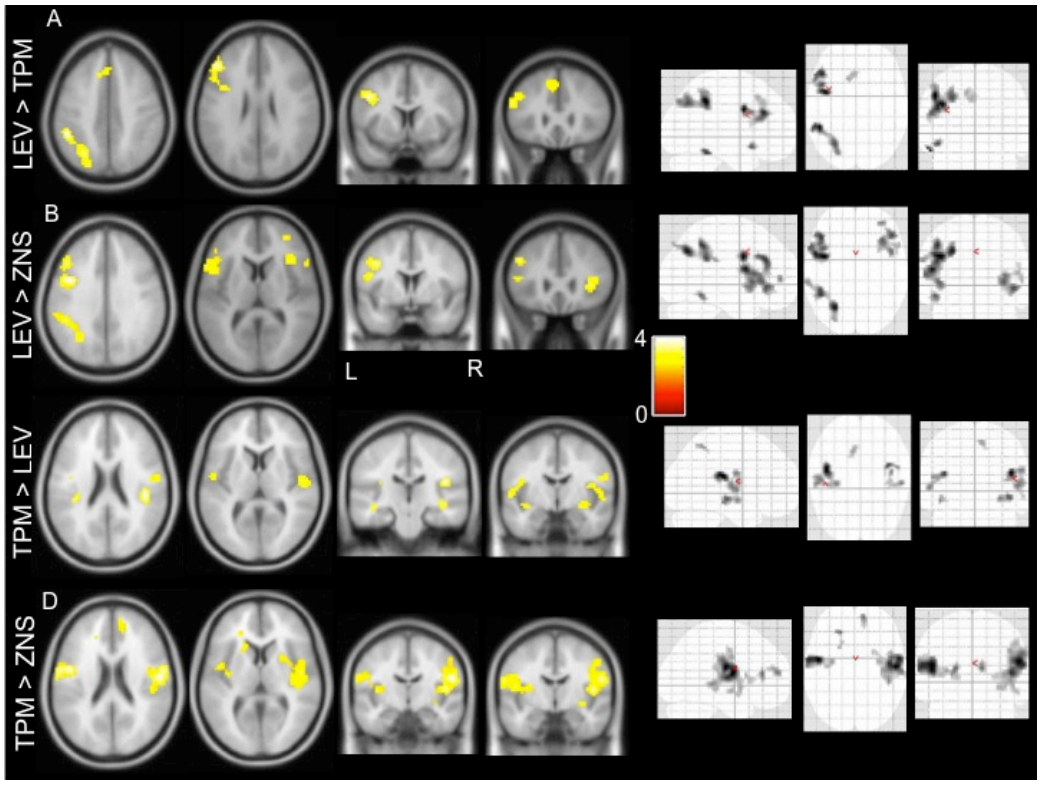

Figure 8.4. Group differences in fMRI activation maps during the verbal fluency task (slice view and glass brain). T-values are demonstrated as colour bars. Patients on TPM and ZNS have less activation in frontal and parietal cognitive networks than patients on LEV: In patients on TPM, activation is reduced in the left middle frontal gyrus (MFG) and left dorsal parietal region (A). In patients on ZNS, activation is reduced in the left MFG and bilateral inferior frontal gyrus (IFG), as well as the left dorsal parietal region (B).

Looking at task-relevant deactivation networks, bilateral lateral temporal regions and rolandic opercula, and the right inferior parietal lobule and supramarginal gyrus are less deactivated in patients on TPM when compared to those on LEV (C).

Compared to ZNS, TPM shows increased activation in the IFG, insular cortex and rolandic operculum on the left, and the insular cortex, inferior parietal lobule, supramarginal gyrus, superior temporal gyrus and rolandic operculum on the right. When inclusively masked with LEV activation maps, differences in the left are mainly due to increased activation of task-relevant regions, and on the right, activated regions mainly lie within task-negative areas, *i.e.* are due to impaired deactivation, when inclusively masked with LEV and ZNS deactivation maps (D), see also Figure 8.3.

$p < 0.005$, 20 voxels threshold extent

L = left, R = right

Table 8.4. Coordinates and peak activations of resultant areas from group comparisons.

	MNI coordinates (X Y Z)	*Z*-score	*p*
patients on LEV > patients on TPM			
left dorsal parietal	-48 -43 43	3.94	< 0.001
left middle frontal gyrus	-39 5 34	3.90	< 0.001
left inferior temporal gyrus	-54 -40 -20	3.55	< 0.001
left superior temporal gyrus	-45 14 -11	3.38	< 0.001
left supplementary motor area	-9 23 49	2.90	0.002
patients on LEV > patients on ZNS			
left inferior frontal gyrus	-42 5 34	4.07	< 0.001
left dorsal parietal	-27 -64 40	3.93	< 0.001
left inferior temporal gyrus	-48 -46 -11	3.35	< 0.001
left middle frontal gyrus	-45 32 28	3.68	< 0.001
right inferior frontal gyrus	48 32 -2	3.51	< 0.001
right middle frontal gyrus	36 50 7	3.20	0.001
patients on TPM > patients on LEV			
left rolandic operculum	-36 -31 19	3.48	< 0.001
left temporal lobe	-42 -25 -11	3.14	0.001
left superior temporal gyrus	-54 -7 4	3.17	0.001
right rolandic operculum/ inferior parietal lobule/ supramarginal gyrus	45 -25 22	3.88	< 0.001
right temporal lobe	42 -19 -8	3.36	< 0.001
right superior temporal gyrus	51 -13 7	3.16	0.001
right precuneus	9 -49 55	2.96	0.002
patients on TPM > patients on ZNS			
left inferior frontal gyrus	-48 -1 19	4.07	< 0.001
left insula	-30 -4 13	3.00	0.001
left anterior cingulate gyrus	-18 35 16	3.35	< 0.001
right rolandic operculum/ inferior parietal lobule/ supramarginal gyrus	54 -13 22	3.98	< 0.001
right insula/ right rolandic	48 -7 10	3.70	< 0.001

operculum/right superior temporal gyrus			
right medial frontal gyrus	12 56 16	3.31	< 0.001

Coordinates are given in MNI space.

LEV = Levetiracetam, MNI = Montreal Neurological Institute, TPM = Topiramate, ZNS = Zonisamide

8.5 Discussion

In this study we demonstrate language paradigm specific fMRI effects with a decrease in frontal lobe and parietal lobe activations common to ZNS and TPM, and impaired deactivation in task-negative networks only seen for TPM.

Our results concur with findings from previous studies on TPM, reporting decreased task-relevant frontal activation or/and impaired deactivation of task-negative networks (Jansen et al., 2006; Szaflarski and Allendorfer, 2012; Tang et al., 2016; Yasuda et al., 2013), and demonstrate both mechanisms in a larger group of patients. Novel findings are that ZNS is associated with similar dysfunctional networks of task-activation, but that impaired deactivation appears to be specific to TPM, as shown both in comparison to both LEV- and ZNS-treated patients.

8.5.1 Effect of Topiramate and Zonisamide on fMRI cognitive networks

The VF fMRI task usually leads to activation of frontal lobe areas, including most consistently the dominant IFG, MFG, anterior cingulate and pre-central cortices, as well as the insular, superior temporal and parietal cortices, and the cerebellum (contralateral to frontal activation) (Friedman et al., 1998; Phelps et al., 1997; Woermann et al., 2003). Dorsolateral frontal and parietal cortices activated by the VF task are also implicated in functional networks of working memory and attention (Coull, 1998; Owen et al., 2005). Given the low-demand control condition in the VF task employed in this study, activation of cognitive networks supporting general task performance, *i.e.* the working memory and sustained attention system, become apparent with increasing task demand, in

addition to activation of language specific frontal networks (Binder et al., 2009). Hence decreased activation in both regions relevant for expressive language function (*i.e.* IFG, MFG) and general cognitive task performance, *i.e.* the parietal cortex for sustained attention and the fronto-parietal working memory network, suggest suppression of several higher level cognitive domains by TPM and ZNS.

8.5.2 Effect of TPM on task-related deactivation

In TPM-treated patients, fMRI changes involved both activation and deactivation networks. Task-related deactivation refers to a decrease in BOLD signal during demanding motor or cognitive tasks, as compared to less demanding states, such as resting. Deactivation likely occurs because neural processes during these less demanding states are interrupted by engagement with the task and a shift from internal to external information processing. Successful task execution has been associated with effective deactivation of task-negative areas (Raichle et al., 2001; Seghier and Price, 2012). It has recently been demonstrated that the DMN is segregated into subspecialized nodes and, more relevant to our study, there is functional heterogeneity across DMN nodes with respect to different language tasks (Andrews-Hanna, 2012; Seghier and Price, 2012). In addition, areas involved in semantic and language processing show a large overlap with regions of the default mode network (*i.e.* angular gyrus, medial prefrontal cortex, IFG, posterior cingulate, ventral temporal lobe) (Binder et al., 2009). Deactivation in those overlapping regions can be modulated by both task *content, i.e.* high semantic demands reducing deactivation, and increased task *demands* or difficulty leading to increased deactivation (Binder et al., 2009; Seghier and Price, 2012). In our study, patients on TPM fail to deactivate task-relevant DMN nodes in comparison to patients taking ZNS or LEV, associated

with more cognitive impairment than those on ZNS, and these include areas implicated in language processing (*i.e.* right inferior parietal lobule, supramarginal gyrus). In addition, direct comparison to ZNS reveals that TPM leads to failed deactivation of language-task relevant DMN nodes on the right, but increased activation of language-relevant task positive regions on the left (Figure 8.3 D, 8.4 D). The latter, as demonstrated by psychometric out-of-scanner data, is ineffective.

8.5.3 Strength and limitations

A particular strength of our study is the big sample size. As a limitation, the statistical threshold used for the second level analysis, *i.e.* $p < 0.005$ uncorrected, 20 voxel threshold extent, enables an exploratory view of the differences between AED treatment groups, though peak activations within implicated regions almost all survive $p < 0.001$, uncorrected (Table 8.4). Findings will need to be confirmed in a follow-up study with larger patient groups.

Additional limitations include a potential case selection bias as our study only includes patients who continued treatment on TPM and ZNS and hence may have benefitted more and experienced fewer side effects than those who stopped it. A further potential confounder is the reason why a particular medication was chosen for a patient. All three drugs are broad-spectrum AED with an uncomplicated interaction profile with other AED and have been established for several years in the treatment of epilepsy in general, and in polytherapy in refractory epilepsy (Carmichael et al., 2013; Mbizvo et al., 2012; Pulman et al., 2014). However, we cannot control for treatment preferences in certain patients, e.g. choosing TPM in those who also suffer from migraines.

More than ten consultants are involved in epilepsy treatment at our centre, supporting that the AED profile of our groups is not driven by personal choices of a few individuals; however, AED choices may differ in our epilepsy centre to those in others. This may weaken the generalizability of our findings.

In addition, the majority of patients were on co-medication and these may have contributed to both poor cognitive performance and observed fMRI activation patterns. Irrespective of specific AED effects, it has been shown that every additional AED leads to further cognitive impairment (Witt et al., 2015). AED plasma concentrations were not known at time of scanning. Though we cannot fully control for effect of co-medication, we matched groups for the median number of AED and individual co-medication AED were included as a regressor of no interest into the fMRI analysis model.

Also, out of scanner psychometric data was only available in a subset of patients.

Due to the retrospective study design, the effect of seizures on our findings could not be quantified in terms of frequency, severity or proximity to scan time. However, all patients suffered from refractory epilepsy and we therefore assume similar effects of seizures in all groups.

Though all patients had focal epilepsy, different epilepsy syndromes were included (Table 8.2). Our study characterizes TPM and ZNS related disruption of language and working memory networks in a relatively large group of presurgical candidates of a big tertiary epilepsy referral centre. Though our findings are not fully generalizable as medical treatment strategies and drug choices may differ across epilepsy centres and countries observed fMRI results in this study still provide valuable information to interpret clinical language fMRI scans in a variety of patients.

8.5.4 Clinical applications and future directions

With respect to clinical applications, task-, region- and AED-specific effects of TPM and ZNS may help to identify patients at risk of developing AED-related side effects at an early stage of treatment. Identifying language lateralization with fMRI is crucial for the risk assessment during planning for epilepsy surgery (Duncan et al., 2016). It would thus be important to establish whether fMRI changes due to TPM and ZNS can lead to mis-lateralization of language. In this study, as groups were matched for LI to increase the yield by including patients irrespective of language lateralization, we cannot comment on a potential effect of TPM and ZNS on LIs. In addition, a prospective longitudinal study, enabling fMRI and psychometric data collection before and when initiated on TPM and ZNS (ideally with plasma levels) will be more appropriate to answer this question.

Chapter 9: Structural imaging biomarkers of sudden unexpected death in epilepsy

9.1 Summary

Rationale: Sudden unexpected death in epilepsy (SUDEP) is a major cause of premature death in people with epilepsy. We aimed to assess whether structural changes potentially attributable to sudden death pathogenesis were present on MRI in people who subsequently died of sudden unexpected death in epilepsy.

Methods: In a retrospective, voxel-based analysis of T1 volume scans, we compared grey matter volumes (GMV) in 12 cases of SUDEP (two definite, ten probable; eight males), acquired two years (Median, interquartile range [IQR] 2.8) before death (Median (IQR) age at scanning 33.5 (22) years), with 34 people at high risk (age 30.5 (12); 19 males), 19 at low risk (age 30 (7.5); 12 males) of sudden death, and 15 healthy controls (age 37 (16); seven males). At risk subjects were defined based on risk factors of SUDEP identified in a recent combined risk factor analysis.

Results: We identified increased GMV in the right anterior hippocampus/ amygdala and parahippocampus in SUDEP cases and people at high risk, when compared to those at low risk and controls. Compared to controls, posterior thalamic GMV, an area mediating oxygen regulation, was reduced in cases of SUDEP and subjects at high risk. The extent of reduction correlated with disease duration in all subjects with epilepsy. Increased amygdalo-hippocampal GMV with right-sided changes is consistent with histopathological findings reported in sudden infant death syndrome. We speculate that the right-sided predominance reflects asymmetric central influences on autonomic outflow, contributing to cardiac arrhythmia. Pulvinar damage may impair

hypoxia regulation. The imaging findings in SUDEP and people at high risk may be useful as a biomarker for risk-stratification in future studies.

9.2 Introduction

The incidence of sudden death is 20-fold higher in people with epilepsy than in the general population; sudden unexpected death in epilepsy (SUDEP) is the most common cause of premature death in people with chronic epilepsy. There is currently little understanding of the underlying mechanisms of SUDEP, and post mortem histopathology has shown no pathognomonic characteristics (Shorvon and Tomson, 2011; Surges and Sander, 2012). Meta-analyses of SUDEP risk factors (Hesdorffer et al., 2011; Ryvlin et al., 2013) have identified frequent convulsive seizures (>= 3/year) as a major risk factor and several studies indicate that unsupervised nocturnal seizures significantly contribute to SUDEP risk (Lamberts et al., 2012). The Mortality in Epilepsy Monitoring Unit Study (MORTEMUS) reported a consistent pattern in video-EEG monitored SUDEP cases, of a convulsive seizure, followed by early and fatal cardiorespiratory dysfunction (Ryvlin et al., 2013). Some studies support a primary respiratory cause with central apnoea, which has been related to postictal generalized EEG suppression, indicating profound depression of central nervous system function (Lhatoo et al., 2010). Other studies report primary peri-ictal cardiac arrhythmias and impaired heart rate variability accompanying SUDEP (Surges et al., 2010).

One recent imaging investigation (Mueller et al., 2014) reported severe volume loss in the dorsal mesencephalon in two SUDEP cases. A resting-state functional connectivity study identified reduced functional connectivity between the pons and right thalamus, the midbrain and right thalamus, the anterior cingulate cortex bilaterally and the thalamus, and the right and left thalamus in people at high risk compared to those at low risk of SUDEP (Tang et al., 2014). Imaging studies in other conditions with high risk of sudden death have also shown structural changes in brain regions bearing autonomic regulatory or

respiratory functions, *i.e.* the dorsal and ventral medulla, putamen, and bilateral insular cortices in recent-onset obstructive sleep apnoea (Kumar et al., 2014), and the hypothalamus, posterior thalamus, caudal raphe, locus coeruleus, insular cortex and lateral medulla in congenital central hypoventilation syndrome. People suffering from the latter condition are especially at risk for sudden death (Patwari et al., 2010). Neuropathological studies in sudden infant death syndrome (SIDS) report brain stem abnormalities, *i.e.* brain stem gliosis and defects of neurotransmission in the medulla (Paine et al., 2014). Dentate gyrus abnormalities in the hippocampus were reported in a large subset of 153 SIDS, and may reflect defective neuronal migration and proliferation (Kinney et al., 2009a, 2015).

Mice carrying mutations in the K1.1v potassium and Scn1a sodium channels have many phenotypes of human SUDEP, e.g. frequent convulsive seizures and premature death. A recent study in these mutant mice demonstrated that cortical EEG suppression coincided with spreading depolarization in the dorsal medulla, a region controlling cardiorespiratory pace making. Depolarizing blockade of these cells prevents normal autoresuscitation and produces cardiorespiratory arrest (Aiba and Noebels, 2015).

To elucidate which brain regions may be implicated in SUDEP, we investigated whether regional abnormalities in grey matter volume appear in those who had SUDEP, compared to healthy controls. Due to the low incidence of SUDEP, exploring enriched risk groups has been suggested as means to increase the yield of future studies (Ryvlin et al., 2013). We explored whether regional imaging findings in people who died of SUDEP can be reproduced in a larger cohort of people at high risk for SUDEP. To assess whether imaging findings are common to SUDEP and those at high risk, independent from other epilepsy-related factors, we compared SUDEP cases and those at high risk to a

population presumed to be at low risk of SUDEP. We also compared people at high risk and low risk of SUDEP to healthy controls.

9.3 Methods

9.3.1 Study population

This retrospective study was conducted at a UK tertiary referral centre for epilepsy as part of database research on the “Prevention and Risk Identification of SUDEP”, approved by the National Research Ethics Committee (14/SW/0021).

The scans for SUDEP cases, those at low and high risk of SUDEP, and healthy controls were obtained from an overlapping period of case ascertainment, ensuring same imaging protocols were used for acquisition.

People with epilepsy were identified from a general clinical database at the tertiary referral centre. We identified 12 people who died with definite or probable SUDEP, and matched those with 53 living people with epilepsy identified from the same database according to criteria below. All subjects had to have undergone a high-resolution T1 volume scan using the identical 3 Tesla MRI scanner as part of their clinical care. Individuals with major brain lesions, such as those after partial temporal lobe resection, were not included to avoid problems with imaging normalisation. Sufficient clinical data had to be also available to subsequently identify subjects at low or high risk of SUDEP, as described below. All three groups were matched for gender, age, epilepsy syndrome, and epilepsy duration to control for duration-related structural changes. Groups were also matched for lesion pathology where possible.

Healthy controls were comparable to the epilepsy populations for gender and age.

9.3.1.1 SUDEP cases

Those deceased were classified as probable (ten) or definite (two) SUDEP, according to a recent classification (Nashef et al., 2012). The median age at death was 35.5 (Interquartile range [IQR] 2.8) years. Scans were acquired at a median of 2 (IQR 2.8) years ante mortem. Videotelemetry data of seizures were available in five SUDEP cases. Further clinical information on the SUDEP cases are shown in Table 9.1. SUDEP, people at high or low risk, as well as controls, were comparable for gender and age at scan (Table 9.2).

9.3.1.2 People at high or low risk for SUDEP

A risk score was created for each subject according to the most robust epilepsy-specific risk factors for SUDEP identified in recent combined-risk factor analyses (Hesdorffer et al., 2011) that were also implemented in a recent SUDEP imaging study (Tang et al., 2014). Odds ratios for individual SUDEP risk factors were therefore adjusted for different study groups. Those with either nocturnal seizures (OR = 3.9), or frequent (>= 3/year) convulsive seizures (OR = 15.46), were considered “high risk.” Increased SUDEP risk is also associated with young age at disease onset (onset age < 16 years: OR = 1.72), and long disease duration (duration > 15 years: OR = 1.95) (Hesdorffer et al., 2011; Lamberts et al., 2012). For each subject, odds ratios for risk factors were added to define an individual overall risk score. In the SUDEP cohort, 11 of 12 SUDEP cases (91.7%) were correctly identified as high risk subjects if the summed risk score was at least 3.9 (Median risk score 19.1, IQR 16.7). One subject with juvenile myoclonic epilepsy had died, probably from SUDEP, but was not known to have suffered from nocturnal seizures nor frequent convulsive seizures. A

cut-off of 3.9 was therefore employed to stratify others into those with high (>= 3.9) and low risk (< 3.9) of SUDEP.

Individual risk scores and pathology identifed on MRI of people at low and high risk for SUDEP are listed in Table 9.5.

SUDEP cases, and those at low and high risk were matched for epilepsy syndrome (SUDEP: 1/12 generalised genetic epilepsy; high risk: 0/34; low risk: 3/19), and as far as possible for type of pathology (Table 9.3). We were primarily interested in identifying common structures and pathophysiological mechanisms underlying SUDEP and high risk for SUDEP, and the majority of those at low risk (10/19), and high risk (22/34), had no identifiable lesions on a high-resolution 3-Tesla epilepsy protocol clinical MRI brain scan. Videotelemetry data of seizures were available in 30/34 of those at high risk, and 7/19 at low risk. Further information regarding epilepsy classification (as per videotelemetry and/or history) is shown in Table 9.4.

9.3.1.3 Controls

Scans of 15 age- and gender-matched healthy controls were included from a previous study (Stretton et al., 2013). All controls had normal MRI scans

Table 9.1. Additional clinical characteristics of the SUDEP cohort

	Epilepsy syndrome	SUDEP Category	Lesion on visual inspection of MRI by neuroradiologist	Duration tonic phase (sec)	PGES	Duration PGES (sec)
1	Juvenile myoclonic epilepsy	Probable	no	N/A	N/A	N/A
2	Focal, left temporal Primary generalized	Probable	Bulky left amygdala with mild FLAIR signal increase	N/A	no	N/A
3	Focal, bitemporal	Probable	no	11	yes	30-43
4	Focal, probably bitemporal	Probable	no	N/A	N/A	N/A
5	Multifocal, left mesial temporal and frontal	Probable	Left hippocampal sclerosis	10	yes	33
6	Focal, frontal	Probable	no	N/A	N/A	N/A
7	Focal, unclassified	Definite	Bilateral periventricular leucomalacia	N/A	N/A	N/A
8	Focal, frontal	Probable	left hippocampal sclerosis	N/A	yes	5
9	Focal, left hemisphere neocortical	definite	Cavernoma left superior frontal gyrus	6 - 23	no	N/A
10	Unclassified	Probable	Cavernoma right inferior frontal, in white matter	N/A	N/A	N/A

11	Focal, probably bitemporal	Probable	Enlarged left amygdala > hippocampus	N/A	N/A	N/A
12	Focal, left hemisphere	Probable	Right superior temporal DNET	N/A	N/A	N/A

DNET = dysembryoplastic neuroepithelial tumor; EEG = electroencephalography; FLAIR = fluid-attenuated inversion recovery;

PGES = Post-ictal generalised EEG suppression; SUDEP = sudden unexpected death in epilepsy

Table 9.2. Demographic and clinical parameters

	SUDEP cases (n=12)	At high risk (n=34)	At low risk (n=19)	Controls (n=15)	df	X^2	*p*
Age at scan (yrs)							
Median (IQR)	33.5 (21.5)	30.5 (12)	30.0 (7.5)	37 (16)	3	2.85	0.241
Age at onset (yrs)							
Median (IQR))	16.5 (10)	13.5 (7)	14 (6)	N/A	2	6.21	0.045
Epilepsy duration (yrs)							
Median (IQR)	11.5 (24.3)	17 (11.25)	15 (15)	N/A	2	5.74	0.057
Gender male	8	19	12	7	3	1.42	0.722*
>3 CSs/year	8	24	0	N/A	2	26.09	0.000*
Nocturnal seizures	8	27	0	N/A	2	31.9	0.000*
polytherapy	4	14	4	N/A	2	2.21	0.347*

Pearson's Chi-Square was employed for dichotomous variables. Since some cells had an expected count less than 5, an exact significance test was selected. Kruskal-Wallis test was employed for all other variables. CS = convulsive seizure; IQR = interquartile range; SUDEP = sudden unexpected death in epilepsy; yrs=years; $p < 0.05$; *indicates exact p

Table 9.3. Structural abnormalities

	Low risk N = 19	High risk N = 34
No lesion	10	22
Hippocampal sclerosis Left/Right	1/0	2/0
Focal cortical dysplasia	3	6
Left/Right	1/2	4/2
	1 left/ 1 right temporo-occipital 1 right parieto-occipital	1 left insular 1 left medial temporal 1 right supramarginal gyrus 1 entire left temporal lobe 1 left inferior parietal 1 right anterior temporal
Cavernoma	2	1
Left/Right	0/2	0/1
	- right temporal pole - right fusiform gyrus	- right temporal pole
DNET	1	0
Left/Right	0/1	
	- left amygdala	
Hamartoma	0	1
		- hypothalamic
Ischaemic lesions	1	1
Left/Right		0/1
	- perinatal, leading to ventriculomegaly	- right parieto-occipital
Unclassified lesions	1	1
Left/Right	1/0	1/0
	- left frontal	- left superior frontal
Lateralization Left/Right	3/5	7/3

DNET = dysembryoplastic neuroepithelial tumor

Table 9.4. Epilepsy classification in the at risk populations

	Low Risk N = 19	High risk N = 34
Videotelemetry data available	7	30
Epilepsy syndrome		
temporal (left/right/bitemporal)	4 (1/1/2)	6 (3/2/1)
temporo-occipital (L/R/non-lateralizing)	2 (0/2/0)	1 (0/0/1)
fronto-temporal (L/R/bilateral)	0	6 (4/1/1)
frontal (L/R/non-lateralizing)	0	6 (1/2/3)
parieto-occipital (L/R)	3 (1/2)	3 (1/2)
hemisphere (L/R)	0	1 (1/0)
Lateralisation	2 left / 5 right / 11 non-lateralized	10 left / 7 right / 13 non-lateralized
Focal, non-localisable	6	6
Idiopathic generalised	3	0

L = left; R = right

Table 9.5. Additive odds ratios and individual pathology demonstrated on MRI

Case	group	total risk score	early onset	long duration	CS >3/year	nocturnal seizures	lesion on MRI
1	Low risk	0	0	0	0	0	right temporal occipital FCD
2	Low risk	1.95	0	1.95	0	0	no lesion
3	Low risk	1.95	0	1.95	0	0	no lesion
4	Low risk	3.67	1.72	1.95	0	0	left superior temporal gyrus non specific focus
5	Low risk	3.67	1.72	1.95	0	0	no lesion
6	Low risk	0	0	0	0	0	no lesion
7	Low risk	3.67	1.72	1.95	0	0	right inferior parietal cystic lesion (likely DNET)

8	Low risk	1.95	0	1.95	0	0	no lesion
9	Low risk	1.72	1.72	0	0	0	no lesion
10	Low risk	1.72	1.72	0	0	0	no lesion
11	Low risk	0	0	0	0	0	no lesion
12	Low risk	0	0	0	0	0	no lesion
13	Low risk	0	0	0	0	0	right anterior temporal/amygdala cavernous haemangioma
14	Low risk	3.67	1.72	1.95	0	0	no lesion
15	Low risk	3.67	1.72	1.95	0	0	hypoxic injury
16	Low risk	0	0	0	0	0	exophytic cavernoma or lipoma left inferior colliculus
17	Low risk	1.72	1.72	0	0	0	left hippocampal cavernoma or DNET/left hippocampal sclerosis
18	Low	3.67	1.72	1.95	0	0	right fusiform carvernoma

	risk						
19	Low risk	1.72	1.72	0	0	0	left hippocampal sclerosis
20	High risk	21.08	1.72	0	15.46	3.9	right hippocampal sclerosis
21	High risk	23.03	1.72	1.95	15.46	3.9	no lesion
22	High risk	5.62	1.72	0	0	3.9	left hippocampal sclerosis
23	High risk	7.57	1.72	1.95	0	3.9	left precentral DNET
24	High risk	15.46	0	0	15.46	0	no lesion
25	High risk	19.13	1.72	1.95	15.46	0	subtle left insular malformation
26	High risk	3.9	0	0	0	3.9	no lesion
27	High risk	19.13	1.72	1.95	15.46	0	right parietal damage or dysplasia
28	High risk	19.36	0	0	15.46	3.9	no lesion

29	High risk	21.08	1.72	0	15.46	3.9	left temporal dysplasia, small left hippocampus
30	High risk	7.57	1.72	1.95	0	3.9	no lesion
31	High risk	5.62	1.72	0	0	3.9	no lesion
32	High risk	19.36	0	0	15.46	3.9	left hippocampal sclerosis
33	High risk	7.57	1.72	1.95	0	3.9	right inferior parietal cortical dysplasia
34	High risk	23.03	1.72	1.95	15.46	3.9	no lesion
35	High risk	3.9	0	0	0	3.9	no lesion
36	High risk	21.31	0	1.95	15.46	3.9	left frontal non specific white matter focus
37	High risk	7.57	1.72	1.95	0	3.9	no lesion
38	High risk	19.36	0	0	15.46	3.9	right superior temporal gyrus/polar haematoma (old)
39	High	23.03	1.72	1.95	15.46	3.9	cerebellar atrophy

	risk						
40	High risk	5.62	1.72	0	0	3.9	no lesion
41	High risk	19.13	1.72	1.95	15.46	0	no lesion
42	High risk	23.03	1.72	1.95	15.46	3.9	mature damage left>right gyrus rectus
43	High risk	21.31	0	1.95	15.46	3.9	no lesion
44	High risk	15.46	0	0	15.46	0	no lesion
45	High risk	7.57	1.72	1.95	0	3.9	hypothalamic hamartoma
46	High risk	23.03	1.72	1.95	15.46	3.9	no lesion
47	High risk	19.13	1.72	1.95	15.46	0	no lesion
48	High risk	19.13	1.72	1.95	15.46	0	no lesion
49	High risk	21.08	1.72	0	15.46	3.9	no lesion

50	High risk	23.03	1.72	1.95	15.46	3.9	no lesion
51	High risk	23.03	1.72	1.95	15.46	3.9	no lesion
52	High risk	21.08	1.72	0	15.46	3.9	left supramarginal gyrus dysplasia
53	High risk	23.03	1.72	1.95	15.46	3.9	no lesion
54	SUDEP	0	0	0	0	0	no lesion
55	SUDEP	23.03	1.72	1.95	15.46	3.9	bulky left amygdala with mild FLAIR signal increase
56	SUDEP	19.36	0	0	15.46	3.9	no lesion
57	SUDEP	15.45	0	0	15.46	0	no lesion
58	SUDEP	19.13	1.72	1.95	15.46	0	left hippocampal sclerosis
59	SUDEP	5.85	0	1.95	0	3.9	no lesion
60	SUDEP	21.08	1.72	0	15.46	3.9	bilateral periventricular leucomalacia
61	SUDEP	23.03	1.72	1.95	15.46	3.9	left hippocampal sclerosis
62	SUDEP	3.9	0	0	0	3.9	cavernoma left superior frontal gyrus
63	SUDEP	21.08	1.72	0	15.46	3.9	cavernoma right inferior frontal, in white matter
64	SUDEP	19.13	1.72	1.95	15.46	0	enlarged left amygdala > hippocampus

65	SUDEP	3.9	0	0	0	3.9	right superior temporal DNET

DNET = dysembryoplastic neuroepithelial tumor, FCD = focal cortical dysplasia, SUDEP = sudden unexpected death in epilepsy

9.3.2 MRI data acquisition

All participants had been previously scanned on the same 3 Tesla GE Signa HDx scanner (General Electric, Milwaukee, Wisconsin, U.S.A.), and were scanned with identical acquisition parameters. We used standard imaging gradients, with a maximum strength of 40 mT/m and slew rate of 150 T/m/s. As part of the clinical sequences, a coronal T1-weighted volumetric (3D) scan was acquired with 170 contiguous 1.1 mm thick slices (matrix 256 × 256, in-plane resolution 0.9375 × 0.9375 mm).

9.3.3 MRI data analysis

We used the Voxel Based Morphometry (VBM) 8 toolbox (http://dbm.neuro.uni-jena.de/vbm), implemented in Statistical Parametric Mapping (SPM) 8 software (http://www.fil.ion.ucl.ac.uk/spm) for data analysis. Preprocessing included spatial normalisation to the Montreal Neurological Institute (MNI) template, segmentation into the different tissue classes (grey matter, white matter, cerebrospinal fluid), and modulation to correct for volume changes due to normalisation. Intersubject registration was optimized by employing the DARTEL (Diffeomorphic Anatomical Registration Through Exponentiated Lie Algebra) algorithm. A quality check implemented in the VBM8 Toolbox did not identify any outliers, and grey matter (GM) images were then smoothed with a 10 mm full-width at half maximum Gaussian kernel (Yasuda et al., 2010). The smoothed GM images were entered into a full-factorial design with group as factor to test for local differences in GM volume between groups. Voxels with GM values <0.2 (absolute threshold masking), were excluded to avoid edge

effects between different tissue types. Age at scan was entered as a nuisance variable into the model.

The statistical threshold was set at $p < 0.001$, with a minimum cluster size of 30 contiguous voxels.

9.3.4 Statistical analysis of demographical and clinical data

Statistical analysis of demographical and clinical data was performed with SPSS Version 20.0 (SPSS Inc., Chicago, IL, USA). Pearson's Chi-Square test with an exact significance test for cells with a count of less than five was used for dichotomous data. Kruskal-Wallis test was employed for all other data (Table 9.2).

9.4 Results

9.4.1 Demographic and clinical data

All groups were comparable for gender and age at scan. Epilepsy groups were generally comparable for clinical parameters, except for factors included in the risk scoring, *i.e.* frequent convulsive seizures, nocturnal seizures, and onset of disease (Table 9.2). Of the epilepsy groups, 66.7 % of SUDEP cases, 35.3% of high risk and 47.3% of low risk had a lesion on the scan (Table 9.3).

9.4.2 Voxel Based Morphometry results

SUDEP cases showed increased grey matter volume within the right anterior hippocampus, and parahippocampal gyrus (Figure 9.1 A), and decreased GMV in the pulvinar of the thalamus bilaterally (Figure 9.1 C), compared to controls. In those at high risk, we found similar changes within these regions, *i.e.* GMV increase in the right hippocampus and parahippocampal gyrus (Figure 9.1 B), and decreased GMV in the left pulvinar (Figure 9.1 C), when compared to controls.

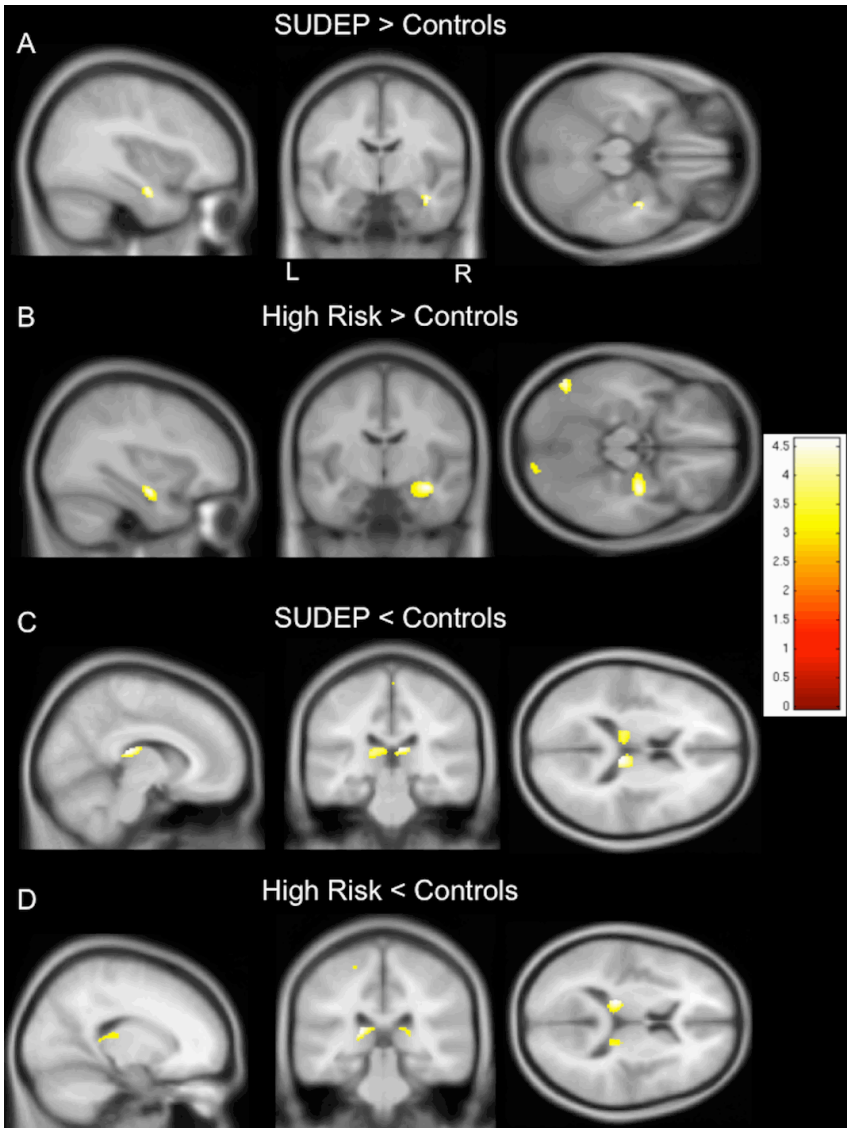

Figure 9.1. Regional grey matter volume differences between SUDEP and people at high risk and controls. A: SUDEP cases show increased grey matter volume in the right hippocampus and parahippocampal gyrus compared to healthy subjects. **B:** Similarly to SUDEP cases, people at high risk show increased grey matter volume in the right hippocampus and parahippocampal gyrus compared to healthy controls. **C:** Compared to controls, grey matter volume is decreased in SUDEP cases in the pulvinar bilaterally. **D:** Likewise, grey matter volume is decreased in those at high risk in the left pulvinar, compared to healthy controls.

T – values are represented in the coloured bars. (p < 0.001, 30 voxel threshold extent)

L = left; R = right

A post-hoc analysis across all cases suggested a negative correlation of GMV within the pulvinar bilaterally with disease duration (Figure 9.2; $p < 0.005$, 30 voxel threshold extent).

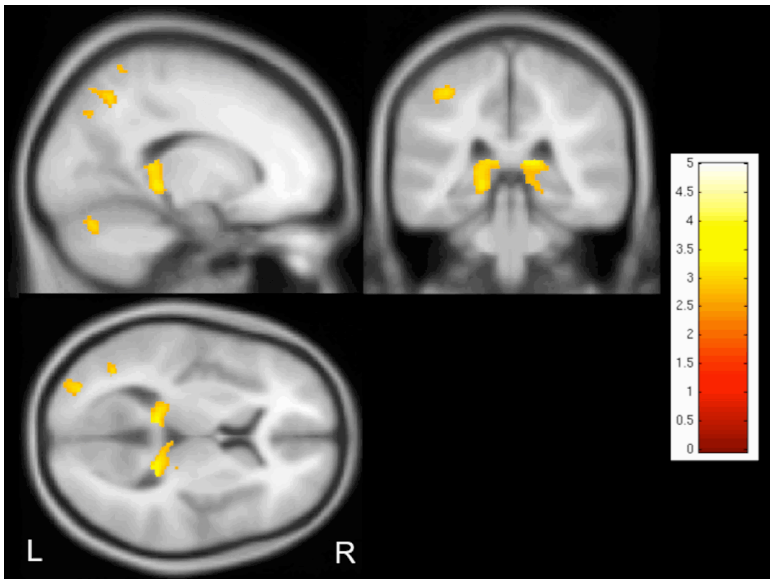

Figure 9.2. Correlation of grey matter volume with disease duration. Regional grey matter volume in bilateral thalamic pulvinar shows a negative correlation with epilepsy duration, i.e. grey matter volume decreases with longer duration ($p < 0.005$, 30 voxel threshold extent). T – values are represented in the coloured bar.
L = left; R = right

Both SUDEP cases and those at high risk showed areas of increased GMV in the right hippocampus and parahippocampal gyrus, compared to those at low risk (threshold of significance $p < 0.05$, 30 voxels threshold extent; Figure 9.3).

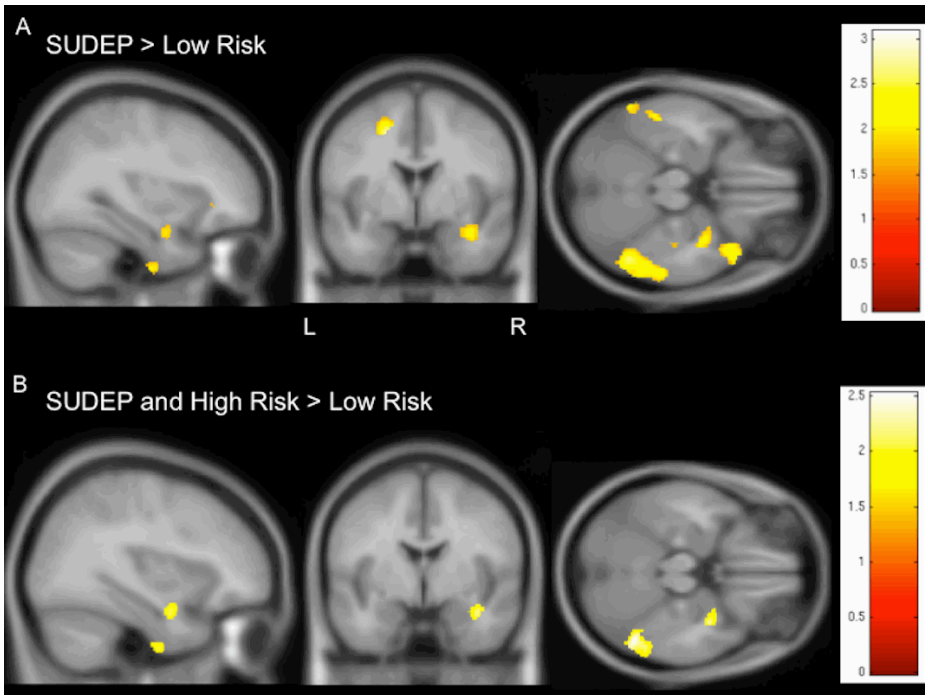

Figure 9.3. Regional grey matter volume differences between SUDEP cases and those at high risk in comparison to people at low risk.

A: Similar to findings in comparison to controls (Fig 9.1 A), but at a lower threshold level ($p < 0.05$, 30 voxels threshold extent), SUDEP cases show increased grey matter volume in the right hippocampus and parahippocampal gyrus in comparison to those at low risk. **B:** People at high risk and SUDEP cases share common areas of increased grey matter volume within the right hippocampus and parahippocampal gyrus when compared to those at low risk (conjunction, $p < 0.05$, 30 voxels threshold extent).

T – values are represented in the coloured bars.

L = left; R = right

9.4.3 Subgroup analyses

To ensure that the findings were not driven by gross brain pathologies, we conducted a subgroup analysis in those at risk who had non-lesional MRI scans (low risk n = 10; high risk n = 22). In the majority of SUDEP cases (66.7%), lesions were evident on clinical scans; hence, due to small sample size, the

same subgroup analysis could not be conducted. Age at scan was entered as a nuisance variable. Compared to controls, those at high risk and without lesions still showed increases in anterior hippocampal GMV, as well as in the amygdala, albeit this time bilaterally (Figure 9.4 A). Similarly, GMV in both hippocampi and amygdalae was increased in people at high risk compared to those at low risk, but more prominent in the right than left amygdala and hippocampus (Figure 9.4 B).

To explore whether findings in the right medial temporal lobe are only related to frequent convulsive seizures, we compared those with more than three convulsive seizures per year to those with fewer convulsive seizures per year in the high risk and SUDEP groups. Fourteen subjects had fewer convulsive seizures (four SUDEP, ten high risk) and 32 had frequent convulsive seizures (eight SUDEP, 24 high risk). Age at scan and gender were entered as nuisance variables. There were no differences within the medial temporal region between both groups. Compared to controls, both groups showed common areas of increased GMV in the right hippocampus (conjunction, $p < 0.005$; Figure 9.5). We also compared total right hippocampal volumes in both groups using an automated segmentation tool (Winston et al., 2013). There were no significant differences in right hippocampal volumes between subjects with frequent and less frequent convulsive seizures (right hippocampal volume in cm^3 in subjects with < 3 convulsive seizures/year: Median 3.036, IQR 0.65; in subjects with >= 3 convulsive seizures/year: Median 2.90, IQR 0.52 cm^3; Mann-Whitney U = 130.000, $p = 0.646$).

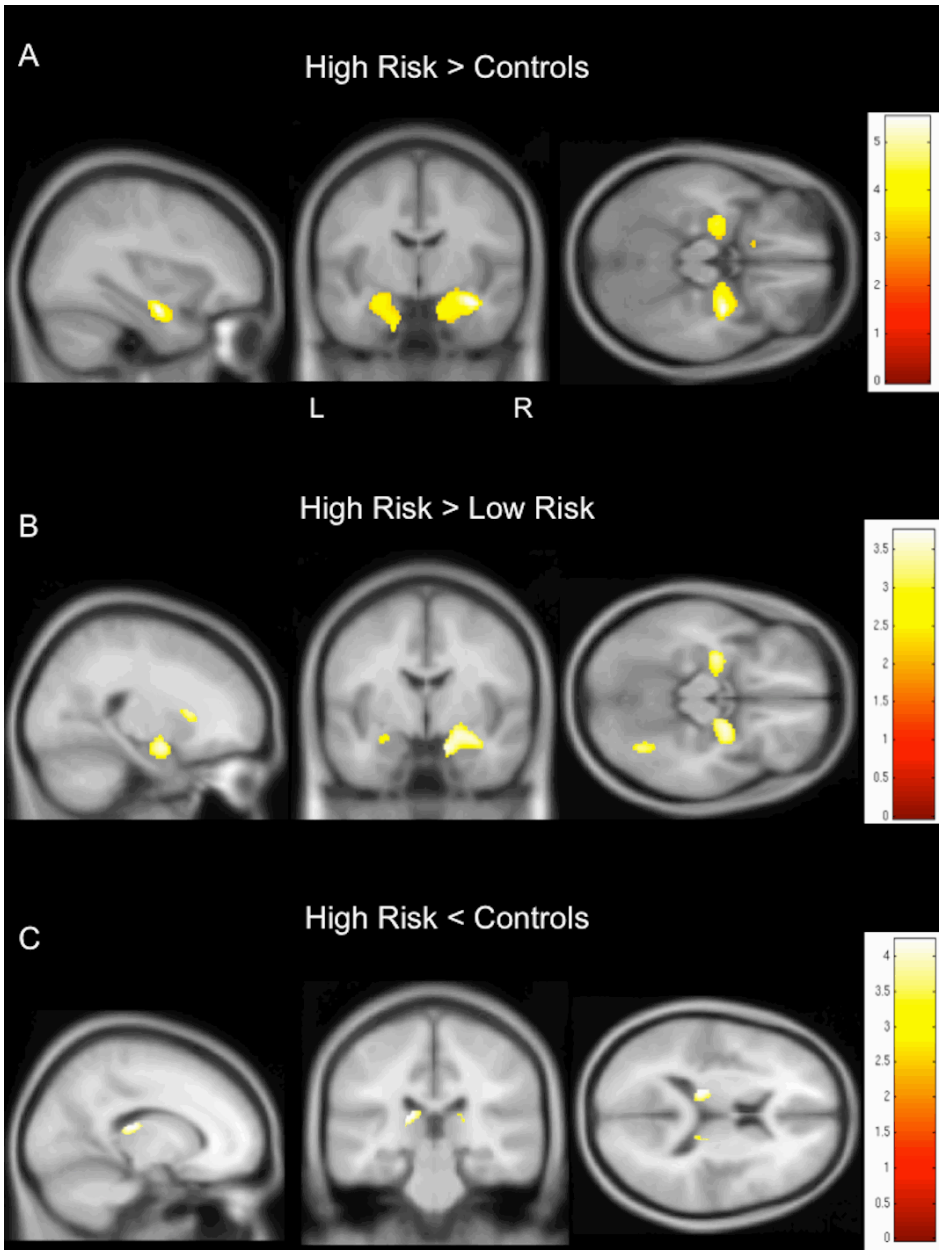

Figure 9.4. Regional grey matter volume differences between those at low and high risk with non-lesional epilepsy and controls. Findings appear similar to previous findings in the whole sample (Figure 9.1), but are more bilateral: People at high risk without identifiable pathology on clinical structural scans show an increase of GMV in both anterior hippocampi and amygdalae when compared to controls (A; $p < 0.001$, 30 voxels threshold extent) and when compared to people at low risk (B; $p < 0.005$, 30 voxels threshold extent). Grey matter volume is decreased in the bilateral posterior thalamus in those at high risk when compared to controls (C; $p < 0.005$, 30 voxels threshold extent).

T – values are represented in the coloured bars

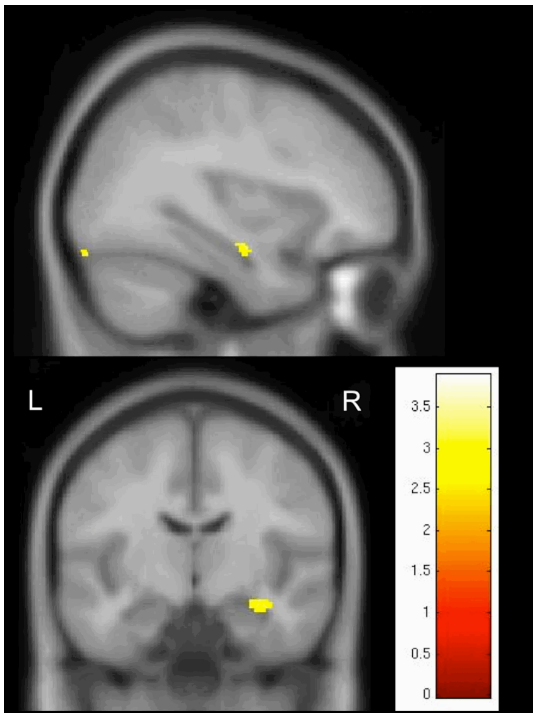

Figure 9.5. Common areas of increased grey matter volume in subjects with frequent and less frequent convulsive seizures compared to controls.
Amongst SUDEP cases and people at high risk of SUDEP, subjects with frequent convulsive seizures (i.e. >= 3/year) and less frequent convulsive seizures (< 3/year) share common areas of increased grey matter volume in the right hippocampus when compared to healthy controls. (conjunction, $p < 0.005$); T – values are represented in the coloured bars.

To relate seizure onset site to right medial temporal findings, subjects with right temporal seizure onset were compared to those with a different, right extratemporal or left hemisphere onset. Ictal EEG data was available in nine SUDEP, 30 high risk and four low risk individuals. In six high risk and one SUDEP case, seizure onset could not be localised and these cases were therefore excluded. There were no differences between these two groups in volumetric findings. In comparison to controls, both groups showed an increase in GMV in the right hippocampus ($p < 0.005$, 30 voxels threshold extent; Figure 9.6).

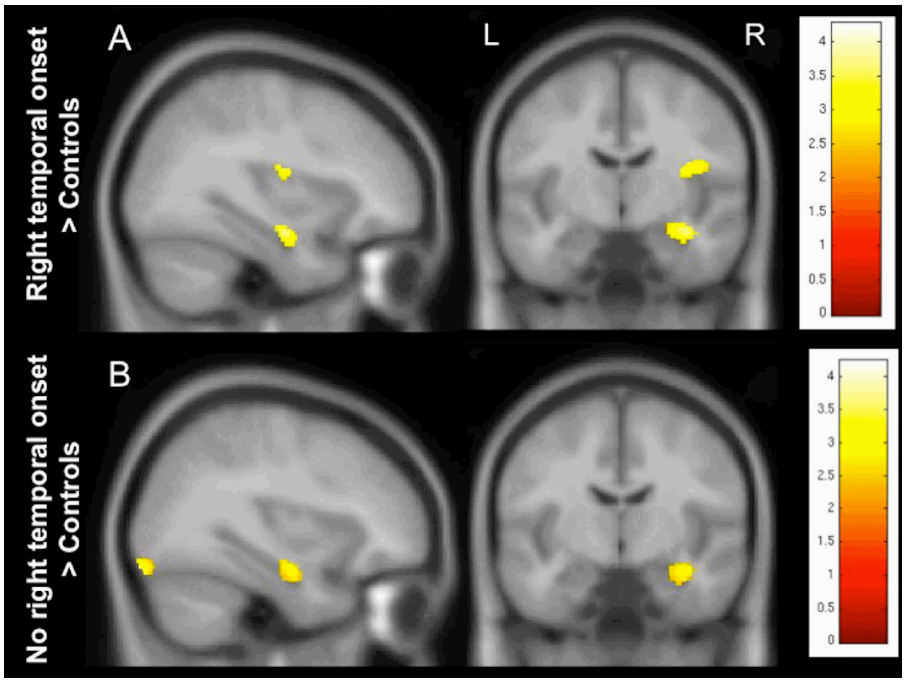

Figure 9.6. Grey matter volume changes in subjects with and without right temporal seizure onset. In comparison to healthy controls, subjects with right temporal seizure onset (Figure 9.6 A), as well as those without (Figure 9.6 B) showed an increase of grey matter volume in the right hippocampus ($p < 0.005$, 30 voxels threshold extent).

T – values are represented in the coloured bars.

L = left; R = right

9.5 Discussion

9.5.1 Anatomical differences between people with SUDEP and high risk versus those at low risk

We identified increased GMV within the right hippocampus and parahippocampal gyrus in SUDEP cases and in people at high risk for SUDEP, compared to people at low risk and controls. There was increased GMV in both hippocampi, extending to the amygdala when comparing non-lesional high and low risk people.

The posterior thalamus (pulvinar) showed disease duration dependent GMV reduction in all patient groups.

MRIs of all cases and controls were subsequently reviewed again by an experienced neuroradiologist, specifically looking for the presence or absence of hippocampal pathology (Table 9.1, Table 9.3). No new lesions within these regions were identified on visual inspection of individual cases, suggesting that the findings are at a group level.

Neuropathological studies in sudden unexplained death in childhood (SUDC) and in sudden infant death syndrome (SIDS) have found abnormalities in the same region; dentate gyrus abnormalities in a large subset of 153 SIDS cases (Kinney et al., 2015) were interpreted as a developmental vulnerability, potentially leading to respiratory/ autonomic instability, or even autonomic seizures and death during sleep when challenged by homeostatic stressors. Hippocampal and temporal lobe anomalies were also described in 62% of SUDC cases (Kinney et al., 2009a). Microdysgenetic features of the hippocampal formation included dentate gyrus and subicular anomalies, granular nodular heterotopia, subventricular neuroblasts and hamartia, all

indicative of aberrant neurodevelopment. Similar to SUDEP cases, those SUDC individuals with structural anomalies were found dead during sleep and in the prone position, and more commonly had an individual or family history of febrile seizures, creating a potential link between hippocampal/temporal lobe maldevelopment, susceptibility to seizures, and sudden death.

Increase in GMV, which has appeared in several epilepsy syndromes in previous VBM studies, has been suggested as indicative of dystopic neurons and diminished grey-white matter demarcation (Yasuda et al., 2010), and findings in the current study may therefore reflect abnormal neurodevelopmental processes. Neuropathological studies in SUDEP show that pathology can be present in the hippocampus (e.g. gliosis) (Zhuo et al., 2012). There are so far, however, no quantitative neuropathological studies of the hippocampus in SUDEP, which would be needed to confirm any subtle abnormalities such as microdysgenesis.

Increased grey matter volumes in the hippocampus may also represent gliosis. Gliosis is a response to injury, and includes neuronal and synaptic functional alterations (Sofroniew, 2009) that have been associated with hyperexcitability in epilepsy. Gliosis within the hippocampus may therefore alter neuronal activity facilitating the risk of SUDEP, e.g. through hyperexcitability and/or limbic network dysfunction implicating also autonomic function (Binder and Steinhäuser, 2006).

A recent study evaluating structural imaging prediction patterns for seizure freedom after surgery in temporal lobe epilepsy found unilateral or bilateral atrophy of the hippocampus, amygdala and entorhinal cortex in most subjects, although one subgroup showed bilaterally increased hippocampal and amygdala volumes (Bernhardt et al., 2015). Subjects in this group were more likely to have unsuccessful epilepsy surgery, supporting the concept that gliosis

may facilitate processes of treatment-resistant disease. Histopathology confirmed hippocampal gliosis in almost all subjects of this subgroup. Astrogliosis and cellular hypertrophy have been described in neuropathological studies in hippocampal tissue of subjects with refractory temporal lobe epilepsy (Das et al., 2012). Mild gliosis is also present in cases of amygdala enlargement (Minami et al., 2015).

Longitudinal VBM studies report a decrease of GMV in mesiotemporal structures and the thalamus with longer disease duration and more active disease, *i.e.* frequent seizures (Bernhardt et al., 2009; Coan et al., 2009). Similarly, changes in the posterior thalamus correlate with disease duration in our cohort and this suggests a dynamic origin of GMV alterations in our study. A potential mechanism for gliosis in epilepsy could be repeated hypoxic insults, particularly through convulsive seizures (Macey et al., 2009).

That increased grey matter volume may represent gliosis and plasticity following neural injury (Yasuda et al., 2010) is corroborated by data in other sudden death entities: Increased grey matter volume in the putamen appears in people with newly-diagnosed obstructive sleep apnoea, who are subjected to repeated hypoxic episodes, with the increased volumes usually attributed to transitional processes in glial death accompanying the neural injury in the syndrome (Kumar et al., 2014).

9.5.2 Association with autonomic dysfunction and significance of laterality of findings

Several functional imaging studies in humans (e.g. (Shoemaker et al., 2012, 2015)), and stimulation studies in animals (Terreberry and Neafsey, 1987) have identified the hippocampus as an essential component of limbic circuitry

modulating autonomic function, with substantial influences on blood pressure regulation (Harper et al., 2000).

Major hippocampal influence on autonomic activity through efferent projections can also be assumed from intracerebral stimulation studies in people with refractory epilepsy (Catenoix et al., 2011). These influences are corroborated by reports of people with mesial temporal lobe epilepsy who show decreased heart rate variability (HRV) in relation to seizures and interictal epileptic discharges, which were more pronounced during sleep, when most cases of SUDEP occur (Moseley et al., 2011). Of interest, HRV normalizes in some after successful TLE surgery (Hilz et al., 2002).

Hippocampal grey matter volume increases in our cohort may partially underlie seizure generation and ictal and periictal autonomic dysfunction. However, increased right hippocampal grey matter volume was even present in those individuals with known right medial temporal epilepsy when compared to healthy controls (no cases of hippocampal sclerosis in either group). The increased grey matter volume was highly surprising, as longitudinal VBM data describe progressive atrophy of the ipsilateral hippocampus in the medial temporal lobe, especially in those people with higher seizure frequency and longer epilepsy duration, *i.e.* higher SUDEP risk (Bernhardt et al., 2009; Coan et al., 2009). This may suggest that our findings are not associated with a primarily seizure-related autonomic dysfunction; but they may be associated with an interictal autonomic dysregulation. At this time this is a speculative suggestion, and needs investigation of autonomic function in similar cohorts.

9.5.3 Asymmetry of grey matter volume increases

A significant aspect of the grey matter volume hippocampal increase in SUDEP cases and people at high risk was the asymmetry, with the volume changes on the right side. The lateralization of tissue change in an autonomic regulatory area poses a serious concern for sympathetic and parasympathetic outflow. If laterality on sympathetic influences is preserved to medullary output nuclei, the consequences to cardiac arrhythmia generation are severe, since asymmetric sympathetic outflow leads to such phenomena as potentially fatal long QT syndrome (Schwartz, 1998). The right insula plays a more prominent role with sympathetic regulation, while parasympathetic regulation is primarily mediated on the left insula (Oppenheimer, 2006) as determined by a series of stimulation, lesion, stroke, and imaging studies, including human epilepsy surgical studies (Oppenheimer et al., 1992). Both injury to the right limbic system and direct insular stimulation have been associated with sympathetic overregulation (Oppenheimer, 2006). Sudden death after acute right-sided insular strokes and increased complex arrhythmias appear more often than in any other lesion localization (Sörös and Hachinski, 2012). Right insular injury in obstructive sleep apnoea show distorted blood pressure recovery patterns to a challenge (Harper et al., 2003; Henderson et al., 2003) and right hemisphere strokes, particularly when involving the insula, are accompanied by increased nocturnal blood pressure, higher noradrenaline levels and QTc prolongations (Oppenheimer, 2006). The insular effects appear to be mediated by projections to the ventral medial frontal cortex, hypothalamus, and hippocampus through integrated circuitry (Shoemaker et al., 2015). The lateralized (right) increased mesiotemporal grey matter volume in our cohort may contribute to chronic, asymmetric hyper-sympathetic activation, or a sympathetic system lacking in

appropriate responsiveness, which would contribute to mechanisms that pose a risk for sudden death.

Similar scenarios develop for obstructive sleep apnea and for heart failure, which induce severe injury preferentially in the right insula, and consequential very high resting, and unresponsive, sympathetic tone (Macey et al., 2002; Woo et al., 2005). An imbalance between parasympathetic and sympathetic drive places an individual at risk, resulting in a tendency to postictal bradycardia/asystole as noted in the MORTEMUS study (Ryvlin et al., 2013).

9.5.4 Decreased grey matter volume in the posterior thalamus

A second major finding was that grey matter volume was reduced in the posterior thalamus, and correlated with disease duration. The finding was not unique to SUDEP. A decrease of grey matter volume in the posterior thalamus correlated with disease duration in all people with epilepsy (Figure 9.2), and one may speculate that those changes may develop in low risk people, given sufficient duration of seizures. However, the finding of posterior thalamic GMV should be taken in the context of roles for that structure in respiratory regulation. Substantial evidence, ranging from lesion and stimulation studies in the foetal lamb (Koos et al., 1998, 2004), to fMRI studies in adolescents and children with congenital central hypoventilation syndrome (Macey et al., 2005) show the significant role of the posterior thalamus in mediating breathing responses following manipulation of oxygen levels, with special participation in the inhibition of breathing following hypoxic exposure (Koos et al., 1998, 2004). We speculate that injury to the posterior thalamus is common in people with epilepsy, that the evidence suggests that disease duration potentiates that injury, and that such injury poses particular risk to the hypoxia normally

accompanying ictal episodes, causing thalamic structures to fail to adequately recover from low oxygen. A thalamic role must, however, be viewed in the context that in people who succumbed to SUDEP or who were at high risk also were burdened with right-sided grey matter volume increases in the hippocampal region, which would compromise appropriate blood pressure responses that accompany apnoea. Thus, the combination of injury, diminished posterior thalamic and altered right-sided hippocampal grey matter volume may impose a set of circumstances leading to vital failure.

The mechanisms underlying decreased thalamic grey matter volume should be considered; the decline emerges in several epilepsy syndromes (Yasuda et al., 2010), and appears to be, in part, independent of epilepsy severity, presence of MRI lesions, and duration (Keller et al., 2002). Strong relationships of disease duration and declines in grey matter volume and changes in white matter tract microstructure, *i.e.* mean fractional anisotropy (FA) declines, have been described, and may underlie progressive brain changes in response to active disease, *i.e.* recurrent seizures (Keller et al., 2012).

High risk for SUDEP has been reported in those who fail epilepsy surgery (Sperling et al., 2005). Persistent seizures in subjects who had undergone amygdalo-hippocampectomy for unilateral temporal lobe epilepsy were associated with pre-operative atrophy of bilateral dorsomedial and pulvinar thalamic regions (Keller et al., 2015), with the investigators arguing that these regions are important hubs of seizure modulation and spread. We suggest that the risk may stem from failure of a combined interaction of breathing and blood pressure control.

9.5.5 Limitations

The criteria used to define our risk groups, and the cut-off between high and low risk, were arbitrary. The finding that SUDEP and those at high risk show similar patterns is consistent with our definition of risk groups. Eleven of 12 SUDEP cases were classified as high risk with our criteria.

A major limitation of our study is to disentangle whether our finding of right hippocampal GMV increase is a specific SUDEP risk factor or rather a marker of severe epilepsy.

As there was only one low risk case in our SUDEP group, we could not establish whether increased right hippocampal GMV is present in SUDEP cases despite being labelled low risk. This would have marked our finding as more SUDEP specific. *In vivo* imaging biomarkers of SUDEP risk should be present in both, people who later on died from, and those at high risk of, SUDEP. We argue that the smaller the difference we observe between those two groups, the better our classification and definition of high risk criteria. Similarly, main risk factors for SUDEP, like frequent, uncontrolled convulsive seizures, will have to be present in both SUDEP and high risk groups (Hesdorffer et al., 2011), and hence, are also the major distinguishing factor of high risk versus low risk subjects in our study. By the nature of SUDEP and our study, it is therefore impossible to fully disentangle the effect of severe epilepsy from a specific SUDEP biomarker itself.

Due to methodological challenges (Ashburner and Ridgway, 2012), there are only few longitudinal VBM studies in people with mesial temporal lobe epilepsy. All of them show grey matter atrophy within mesial temporal structures and beyond (e.g. thalamus) over time, which are more progressive with longer disease duration and higher seizure frequency (Bernhardt et al., 2009; Coan et al., 2009). Evaluation of subregional mesiotemporal disease progression

revealed that progressive atrophy particularly involves the anterior part of the hippocampus (Bernhardt et al., 2013). These reports are in clear contrast to our findings of increased GMV particularly in the anterior hippocampus and suggest that these are not only caused by frequent seizures. There are poor data on exact seizure counts in our groups, but when subjects in the high risk and SUDEP groups where dichotomized into those with frequent (*i.e.* > 3 convulsive seizures/year) and those with less frequent convulsive seizures, there were no significant group differences within the right hippocampus but both groups showed common areas of increased right hippocampal GMV when compared to healthy controls (Figure 9.5). In addition, total right hippocampal volume measures did not differ between groups. This underscores our argument that the findings represent more specific SUDEP markers than just markers of severe epilepsy.

In keeping with the longitudinal data, posterior thalamic grey matter atrophy correlates with disease duration in our cohort and we can therefore confirm that this finding is not a specific SUDEP biomarker.

We appreciate that epilepsy groups in this study combine various different epilepsy subtypes, and include people with lesional and non-lesional MRI scans (Table 9.3). Right hippocampal sclerosis was, however, not present in either epilepsy group, and therefore does not explain differences in right hippocampal GMV. Structural abnormalities were common among our SUDEP population (66.7% of cases), and we acknowledge that our SUDEP group may therefore not be representative of all SUDEP cases.

A previous study (Mueller et al., 2014) described decreased midbrain volume using graph analysis methodology in two SUDEP cases compared to controls. We did not aim to examine brainstem volumes, although our whole-brain analysis included the brainstem; we found no abnormal changes in the brainstem within any group. Voxel based morphometry has substantial

limitations in evaluating brainstem segmentation, due to the difficulty in resolving internal brainstem architecture reliably and consistently (Lamberts et al., 2012). Disturbances in brainstem attributes may be better evaluated with newer procedures for examining tissue changes, such as diffusion MRI.

9.5.6 Conclusions

Increased right hippocampal and parahippocampal GMV and GMV decline in the posterior thalamus appears to be related to SUDEP risk. In the case of GMV increases, the relationship is independent of markers of severe epilepsy, such as frequent convulsive seizures. The volume increases are potentially of dynamic origin, representing gliosis in response to repetitive injury from severe epilepsy, while the thalamic volume declines may result from excitotoxic or other injury sources. The thalamic injury may lead to an inability to recover breathing to a hypoxic challenge from apnoea, while the hippocampal/parahippocampal pathology may contribute to asymmetric influences on autonomic outflow, establishing circumstances for cardiac arrhythmia and hypotension. The structural changes may be useful biomarkers to assist determination of pathophysiology of SUDEP.

Chapter 10: Conclusions and outlook

10.1 Imaging endophenotypes in juvenile myoclonic epilepsy

Using fMRI and a working memory paradigm, we identified a functional endophenotype in patients with JME and their unaffected siblings. Our findings underscore previous results in JME from our group, *i.e.* attenuated deactivation of the motor system and increased functional and structural connectivity between fronto-parietal cognitive networks and the motor cortex. Similar functional findings in unaffected siblings support our hypothesis of a genetically determined neurodevelopmental condition.

Though the findings offer a pathophysiological explanation for both subtle frontal lobe cognitive impairment and cognitively triggered jerks in JME, their syndrome specificity is yet to be proven. Reflex mechanisms have been described in other epilepsy syndromes, particularly in genetic generalised epilepsies, and impaired functional segregation of large scale networks is likely a common pathomechanism of GGE (Badawy et al., 2013; Koepp et al., 2016). Future studies ideally employing the same fMRI working memory paradigm in other GGE syndromes, such as childhood and juvenile absence epilepsies, are necessary to establish whether our findings are truly syndrome specific for JME.

One may criticize that the endophenotypes described in this work have only been identified at group level so far, rendering practical applications at single subject level, e.g. identifying “cases” for genetic studies, difficult (Berkovic and Jackson, 2014). One possible application for gene discovery is to use the described functional imaging findings as a quantitative trait in a probabilistic approach in conjunction with genome-wide association, as previously employed

in schizophrenia (Potkin et al., 2009). In addition, studies ideally in untreated, newly-diagnosed patient groups, removing confounding factors of treatment and disease duration, may help to eventually translate findings to the single subject level.

10.2 Pharmacological fMRI

In two retrospective studies in patients with refractory epilepsy, I was able to show drug specific effects on cognitive networks. Levetiracetam lead to normalisation of mesial temporal lobe deactivation. Our study design allowed us to show that this was a syndrome and task specific effect, *i.e.* it was observed in the right temporal lobe during a non-verbal working memory task in in right TLE, and in the left temporal lobe during a verbal working memory task in left TLE. Topiramate and Zonisamide were associated with a dysfunction of language, sustained-attention and working memory specific activation networks. This included a decrease of activation in task-relevant regions. In addition, TPM showed regionally and task specific impaired attenuation of task-negative networks. This was in keeping with an overall poorer cognitive performance than observed for ZNS in this study, and with the clinical experience that ZNS has less negative effects on cognition than TPM.

Limitations of these studies are, that they were both conducted in patients with chronic and refractory epilepsy, in who one expects a higher degree of cognitive impairment due to disease duration and uncontrolled seizures than for example in recent-onset patients who are treatment-responders. In addition, the majority of patients were on co-medication. Even though we included co-medications as regressor of no interest into our statistical models, we could not fully control for AED interactions, as well as additive detrimental effects on cognitive function due to polytherapy (Witt et al., 2015).

To study more specific AED effects and their dynamic changes over disease duration and/or their interaction with the disease, future studies will have to prospectively assess the effects of AEDs on both cognitive and epileptogenic networks. Ideally AEDs should be studied in mono-therapy, or at least as first

add-on drug to reduce medication confounders, and pre- and post treatment initiation.

Furthermore, it has been suggested by other researchers in the field (Borsook et al., 2013), that drug efficacy is probably best studied via functional connectivity analysis, whereas task-based regional activation may be more appropriate for evaluation of specific cognitive side effects.

Longitudinal resting state and task-based imaging studies may thus enable us to understand long-term drug effects on specific cognitive or more disease related networks. They may help to understand whether chronic AED exposure can eventually lead to normalisation of aberrant, disease/seizure-related functional networks, and mechanisms in non-responders, or more dynamic changes, such as development of treatment resistance to a substance that previously lead to long-term symptom benefit.

Overall, ph-MRI studies in epilepsy are sparse. However, we know from studies in other disease entities, particularly affective disorders and pain research (Nathan et al., 2014), that ph-MRI studies show consistent and reproducible changes on disease relevant networks and prove sufficiently sensitive to detect dose-dependent network changes early, prior to clinical change, and can predict long-term efficacy, providing promising new tools for a personalised treatment planning and future CNS drug-development.

10.3 Imaging markers of sudden death in epilepsy

Our structural imaging analysis in patients who either died or were at high risk of sudden unexpected death in epilepsy (SUDEP) showed increased right hippocampal and parahippocampal grey matter volume (GMV) and GMV decline in the posterior thalamus.

In our exploratory analysis in a relatively small data set, we could not yet disentangle whether the abnormalities indicate seizure-induced damage/ response to repetitive seizure-related damage, *i.e.* gliosis, or signify a-priori changes. The latter is intriguing given similar changes in sudden infant and childhood death cases, though not on imaging but in neuropathological studies (Kinney et al., 2009a, 2015). Implicated regions lie within autonomic regulatory circuits, as well as within or in proximity to critical epilepsy/seizure network hubs, and are therefore interesting targets for further exploration in future studies.

A further problem that other studies exploring SUDEP biomarkers also face is the specificity of our findings in the context of potential effects of high disease load, which in itself is a risk factor for SUDEP.

Apart from the obvious next steps to try to confirm or refute our findings in larger data-sets, additional directions could be a refinement of risk stratification through electrographic and autonomic data from video-telemetry units and a multimodal imaging approach including functional and structural connectivity, as well as looking at neuroimaging data across (neurological) sudden death entities, such as sleep apnoea and stroke.

References

Abou-Khalil, B.W., 2016. Antiepileptic Drugs. Contin. Minneap. Minn 22, 132–156. doi:10.1212/CON.0000000000000289

Aiba, I., Noebels, J.L., 2015. Spreading depolarization in the brainstem mediates sudden cardiorespiratory arrest in mouse SUDEP models. Sci. Transl. Med. 7, 282ra46. doi:10.1126/scitranslmed.aaa4050

Akgun, Y., Soysal, A., Atakli, D., Yuksel, B., Dayan, C., Arpaci, B., 2009. Cortical excitability in juvenile myoclonic epileptic patients and their asymptomatic siblings: a transcranial magnetic stimulation study. Seizure 18, 387–391. doi:10.1016/j.seizure.2009.02.002

Aldenkamp, A.P., Baker, G., Mulder, O.G., Chadwick, D., Cooper, P., Doelman, J., Duncan, R., Gassmann-Mayer, C., de Haan, G.J., Hughson, C., Hulsman, J., Overweg, J., Pledger, G., Rentmeester, T.W., Riaz, H., Wroe, S., 2000. A multicenter, randomized clinical study to evaluate the effect on cognitive function of topiramate compared with valproate as add-on therapy to carbamazepine in patients with partial-onset seizures. Epilepsia 41, 1167–1178.

Alhusaini, S., Ronan, L., Scanlon, C., Whelan, C.D., Doherty, C.P., Delanty, N., Fitzsimons, M., 2013. Regional increase of cerebral cortex thickness in juvenile myoclonic epilepsy. Epilepsia 54, e138-141. doi:10.1111/epi.12330

Andrews-Hanna, J.R., 2012. The brain's default network and its adaptive role in internal mentation. Neurosci. Rev. J. Bringing Neurobiol. Neurol. Psychiatry 18, 251–270. doi:10.1177/1073858411403316

Annegers, J.F., Coan, S.P., Hauser, W.A., Leestma, J., 2000. Epilepsy, vagal nerve stimulation by the NCP system, all-cause mortality, and sudden, unexpected, unexplained death. Epilepsia 41, 549–553.

Appleton, R., Beirne, M., Acomb, B., 2000. Photosensitivity in juvenile myoclonic epilepsy. Seizure 9, 108–111. doi:10.1053/seiz.1999.0376

Arif, H., Buchsbaum, R., Weintraub, D., Pierro, J., Resor, S.R., Hirsch, L.J., 2009. Patient-reported cognitive side effects of antiepileptic drugs: predictors and comparison of all commonly used antiepileptic drugs. Epilepsy Behav. EB 14, 202–209. doi:10.1016/j.yebeh.2008.10.017

Ashburner, J., 2007. A fast diffeomorphic image registration algorithm. NeuroImage 38, 95–113. doi:10.1016/j.neuroimage.2007.07.007

Ashburner, J., Andersson, J.L., Friston, K.J., 2000. Image registration using a symmetric prior--in three dimensions. Hum. Brain Mapp. 9, 212–225.

Ashburner, J., Friston, K.J., 2000. Voxel-based morphometry--the methods. NeuroImage 11, 805–821. doi:10.1006/nimg.2000.0582

Ashburner, J., Ridgway, G.R., 2012. Symmetric diffeomorphic modeling of longitudinal structural MRI. Front. Neurosci. 6, 197. doi:10.3389/fnins.2012.00197

Atakli, D., Soysal, A., Atay, T., Altintas, H., Arpaci, B., Baybas, S., 1999. Somatosensory evoked potentials and EEG findings in siblings of juvenile myoclonic epilepsy patients. Epileptic Disord. Int. Epilepsy J. Videotape 1, 173–177.

Badawy, R.A.B., Vogrin, S.J., Lai, A., Cook, M.J., 2013. Capturing the epileptic trait: cortical excitability measures in patients and their unaffected siblings. Brain J. Neurol. 136, 1177–1191. doi:10.1093/brain/awt047

Bagnall, R.D., Crompton, D.E., Petrovski, S., Lam, L., Cutmore, C., Garry, S.I., Sadleir, L.G., Dibbens, L.M., Cairns, A., Kivity, S., Afawi, Z., Regan,

B.M., Duflou, J., Berkovic, S.F., Scheffer, I.E., Semsarian, C., 2015. Exome-based analysis of cardiac arrhythmia, respiratory control and epilepsy genes in sudden unexpected death in epilepsy. Ann. Neurol. doi:10.1002/ana.24596

Bakker, A., Albert, M.S., Krauss, G., Speck, C.L., Gallagher, M., 2015. Response of the medial temporal lobe network in amnestic mild cognitive impairment to therapeutic intervention assessed by fMRI and memory task performance. NeuroImage Clin. 7, 688–698. doi:10.1016/j.nicl.2015.02.009

Bakker, A., Krauss, G.L., Albert, M.S., Speck, C.L., Jones, L.R., Stark, C.E., Yassa, M.A., Bassett, S.S., Shelton, A.L., Gallagher, M., 2012. Reduction of hippocampal hyperactivity improves cognition in amnestic mild cognitive impairment. Neuron 74, 467–474. doi:10.1016/j.neuron.2012.03.023

Bateman, L.M., Li, C.-S., Lin, T.-C., Seyal, M., 2010. Serotonin reuptake inhibitors are associated with reduced severity of ictal hypoxemia in medically refractory partial epilepsy. Epilepsia 51, 2211–2214. doi:10.1111/j.1528-1167.2010.02594.x

Bateman, L.M., Li, C.-S., Seyal, M., 2008. Ictal hypoxemia in localization-related epilepsy: analysis of incidence, severity and risk factors. Brain J. Neurol. 131, 3239–3245. doi:10.1093/brain/awn277

Baxendale, S., Thompson, P.J., Duncan, J.S., 2008. Improvements in memory function following anterior temporal lobe resection for epilepsy. Neurology 71, 1319–1325. doi:10.1212/01.wnl.0000319699.04265.fd

Beltramini, G.C., Cendes, F., Yasuda, C.L., 2015. The effects of antiepileptic drugs on cognitive functional magnetic resonance imaging. Quant. Imaging Med. Surg. 5, 238–246. doi:10.3978/j.issn.2223-4292.2015.01.04

Beniczky, S., Guaranha, M.S.B., Conradsen, I., Singh, M.B., Rutar, V., Lorber, B., Braga, P., Fressola, A.B., Inoue, Y., Yacubian, E.M.T., Wolf, P., 2012. Modulation of epileptiform EEG discharges in juvenile myoclonic epilepsy: an investigation of reflex epileptic traits. Epilepsia 53, 832–839. doi:10.1111/j.1528-1167.2012.03454.x

Berg, A.T., Berkovic, S.F., Brodie, M.J., Buchhalter, J., Cross, J.H., van Emde Boas, W., Engel, J., French, J., Glauser, T.A., Mathern, G.W., Moshé, S.L., Nordli, D., Plouin, P., Scheffer, I.E., 2010. Revised terminology and concepts for organization of seizures and epilepsies: report of the ILAE Commission on Classification and Terminology, 2005-2009. Epilepsia 51, 676–685. doi:10.1111/j.1528-1167.2010.02522.x

Berg, A.T., Millichap, J.J., 2013. The 2010 revised classification of seizures and epilepsy. Contin. Minneap. Minn 19, 571–597. doi:10.1212/01.CON.0000431377.44312.9e

Berkovic, S.F., Jackson, G.D., 2014. “Idiopathic” no more! Abnormal interaction of large-scale brain networks in generalized epilepsy. Brain J. Neurol. 137, 2400–2402. doi:10.1093/brain/awu194

Bernasconi, A., Bernasconi, N., Bernhardt, B.C., Schrader, D., 2011. Advances in MRI for “cryptogenic” epilepsies. Nat. Rev. Neurol. 7, 99–108. doi:10.1038/nrneurol.2010.199

Bernhardt, B.C., Chen, Z., He, Y., Evans, A.C., Bernasconi, N., 2011. Graph-theoretical analysis reveals disrupted small-world organization of cortical thickness correlation networks in temporal lobe epilepsy. Cereb. Cortex N. Y. N 1991 21, 2147–2157. doi:10.1093/cercor/bhq291

Bernhardt, B.C., Hong, S.-J., Bernasconi, A., Bernasconi, N., 2015. Magnetic resonance imaging pattern learning in temporal lobe epilepsy:

classification and prognostics. Ann. Neurol. 77, 436–446. doi:10.1002/ana.24341
Bernhardt, B.C., Kim, H., Bernasconi, N., 2013. Patterns of subregional mesiotemporal disease progression in temporal lobe epilepsy. Neurology 81, 1840–1847. doi:10.1212/01.wnl.0000436069.20513.92
Bernhardt, B.C., Worsley, K.J., Kim, H., Evans, A.C., Bernasconi, A., Bernasconi, N., 2009. Longitudinal and cross-sectional analysis of atrophy in pharmacoresistant temporal lobe epilepsy. Neurology 72, 1747–1754. doi:10.1212/01.wnl.0000345969.57574.f5
Bianchi, A., Viaggi, S., Chiossi, E., LICE Episcreen Group, 2003. Family study of epilepsy in first degree relatives: data from the Italian Episcreen Study. Seizure 12, 203–210.
Bigos, K.L., Weinberger, D.R., 2010. Imaging genetics--days of future past. NeuroImage 53, 804–809. doi:10.1016/j.neuroimage.2010.01.035
Binder, D.K., Steinhäuser, C., 2006. Functional changes in astroglial cells in epilepsy. Glia 54, 358–368. doi:10.1002/glia.20394
Binder, J.R., Desai, R.H., Graves, W.W., Conant, L.L., 2009. Where is the semantic system? A critical review and meta-analysis of 120 functional neuroimaging studies. Cereb. Cortex N. Y. N 1991 19, 2767–2796. doi:10.1093/cercor/bhp055
Binnie, C.D., 2003. Cognitive impairment during epileptiform discharges: is it ever justifiable to treat the EEG? Lancet Neurol. 2, 725–730.
Blokland, G.A.M., McMahon, K.L., Thompson, P.M., Martin, N.G., de Zubicaray, G.I., Wright, M.J., 2011. Heritability of working memory brain activation. J. Neurosci. Off. J. Soc. Neurosci. 31, 10882–10890. doi:10.1523/JNEUROSCI.5334-10.2011
Blum, D., Meador, K., Biton, V., Fakhoury, T., Shneker, B., Chung, S., Mills, K., Hammer, A., Isojärvi, J., 2006. Cognitive effects of lamotrigine compared with topiramate in patients with epilepsy. Neurology 67, 400–406. doi:10.1212/01.wnl.0000232737.72555.06
Blumenfeld, H., 2005. Consciousness and epilepsy: why are patients with absence seizures absent? Prog. Brain Res. 150, 271–286. doi:10.1016/S0079-6123(05)50020-7
Bootsma, H.P.R., Ricker, L., Diepman, L., Gehring, J., Hulsman, J., Lambrechts, D., Leenen, L., Majoie, M., Schellekens, A., de Krom, M., Aldenkamp, A.P., 2008. Long-term effects of levetiracetam and topiramate in clinical practice: A head-to-head comparison. Seizure 17, 19–26. doi:10.1016/j.seizure.2007.05.019
Borsook, D., Becerra, L., Fava, M., 2013. Use of functional imaging across clinical phases in CNS drug development. Transl. Psychiatry 3, e282. doi:10.1038/tp.2013.43
Borsook, D., Becerra, L., Hargreaves, R., 2006. A role for fMRI in optimizing CNS drug development. Nat. Rev. Drug Discov. 5, 411–424. doi:10.1038/nrd2027
Bullmore, E., 2012. The future of functional MRI in clinical medicine. NeuroImage 62, 1267–1271. doi:10.1016/j.neuroimage.2012.01.026
Burns, T.G., Lee, G.P., McCormick, M.L., Pettoni, A.N., Flamini, J.R., Cohen, M., 2009. Carbonic anhydrase-inhibiting medications and the intracarotid amobarbital procedure in children. Epilepsy Behav. EB 15, 240–244. doi:10.1016/j.yebeh.2009.01.006
Callicott, J.H., Egan, M.F., Mattay, V.S., Bertolino, A., Bone, A.D., Verchinksi, B., Weinberger, D.R., 2003. Abnormal fMRI response of the dorsolateral prefrontal cortex in cognitively intact siblings of patients with schizophrenia. Am. J. Psychiatry 160, 709–719. doi:10.1176/appi.ajp.160.4.709

Camfield, C.S., Camfield, P.R., 2009. Juvenile myoclonic epilepsy 25 years after seizure onset: a population-based study. Neurology 73, 1041–1045. doi:10.1212/WNL.0b013e3181b9c86f

Cannon, T.D., Keller, M.C., 2006. Endophenotypes in the genetic analyses of mental disorders. Annu. Rev. Clin. Psychol. 2, 267–290. doi:10.1146/annurev.clinpsy.2.022305.095232

Cao, B., Tang, Y., Li, J., Zhang, X., Shang, H.-F., Zhou, D., 2013. A meta-analysis of voxel-based morphometry studies on gray matter volume alteration in juvenile myoclonic epilepsy. Epilepsy Res. 106, 370–377. doi:10.1016/j.eplepsyres.2013.07.003

Carmichael, K., Pulman, J., Lakhan, S.E., Parikh, P., Marson, A.G., 2013. Zonisamide add-on for drug-resistant partial epilepsy. Cochrane Database Syst. Rev. CD001416. doi:10.1002/14651858.CD001416.pub3

Catenoix, H., Magnin, M., Mauguière, F., Ryvlin, P., 2011. Evoked potential study of hippocampal efferent projections in the human brain. Clin. Neurophysiol. Off. J. Int. Fed. Clin. Neurophysiol. 122, 2488–2497. doi:10.1016/j.clinph.2011.05.007

Coan, A.C., Appenzeller, S., Bonilha, L., Li, L.M., Cendes, F., 2009. Seizure frequency and lateralization affect progression of atrophy in temporal lobe epilepsy. Neurology 73, 834–842. doi:10.1212/WNL.0b013e3181b783dd

Corey, L.A., Pellock, J.M., Kjeldsen, M.J., Nakken, K.O., 2011. Importance of genetic factors in the occurrence of epilepsy syndrome type: a twin study. Epilepsy Res. 97, 103–111. doi:10.1016/j.eplepsyres.2011.07.018

Coull, J.T., 1998. Neural correlates of attention and arousal: insights from electrophysiology, functional neuroimaging and psychopharmacology. Prog. Neurobiol. 55, 343–361.

Cousijn, H., Rijpkema, M., Qin, S., van Wingen, G.A., Fernández, G., 2012. Phasic deactivation of the medial temporal lobe enables working memory processing under stress. NeuroImage 59, 1161–1167. doi:10.1016/j.neuroimage.2011.09.027

Das, A., Wallace, G.C., Holmes, C., McDowell, M.L., Smith, J.A., Marshall, J.D., Bonilha, L., Edwards, J.C., Glazier, S.S., Ray, S.K., Banik, N.L., 2012. Hippocampal tissue of patients with refractory temporal lobe epilepsy is associated with astrocyte activation, inflammation, and altered expression of channels and receptors. Neuroscience 220, 237–246. doi:10.1016/j.neuroscience.2012.06.002

de Araujo Filho, G.M., Yacubian, E.M.T., 2013. Juvenile myoclonic epilepsy: psychiatric comorbidity and impact on outcome. Epilepsy Behav. EB 28 Suppl 1, S74-80. doi:10.1016/j.yebeh.2013.03.026

De Ciantis, A., Muti, M., Piccolini, C., Principi, M., Di Renzo, A., De Ciantis, R., Frondizi, D., Iannone, G., Ottaviano, P., Piccirilli, M., 2008. A functional MRI study of language disturbances in subjects with migraine headache during treatment with topiramate. Neurol. Sci. Off. J. Ital. Neurol. Soc. Ital. Soc. Clin. Neurophysiol. 29 Suppl 1, S141-143. doi:10.1007/s10072-008-0906-5

de Nijs, L., Wolkoff, N., Grisar, T., Lakaye, B., 2013. Juvenile myoclonic epilepsy as a possible neurodevelopmental disease: role of EFHC1 or Myoclonin1. Epilepsy Behav. EB 28 Suppl 1, S58-60. doi:10.1016/j.yebeh.2012.06.034

Delgado-Escueta, A.V., Koeleman, B.P.C., Bailey, J.N., Medina, M.T., Durón, R.M., 2013. The quest for juvenile myoclonic epilepsy genes. Epilepsy Behav. EB 28 Suppl 1, S52-57. doi:10.1016/j.yebeh.2012.06.033

Devinsky, O., Gershengorn, J., Brown, E., Perrine, K., Vazquez, B., Luciano, D., 1997. Frontal functions in juvenile myoclonic epilepsy. Neuropsychiatry. Neuropsychol. Behav. Neurol. 10, 243–246.

Devinsky, O., Spruill, T., Thurman, D., Friedman, D., 2015. Recognizing and preventing epilepsy-related mortality: A call for action. Neurology. doi:10.1212/WNL.0000000000002253

Dlouhy, B.J., Gehlbach, B.K., Kreple, C.J., Kawasaki, H., Oya, H., Buzza, C., Granner, M.A., Welsh, M.J., Howard, M.A., Wemmie, J.A., Richerson, G.B., 2015. Breathing Inhibited When Seizures Spread to the Amygdala and upon Amygdala Stimulation. J. Neurosci. 35, 10281–10289. doi:10.1523/JNEUROSCI.0888-15.2015

Dodrill, C.B., 1975. Effects of sulthiame upon intellectual, neuropsychological, and social functioning abilities among adult epileptics: comparison with diphenylhydantoin. Epilepsia 16, 617–625.

Duncan, J.S., Winston, G.P., Koepp, M.J., Ourselin, S., 2016. Brain imaging in the assessment for epilepsy surgery. Lancet Neurol. 15, 420–433. doi:10.1016/S1474-4422(15)00383-X

Ecker, C., Marquand, A., Mourão-Miranda, J., Johnston, P., Daly, E.M., Brammer, M.J., Maltezos, S., Murphy, C.M., Robertson, D., Williams, S.C., Murphy, D.G.M., 2010. Describing the brain in autism in five dimensions--magnetic resonance imaging-assisted diagnosis of autism spectrum disorder using a multiparameter classification approach. J. Neurosci. Off. J. Soc. Neurosci. 30, 10612–10623. doi:10.1523/JNEUROSCI.5413-09.2010

Egan, M.F., Goldberg, T.E., Kolachana, B.S., Callicott, J.H., Mazzanti, C.M., Straub, R.E., Goldman, D., Weinberger, D.R., 2001. Effect of COMT Val108/158 Met genotype on frontal lobe function and risk for schizophrenia. Proc. Natl. Acad. Sci. U. S. A. 98, 6917–6922. doi:10.1073/pnas.111134598

Ellis, J., 1996. Prospective memory or the realization of delayed intentions: A conceptual framework for research., in: M. Brandimonte, G. O. Einstein, M. A. McDaniel (Eds.), Prospective Memory: Theory and Applications. Lawrence Erlbaum Associates Publishers, Mahwah, NJ, US, pp. 1–22.

Engel, J., 2011. Biomarkers in epilepsy: introduction. Biomark. Med. 5, 537–544. doi:10.2217/bmm.11.62

Ficker, D.M., So, E.L., Shen, W.K., Annegers, J.F., O'Brien, P.C., Cascino, G.D., Belau, P.G., 1998. Population-based study of the incidence of sudden unexplained death in epilepsy. Neurology 51, 1270–1274.

Filippini, N., MacIntosh, B.J., Hough, M.G., Goodwin, G.M., Frisoni, G.B., Smith, S.M., Matthews, P.M., Beckmann, C.F., Mackay, C.E., 2009. Distinct patterns of brain activity in young carriers of the APOE-epsilon4 allele. Proc. Natl. Acad. Sci. U. S. A. 106, 7209–7214. doi:10.1073/pnas.0811879106

Fisher, R.S., Acevedo, C., Arzimanoglou, A., Bogacz, A., Cross, J.H., Elger, C.E., Engel, J., Forsgren, L., French, J.A., Glynn, M., Hesdorffer, D.C., Lee, B.I., Mathern, G.W., Moshé, S.L., Perucca, E., Scheffer, I.E., Tomson, T., Watanabe, M., Wiebe, S., 2014. ILAE official report: a practical clinical definition of epilepsy. Epilepsia 55, 475–482. doi:10.1111/epi.12550

Fisher, R.S., van Emde Boas, W., Blume, W., Elger, C., Genton, P., Lee, P., Engel, J., 2005. Epileptic seizures and epilepsy: definitions proposed by the International League Against Epilepsy (ILAE) and the International Bureau for Epilepsy (IBE). Epilepsia 46, 470–472. doi:10.1111/j.0013-9580.2005.66104.x

Forsgren, L., Beghi, E., Oun, A., Sillanpää, M., 2005. The epidemiology of epilepsy in Europe - a systematic review. Eur. J. Neurol. 12, 245–253. doi:10.1111/j.1468-1331.2004.00992.x

Friedman, L., Kenny, J.T., Wise, A.L., Wu, D., Stuve, T.A., Miller, D.A., Jesberger, J.A., Lewin, J.S., 1998. Brain activation during silent word generation evaluated with functional MRI. Brain Lang. 64, 231–256. doi:10.1006/brln.1998.1953

Friston, K.J., 2005. Models of brain function in neuroimaging. Annu. Rev. Psychol. 56, 57–87. doi:10.1146/annurev.psych.56.091103.070311

Friston, K.J., Josephs, O., Zarahn, E., Holmes, A.P., Rouquette, S., Poline, J., 2000. To smooth or not to smooth? Bias and efficiency in fMRI time-series analysis. NeuroImage 12, 196–208. doi:10.1006/nimg.2000.0609

Geithner, J., Schneider, F., Wang, Z., Berneiser, J., Herzer, R., Kessler, C., Runge, U., 2012. Predictors for long-term seizure outcome in juvenile myoclonic epilepsy: 25-63 years of follow-up. Epilepsia 53, 1379–1386. doi:10.1111/j.1528-1167.2012.03526.x

Giorgio, A., Watkins, K.E., Chadwick, M., James, S., Winmill, L., Douaud, G., De Stefano, N., Matthews, P.M., Smith, S.M., Johansen-Berg, H., James, A.C., 2010. Longitudinal changes in grey and white matter during adolescence. NeuroImage 49, 94–103. doi:10.1016/j.neuroimage.2009.08.003

Goldman, A.M., 2015. Mechanisms of sudden unexplained death in epilepsy. Curr. Opin. Neurol. 28, 166–174. doi:10.1097/WCO.0000000000000184

Goldman, A.M., Behr, E.R., Semsarian, C., Bagnall, R.D., Sisodiya, S., Cooper, P.N., 2016. Sudden unexpected death in epilepsy genetics: Molecular diagnostics and prevention. Epilepsia 57 Suppl 1, 17–25. doi:10.1111/epi.13232

Gomer, B., Wagner, K., Frings, L., Saar, J., Carius, A., Härle, M., Steinhoff, B.J., Schulze-Bonhage, A., 2007. The influence of antiepileptic drugs on cognition: a comparison of levetiracetam with topiramate. Epilepsy Behav. EB 10, 486–494. doi:10.1016/j.yebeh.2007.02.007

Gottesman, I.I., Gould, T.D., 2003. The endophenotype concept in psychiatry: etymology and strategic intentions. Am. J. Psychiatry 160, 636–645. doi:10.1176/appi.ajp.160.4.636

Guaranha, M.S.B., da Silva Sousa, P., de Araújo-Filho, G.M., Lin, K., Guilhoto, L.M.F.F., Caboclo, L.O.S.F., Yacubian, E.M.T., 2009. Provocative and inhibitory effects of a video-EEG neuropsychologic protocol in juvenile myoclonic epilepsy. Epilepsia 50, 2446–2455. doi:10.1111/j.1528-1167.2009.02126.x

Guaranha, M.S.B., Filho, G.M. de A., Lin, K., Guilhoto, L.M.F.F., Caboclo, L.O.S.F., Yacubian, E.M.T., 2011. Prognosis of juvenile myoclonic epilepsy is related to endophenotypes. Seizure 20, 42–48. doi:10.1016/j.seizure.2010.10.004

Haneef, Z., Levin, H.S., Chiang, S., 2015. Brain Graph Topology Changes Associated with Anti-Epileptic Drug Use. Brain Connect. 5, 284–291. doi:10.1089/brain.2014.0304

Harper, R.M., Bandler, R., Spriggs, D., Alger, J.R., 2000. Lateralized and widespread brain activation during transient blood pressure elevation revealed by magnetic resonance imaging. J. Comp. Neurol. 417, 195–204.

Harper, R.M., Macey, P.M., Henderson, L.A., Woo, M.A., Macey, K.E., Frysinger, R.C., Alger, J.R., Nguyen, K.P., Yan-Go, F.L., 2003. fMRI responses to cold pressor challenges in control and obstructive sleep apnea subjects. J. Appl. Physiol. Bethesda Md 1985 94, 1583–1595. doi:10.1152/japplphysiol.00881.2002

Hartmann, H.A., Colom, L.V., Sutherland, M.L., Noebels, J.L., 1999. Selective localization of cardiac SCN5A sodium channels in limbic regions of rat brain. Nat. Neurosci. 2, 593–595. doi:10.1038/10147

Helmstaedter, C., Aldenkamp, A.P., Baker, G.A., Mazarati, A., Ryvlin, P., Sankar, R., 2014. Disentangling the relationship between epilepsy and its behavioral comorbidities - the need for prospective studies in new-onset epilepsies. Epilepsy Behav. EB 31, 43–47. doi:10.1016/j.yebeh.2013.11.010

Helmstaedter, C., Witt, J.-A., 2010. Cognitive outcome of antiepileptic treatment with levetiracetam versus carbamazepine monotherapy: a non-interventional surveillance trial. Epilepsy Behav. EB 18, 74–80. doi:10.1016/j.yebeh.2010.02.011

Henderson, L.A., Woo, M.A., Macey, P.M., Macey, K.E., Frysinger, R.C., Alger, J.R., Yan-Go, F., Harper, R.M., 2003. Neural responses during Valsalva maneuvers in obstructive sleep apnea syndrome. J. Appl. Physiol. Bethesda Md 1985 94, 1063–1074. doi:10.1152/japplphysiol.00702.2002

Hermann, B., Meador, K.J., Gaillard, W.D., Cramer, J.A., 2010. Cognition across the lifespan: antiepileptic drugs, epilepsy, or both? Epilepsy Behav. EB 17, 1–5. doi:10.1016/j.yebeh.2009.10.019

Hermann, B.P., Jones, J.E., Jackson, D.C., Seidenberg, M., 2012. Starting at the beginning: the neuropsychological status of children with new-onset epilepsies. Epileptic Disord. Int. Epilepsy J. Videotape 14, 12–21. doi:10.1684/epd.2012.0483

Hesdorffer, D.C., Tomson, T., Benn, E., Sander, J.W., Nilsson, L., Langan, Y., Walczak, T.S., Beghi, E., Brodie, M.J., Hauser, A., ILAE Commission on Epidemiology; Subcommission on Mortality, 2011. Combined analysis of risk factors for SUDEP. Epilepsia 52, 1150–1159. doi:10.1111/j.1528-1167.2010.02952.x

Hesdorffer, D.C., Tomson, T., Benn, E., Sander, J.W., Nilsson, L., Langan, Y., Walczak, T.S., Beghi, E., Brodie, M.J., Hauser, W.A., ILAE Commission on Epidemiology (Subcommission on Mortality), 2012. Do antiepileptic drugs or generalized tonic-clonic seizure frequency increase SUDEP risk? A combined analysis. Epilepsia 53, 249–252. doi:10.1111/j.1528-1167.2011.03354.x

Hilz, M.J., Devinsky, O., Doyle, W., Mauerer, A., Dütsch, M., 2002. Decrease of sympathetic cardiovascular modulation after temporal lobe epilepsy surgery. Brain J. Neurol. 125, 985–995.

Hodges, M.R., Wehner, M., Aungst, J., Smith, J.C., Richerson, G.B., 2009. Transgenic mice lacking serotonin neurons have severe apnea and high mortality during development. J. Neurosci. Off. J. Soc. Neurosci. 29, 10341–10349. doi:10.1523/JNEUROSCI.1963-09.2009

Hommet, C., Sauerwein, H.C., De Toffol, B., Lassonde, M., 2006. Idiopathic epileptic syndromes and cognition. Neurosci. Biobehav. Rev. 30, 85–96. doi:10.1016/j.neubiorev.2005.06.004

Iqbal, N., Caswell, H., Muir, R., Cadden, A., Ferguson, S., Mackenzie, H., Watson, P., Duncan, S., 2015. Neuropsychological profiles of patients with juvenile myoclonic epilepsy and their siblings: An extended study. Epilepsia 56, 1301–1308. doi:10.1111/epi.13061

Iqbal, N., Caswell, H.L., Hare, D.J., Pilkington, O., Mercer, S., Duncan, S., 2009. Neuropsychological profiles of patients with juvenile myoclonic epilepsy and their siblings: a preliminary controlled experimental video-EEG case series. Epilepsy Behav. EB 14, 516–521. doi:10.1016/j.yebeh.2008.12.025

Jansen, J.F.A., Aldenkamp, A.P., Marian Majoie, H.J., Reijs, R.P., de Krom, M.C.T.F.M., Hofman, P.A.M., Eline Kooi, M., Nicolay, K., Backes, W.H., 2006. Functional MRI reveals declined prefrontal cortex activation in patients with epilepsy on topiramate therapy. Epilepsy Behav. EB 9, 181–185. doi:10.1016/j.yebeh.2006.05.004

Janz, D., 1985. Epilepsy with impulsive petit mal (juvenile myoclonic epilepsy). Acta Neurol. Scand. 72, 449–459.

Jayalakshmi, S.S., Mohandas, S., Sailaja, S., Borgohain, R., 2006. Clinical and electroencephalographic study of first-degree relatives and probands with juvenile myoclonic epilepsy. Seizure 15, 177–183. doi:10.1016/j.seizure.2005.12.011

Jennum, P., Gyllenborg, J., Kjellberg, J., 2011. The social and economic consequences of epilepsy: a controlled national study. Epilepsia 52, 949–956. doi:10.1111/j.1528-1167.2010.02946.x

Jernigan, T.L., Baaré, W.F.C., Stiles, J., Madsen, K.S., 2011. Postnatal brain development: structural imaging of dynamic neurodevelopmental processes. Prog. Brain Res. 189, 77–92. doi:10.1016/B978-0-444-53884-0.00019-1

Jokeit, H., Okujava, M., Woermann, F.G., 2001. Carbamazepine reduces memory induced activation of mesial temporal lobe structures: a pharmacological fMRI-study. BMC Neurol. 1, 6.

Kaada, B.R., Jasper, H., 1952. Respiratory responses to stimulation of temporal pole, insula, and hippocampal and limbic gyri in man. AMA Arch. Neurol. Psychiatry 68, 609–619.

Kaminski, R.M., Rogawski, M.A., Klitgaard, H., 2014. The potential of antiseizure drugs and agents that act on novel molecular targets as antiepileptogenic treatments. Neurother. J. Am. Soc. Exp. Neurother. 11, 385–400. doi:10.1007/s13311-014-0266-1

Karlsgodt, K.H., Glahn, D.C., van Erp, T.G.M., Therman, S., Huttunen, M., Manninen, M., Kaprio, J., Cohen, M.S., Lönnqvist, J., Cannon, T.D., 2007. The relationship between performance and fMRI signal during working memory in patients with schizophrenia, unaffected co-twins, and control subjects. Schizophr. Res. 89, 191–197. doi:10.1016/j.schres.2006.08.016

Kasteleijn-Nolst Trenité, D.G.A., Schmitz, B., Janz, D., Delgado-Escueta, A.V., Thomas, P., Hirsch, E., Lerche, H., Camfield, C., Baykan, B., Feucht, M., Martínez-Juárez, I.E., Duron, R.M., Medina, M.T., Rubboli, G., Jerney, J., Hermann, B., Yacubian, E., Koutroumanidis, M., Stephani, U., Salas-Puig, J., Reed, R.C., Woermann, F., Wandschneider, B., Bureau, M., Gambardella, A., Koepp, M.J., Gelisse, P., Gurses, C., Crespel, A., Nguyen-Michel, V.H., Ferlazzo, E., Grisar, T., Helbig, I., Koeleman, B.P.C., Striano, P., Trimble, M., Buono, R., Cossette, P., Represa, A., Dravet, C., Serafini, A., Berglund, I.S.-, Sisodiya, S.M., Yamakawa, K., Genton, P., 2013. Consensus on diagnosis and management of JME: From founder's observations to current trends. Epilepsy Behav. EB 28 Suppl 1, S87-90. doi:10.1016/j.yebeh.2012.11.051

Keller, S.S., Mackay, C.E., Barrick, T.R., Wieshmann, U.C., Howard, M.A., Roberts, N., 2002. Voxel-based morphometric comparison of hippocampal and extrahippocampal abnormalities in patients with left and right hippocampal atrophy. NeuroImage 16, 23–31. doi:10.1006/nimg.2001.1072

Keller, S.S., Richardson, M.P., Schoene-Bake, J.-C., O'Muircheartaigh, J., Elkommos, S., Kreilkamp, B., Goh, Y.Y., Marson, A.G., Elger, C., Weber, B., 2015. Thalamotemporal alteration and postoperative

seizures in temporal lobe epilepsy. Ann. Neurol. 77, 760–774. doi:10.1002/ana.24376
Keller, S.S., Schoene-Bake, J.-C., Gerdes, J.S., Weber, B., Deppe, M., 2012. Concomitant fractional anisotropy and volumetric abnormalities in temporal lobe epilepsy: cross-sectional evidence for progressive neurologic injury. PloS One 7, e46791. doi:10.1371/journal.pone.0046791
Kinney, H.C., Chadwick, A.E., Crandall, L.A., Grafe, M., Armstrong, D.L., Kupsky, W.J., Trachtenberg, F.L., Krous, H.F., 2009a. Sudden death, febrile seizures, and hippocampal and temporal lobe maldevelopment in toddlers: a new entity. Pediatr. Dev. Pathol. Off. J. Soc. Pediatr. Pathol. Paediatr. Pathol. Soc. 12, 455–463. doi:10.2350/08-09-0542.1
Kinney, H.C., Cryan, J.B., Haynes, R.L., Paterson, D.S., Haas, E.A., Mena, O.J., Minter, M., Journey, K.W., Trachtenberg, F.L., Goldstein, R.D., Armstrong, D.D., 2015. Dentate gyrus abnormalities in sudden unexplained death in infants: morphological marker of underlying brain vulnerability. Acta Neuropathol. (Berl.) 129, 65–80. doi:10.1007/s00401-014-1357-0
Kinney, H.C., Richerson, G.B., Dymecki, S.M., Darnall, R.A., Nattie, E.E., 2009b. The brainstem and serotonin in the sudden infant death syndrome. Annu. Rev. Pathol. 4, 517–550. doi:10.1146/annurev.pathol.4.110807.092322
Kliegel, M., McDaniel, M.A., Einstein, G.O., 2000. Plan formation, retention, and execution in prospective memory: a new approach and age-related effects. Mem. Cognit. 28, 1041–1049.
Koepp, M.J., 2016. The help of biomarkers in the prevention of epilepsy. Lancet Neurol. 15, 782–784. doi:10.1016/S1474-4422(16)30081-3
Koepp, M.J., 2011. Gender and drug effects on neuroimaging in epilepsy. Epilepsia 52 Suppl 4, 35–37. doi:10.1111/j.1528-1167.2011.03150.x
Koepp, M.J., Caciagli, L., Pressler, R.M., Lehnertz, K., Beniczky, S., 2016. Reflex seizures, traits, and epilepsies: from physiology to pathology. Lancet Neurol. 15, 92–105. doi:10.1016/S1474-4422(15)00219-7
Koepp, M.J., Richardson, M.P., Brooks, D.J., Cunningham, V.J., Duncan, J.S., 1997. Central benzodiazepine/gamma-aminobutyric acid A receptors in idiopathic generalized epilepsy: an [11C]flumazenil positron emission tomography study. Epilepsia 38, 1089–1097.
Koepp, M.J., Thomas, R.H., Wandschneider, B., Berkovic, S.F., Schmidt, D., 2014. Concepts and controversies of juvenile myoclonic epilepsy: still an enigmatic epilepsy. Expert Rev. Neurother. 14, 819–831. doi:10.1586/14737175.2014.928203
Koos, B.J., Chau, A., Matsuura, M., Punla, O., Kruger, L., 1998. Thalamic locus mediates hypoxic inhibition of breathing in fetal sheep. J. Neurophysiol. 79, 2383–2393.
Koos, B.J., Kawasaki, Y., Hari, A., Bohorquez, F., Jan, C., Roostaeian, J., Wilson, C.L., Kruger, L., 2004. Electrical stimulation of the posteromedial thalamus modulates breathing in unanesthetized fetal sheep. J. Appl. Physiol. Bethesda Md 1985 96, 115–123. doi:10.1152/japplphysiol.00517.2003
Krous, H.F., Beckwith, J.B., Byard, R.W., Rognum, T.O., Bajanowski, T., Corey, T., Cutz, E., Hanzlick, R., Keens, T.G., Mitchell, E.A., 2004. Sudden infant death syndrome and unclassified sudden infant deaths: a definitional and diagnostic approach. Pediatrics 114, 234–238.
Krous, H.F., Chadwick, A.E., Crandall, L., Nadeau-Manning, J.M., 2005. Sudden unexpected death in childhood: a report of 50 cases. Pediatr.

Dev. Pathol. Off. J. Soc. Pediatr. Pathol. Paediatr. Pathol. Soc. 8, 307–319. doi:10.1007/s10024-005-1155-8
Kumar, R., Farahvar, S., Ogren, J.A., Macey, P.M., Thompson, P.M., Woo, M.A., Yan-Go, F.L., Harper, R.M., 2014. Brain putamen volume changes in newly-diagnosed patients with obstructive sleep apnea. NeuroImage Clin. 4, 383–391. doi:10.1016/j.nicl.2014.01.009
Kumari, V., Peters, E.R., Fannon, D., Antonova, E., Premkumar, P., Anilkumar, A.P., Williams, S.C.R., Kuipers, E., 2009. Dorsolateral prefrontal cortex activity predicts responsiveness to cognitive-behavioral therapy in schizophrenia. Biol. Psychiatry 66, 594–602. doi:10.1016/j.biopsych.2009.04.036
Kwan, P., Brodie, M.J., 2000. Early identification of refractory epilepsy. N. Engl. J. Med. 342, 314–319. doi:10.1056/NEJM200002033420503
Kwon, O.-Y., Park, S.-P., 2013. Zonisamide decreases current-source density of high Beta frequency of electroencephalogram. J. Epilepsy Res. 3, 63–69. doi:10.14581/jer.13012
Laird, A.R., Fox, P.M., Eickhoff, S.B., Turner, J.A., Ray, K.L., McKay, D.R., Glahn, D.C., Beckmann, C.F., Smith, S.M., Fox, P.T., 2011. Behavioral interpretations of intrinsic connectivity networks. J. Cogn. Neurosci. 23, 4022–4037. doi:10.1162/jocn_a_00077
Lamberts, R.J., Thijs, R.D., Laffan, A., Langan, Y., Sander, J.W., 2012. Sudden unexpected death in epilepsy: people with nocturnal seizures may be at highest risk. Epilepsia 53, 253–257. doi:10.1111/j.1528-1167.2011.03360.x
Langan, Y., Nashef, L., Sander, J.W., 2005. Case-control study of SUDEP. Neurology 64, 1131–1133. doi:10.1212/01.WNL.0000156352.61328.CB
Leu, C., Balestrini, S., Maher, B., Hernández-Hernández, L., Gormley, P., Hämäläinen, E., Heggeli, K., Schoeler, N., Novy, J., Willis, J., Plagnol, V., Ellis, R., Reavey, E., O'Regan, M., Pickrell, W.O., Thomas, R.H., Chung, S.-K., Delanty, N., McMahon, J.M., Malone, S., Sadleir, L.G., Berkovic, S.F., Nashef, L., Zuberi, S.M., Rees, M.I., Cavalleri, G.L., Sander, J.W., Hughes, E., Helen Cross, J., Scheffer, I.E., Palotie, A., Sisodiya, S.M., 2015. Genome-wide Polygenic Burden of Rare Deleterious Variants in Sudden Unexpected Death in Epilepsy. EBioMedicine 2, 1063–1070. doi:10.1016/j.ebiom.2015.07.005
Levav, M., Mirsky, A.F., Herault, J., Xiong, L., Amir, N., Andermann, E., 2002. Familial association of neuropsychological traits in patients with generalized and partial seizure disorders. J. Clin. Exp. Neuropsychol. 24, 311–326. doi:10.1076/jcen.24.3.311.985
Lhatoo, S.D., Faulkner, H.J., Dembny, K., Trippick, K., Johnson, C., Bird, J.M., 2010. An electroclinical case-control study of sudden unexpected death in epilepsy. Ann. Neurol. 68, 787–796. doi:10.1002/ana.22101
Liebenthal, J.A., Wu, S., Rose, S., Ebersole, J.S., Tao, J.X., 2015. Association of prone position with sudden unexpected death in epilepsy. Neurology 84, 703–709. doi:10.1212/WNL.0000000000001260
Lieberman, M.D., Cunningham, W.A., 2009. Type I and Type II error concerns in fMRI research: re-balancing the scale. Soc. Cogn. Affect. Neurosci. 4, 423–428. doi:10.1093/scan/nsp052
Lin, J.J., Dabbs, K., Riley, J.D., Jones, J.E., Jackson, D.C., Hsu, D.A., Stafstrom, C.E., Seidenberg, M., Hermann, B.P., 2014. Neurodevelopment in new-onset juvenile myoclonic epilepsy over the first 2 years. Ann. Neurol. 76, 660–668. doi:10.1002/ana.24240
Lin, K., de Araujo Filho, G.M., Pascalicchio, T.F., Silva, I., Tudesco, I.S.S., Guaranha, M.S.B., Carrete Júnior, H., Jackowski, A.P., Yacubian, E.M.T., 2013. Hippocampal atrophy and memory dysfunction in patients

with juvenile myoclonic epilepsy. Epilepsy Behav. EB 29, 247–251. doi:10.1016/j.yebeh.2013.06.034
Logothetis, N.K., 2008. What we can do and what we cannot do with fMRI. Nature 453, 869–878. doi:10.1038/nature06976
Loring, D.W., Williamson, D.J., Meador, K.J., Wiegand, F., Hulihan, J., 2011. Topiramate dose effects on cognition: a randomized double-blind study. Neurology 76, 131–137. doi:10.1212/WNL.0b013e318206ca02
Macey, P.M., Henderson, L.A., Macey, K.E., Alger, J.R., Frysinger, R.C., Woo, M.A., Harper, R.K., Yan-Go, F.L., Harper, R.M., 2002. Brain morphology associated with obstructive sleep apnea. Am. J. Respir. Crit. Care Med. 166, 1382–1387. doi:10.1164/rccm.200201-050OC
Macey, P.M., Richard, C.A., Kumar, R., Woo, M.A., Ogren, J.A., Avedissian, C., Thompson, P.M., Harper, R.M., 2009. Hippocampal volume reduction in congenital central hypoventilation syndrome. PloS One 4, e6436. doi:10.1371/journal.pone.0006436
Macey, P.M., Woo, M.A., Macey, K.E., Keens, T.G., Saeed, M.M., Alger, J.R., Harper, R.M., 2005. Hypoxia reveals posterior thalamic, cerebellar, midbrain, and limbic deficits in congenital central hypoventilation syndrome. J. Appl. Physiol. Bethesda Md 1985 98, 958–969. doi:10.1152/japplphysiol.00969.2004
Manjón, J.V., Coupé, P., Martí-Bonmatí, L., Collins, D.L., Robles, M., 2010. Adaptive non-local means denoising of MR images with spatially varying noise levels. J. Magn. Reson. Imaging JMRI 31, 192–203. doi:10.1002/jmri.22003
Marini, C., Scheffer, I.E., Crossland, K.M., Grinton, B.E., Phillips, F.L., McMahon, J.M., Turner, S.J., Dean, J.T., Kivity, S., Mazarib, A., Neufeld, M.Y., Korczyn, A.D., Harkin, L.A., Dibbens, L.M., Wallace, R.H., Mulley, J.C., Berkovic, S.F., 2004. Genetic architecture of idiopathic generalized epilepsy: clinical genetic analysis of 55 multiplex families. Epilepsia 45, 467–478. doi:10.1111/j.0013-9580.2004.46803.x
Marson, A.G., Al-Kharusi, A.M., Alwaidh, M., Appleton, R., Baker, G.A., Chadwick, D.W., Cramp, C., Cockerell, O.C., Cooper, P.N., Doughty, J., Eaton, B., Gamble, C., Goulding, P.J., Howell, S.J.L., Hughes, A., Jackson, M., Jacoby, A., Kellett, M., Lawson, G.R., Leach, J.P., Nicolaides, P., Roberts, R., Shackley, P., Shen, J., Smith, D.F., Smith, P.E.M., Smith, C.T., Vanoli, A., Williamson, P.R., SANAD Study group, 2007a. The SANAD study of effectiveness of valproate, lamotrigine, or topiramate for generalised and unclassifiable epilepsy: an unblinded randomised controlled trial. Lancet Lond. Engl. 369, 1016–1026. doi:10.1016/S0140-6736(07)60461-9
Marson, A.G., Al-Kharusi, A.M., Alwaidh, M., Appleton, R., Baker, G.A., Chadwick, D.W., Cramp, C., Cockerell, O.C., Cooper, P.N., Doughty, J., Eaton, B., Gamble, C., Goulding, P.J., Howell, S.J.L., Hughes, A., Jackson, M., Jacoby, A., Kellett, M., Lawson, G.R., Leach, J.P., Nicolaides, P., Roberts, R., Shackley, P., Shen, J., Smith, D.F., Smith, P.E.M., Smith, C.T., Vanoli, A., Williamson, P.R., SANAD Study group, 2007b. The SANAD study of effectiveness of carbamazepine, gabapentin, lamotrigine, oxcarbazepine, or topiramate for treatment of partial epilepsy: an unblinded randomised controlled trial. Lancet Lond. Engl. 369, 1000–1015. doi:10.1016/S0140-6736(07)60460-7
Martin, R., Kuzniecky, R., Ho, S., Hetherington, H., Pan, J., Sinclair, K., Gilliam, F., Faught, E., 1999. Cognitive effects of topiramate, gabapentin, and lamotrigine in healthy young adults. Neurology 52, 321–327.

Massey, C.A., Sowers, L.P., Dlouhy, B.J., Richerson, G.B., 2014. Mechanisms of sudden unexpected death in epilepsy: the pathway to prevention. Nat. Rev. Neurol. 10, 271–282. doi:10.1038/nrneurol.2014.64

Matsuoka, H., Nakamura, M., Ohno, T., Shimabukuro, J., Suzuki, T., Numachi, Y., Awata, S., 2005. The role of cognitive-motor function in precipitation and inhibition of epileptic seizures. Epilepsia 46 Suppl 1, 17–20. doi:10.1111/j.0013-9580.2005.461006.x

Matsuoka, H., Takahashi, T., Sasaki, M., Matsumoto, K., Yoshida, S., Numachi, Y., Saito, H., Ueno, T., Sato, M., 2000. Neuropsychological EEG activation in patients with epilepsy. Brain J. Neurol. 123 (Pt 2), 318–330.

Mayer, T.A., Schroeder, F., May, T.W., Wolf, P.T., 2006. Perioral reflex myoclonias: a controlled study in patients with JME and focal epilepsies. Epilepsia 47, 1059–1067. doi:10.1111/j.1528-1167.2006.00575.x

Mbizvo, G.K., Dixon, P., Hutton, J.L., Marson, A.G., 2012. Levetiracetam add-on for drug-resistant focal epilepsy: an updated Cochrane Review. Cochrane Database Syst. Rev. CD001901. doi:10.1002/14651858.CD001901.pub2

McDonald, C.R., Swartz, B.E., Halgren, E., Patell, A., Daimes, R., Mandelkern, M., 2006. The relationship of regional frontal hypometabolism to executive function: a resting fluorodeoxyglucose PET study of patients with epilepsy and healthy controls. Epilepsy Behav. EB 9, 58–67. doi:10.1016/j.yebeh.2006.04.007

McKenna P, Warrington EK, 1983. Graded Naming Test Manual. NFER-Nelson, Windsor.

Meador, K.J., Loring, D.W., Vahle, V.J., Ray, P.G., Werz, M.A., Fessler, A.J., Ogrocki, P., Schoenberg, M.R., Miller, J.M., Kustra, R.P., 2005. Cognitive and behavioral effects of lamotrigine and topiramate in healthy volunteers. Neurology 64, 2108–2114. doi:10.1212/01.WNL.0000165994.46777.BE

Meencke, H.J., Janz, D., 1985. The significance of microdysgenesia in primary generalized epilepsy: an answer to the considerations of Lyon and Gastaut. Epilepsia 26, 368–371.

Meencke, H.J., Janz, D., 1984. Neuropathological findings in primary generalized epilepsy: a study of eight cases. Epilepsia 25, 8–21.

Mehta, M.A., O'Daly, O.G., 2011. Pharmacological application of fMRI. Methods Mol. Biol. Clifton NJ 711, 551–565. doi:10.1007/978-1-61737-992-5_28

Meyer-Lindenberg, A., 2012. The future of fMRI and genetics research. NeuroImage 62, 1286–1292. doi:10.1016/j.neuroimage.2011.10.063

Minami, N., Morino, M., Uda, T., Komori, T., Nakata, Y., Arai, N., Kohmura, E., Nakano, I., 2015. Surgery for amygdala enlargement with mesial temporal lobe epilepsy: pathological findings and seizure outcome. J. Neurol. Neurosurg. Psychiatry 86, 887–894. doi:10.1136/jnnp-2014-308383

Moseley, B.D., Wirrell, E.C., Nickels, K., Johnson, J.N., Ackerman, M.J., Britton, J., 2011. Electrocardiographic and oximetric changes during partial complex and generalized seizures. Epilepsy Res. 95, 237–245. doi:10.1016/j.eplepsyres.2011.04.005

Mueller, S.G., Bateman, L.M., Laxer, K.D., 2014. Evidence for brainstem network disruption in temporal lobe epilepsy and sudden unexplained death in epilepsy. NeuroImage Clin. 5, 208–216. doi:10.1016/j.nicl.2014.06.010

Mula, M., 2012. Topiramate and cognitive impairment: evidence and clinical implications. Ther. Adv. Drug Saf. 3, 279–289. doi:10.1177/2042098612455357

Mula, M., Trimble, M.R., 2009. Antiepileptic drug-induced cognitive adverse effects: potential mechanisms and contributing factors. CNS Drugs 23, 121–137.
Nair, R.R., Thomas, S.V., 2004. Genetic liability to epilepsy in Kerala State, India. Epilepsy Res. 62, 163–170. doi:10.1016/j.eplepsyres.2004.08.007
Nashef, L., 1997. Sudden unexpected death in epilepsy: terminology and definitions. Epilepsia 38, S6-8. doi:10.1111/j.1528-1157.1997.tb06130.x
Nashef, L., Garner, S., Sander, J.W., Fish, D.R., Shorvon, S.D., 1998. Circumstances of death in sudden death in epilepsy: interviews of bereaved relatives. J. Neurol. Neurosurg. Psychiatry 64, 349–352.
Nashef, L., So, E.L., Ryvlin, P., Tomson, T., 2012. Unifying the definitions of sudden unexpected death in epilepsy. Epilepsia 53, 227–233. doi:10.1111/j.1528-1167.2011.03358.x
Nathan, P.J., Phan, K.L., Harmer, C.J., Mehta, M.A., Bullmore, E.T., 2014. Increasing pharmacological knowledge about human neurological and psychiatric disorders through functional neuroimaging and its application in drug discovery. Curr. Opin. Pharmacol. 14, 54–61. doi:10.1016/j.coph.2013.11.009
Neligan, A., Bell, G.S., Shorvon, S.D., Sander, J.W., 2010. Temporal trends in the mortality of people with epilepsy: a review. Epilepsia 51, 2241–2246. doi:10.1111/j.1528-1167.2010.02711.x
Nelson, HE, 1982. The National Adult Reading Test (NART): Test Manual. NFER-Nelson, Windsor.
Nobili, L., Proserpio, P., Rubboli, G., Montano, N., Didato, G., Tassinari, C.A., 2011. Sudden unexpected death in epilepsy (SUDEP) and sleep. Sleep Med. Rev. 15, 237–246. doi:10.1016/j.smrv.2010.07.006
Ojemann, L.M., Ojemann, G.A., Dodrill, C.B., Crawford, C.A., Holmes, M.D., Dudley, D.L., 2001. Language Disturbances as Side Effects of Topiramate and Zonisamide Therapy. Epilepsy Behav. EB 2, 579–584. doi:10.1006/ebeh.2001.0285
O'Muircheartaigh, J., Vollmar, C., Barker, G.J., Kumari, V., Symms, M.R., Thompson, P., Duncan, J.S., Koepp, M.J., Richardson, M.P., 2012. Abnormal thalamocortical structural and functional connectivity in juvenile myoclonic epilepsy. Brain J. Neurol. 135, 3635–3644. doi:10.1093/brain/aws296
O'Muircheartaigh, J., Vollmar, C., Barker, G.J., Kumari, V., Symms, M.R., Thompson, P., Duncan, J.S., Koepp, M.J., Richardson, M.P., 2011. Focal structural changes and cognitive dysfunction in juvenile myoclonic epilepsy. Neurology 76, 34–40. doi:10.1212/WNL.0b013e318203e93d
Opeskin, K., Kalnins, R.M., Halliday, G., Cartwright, H., Berkovic, S.F., 2000. Idiopathic generalized epilepsy: lack of significant microdysgenesis. Neurology 55, 1101–1106.
Oppenheimer, S., 2006. Cerebrogenic cardiac arrhythmias: cortical lateralization and clinical significance. Clin. Auton. Res. Off. J. Clin. Auton. Res. Soc. 16, 6–11. doi:10.1007/s10286-006-0276-0
Oppenheimer, S.M., Gelb, A., Girvin, J.P., Hachinski, V.C., 1992. Cardiovascular effects of human insular cortex stimulation. Neurology 42, 1727–1732.
Owen, A.M., McMillan, K.M., Laird, A.R., Bullmore, E., 2005. N-back working memory paradigm: a meta-analysis of normative functional neuroimaging studies. Hum. Brain Mapp. 25, 46–59. doi:10.1002/hbm.20131
Paine, S.M.L., Jacques, T.S., Sebire, N.J., 2014. Review: Neuropathological features of unexplained sudden unexpected death in infancy: current

evidence and controversies. Neuropathol. Appl. Neurobiol. 40, 364–384. doi:10.1111/nan.12095

Pascalicchio, T.F., de Araujo Filho, G.M., da Silva Noffs, M.H., Lin, K., Caboclo, L.O.S.F., Vidal-Dourado, M., Ferreira Guilhoto, L.M.F., Yacubian, E.M.T., 2007. Neuropsychological profile of patients with juvenile myoclonic epilepsy: a controlled study of 50 patients. Epilepsy Behav. EB 10, 263–267. doi:10.1016/j.yebeh.2006.11.012

Patwari, P.P., Carroll, M.S., Rand, C.M., Kumar, R., Harper, R., Weese-Mayer, D.E., 2010. Congenital central hypoventilation syndrome and the PHOX2B gene: a model of respiratory and autonomic dysregulation. Respir. Physiol. Neurobiol. 173, 322–335. doi:10.1016/j.resp.2010.06.013

Perlstein, W.M., Carter, C.S., Noll, D.C., Cohen, J.D., 2001. Relation of prefrontal cortex dysfunction to working memory and symptoms in schizophrenia. Am. J. Psychiatry 158, 1105–1113. doi:10.1176/appi.ajp.158.7.1105

Phelps, E.A., Hyder, F., Blamire, A.M., Shulman, R.G., 1997. FMRI of the prefrontal cortex during overt verbal fluency. Neuroreport 8, 561–565.

Piazzini, A., Turner, K., Vignoli, A., Canger, R., Canevini, M.P., 2008. Frontal cognitive dysfunction in juvenile myoclonic epilepsy. Epilepsia 49, 657–662. doi:10.1111/j.1528-1167.2007.01482.x

Pitkänen, A., Löscher, W., Vezzani, A., Becker, A.J., Simonato, M., Lukasiuk, K., Gröhn, O., Bankstahl, J.P., Friedman, A., Aronica, E., Gorter, J.A., Ravizza, T., Sisodiya, S.M., Kokaia, M., Beck, H., 2016. Advances in the development of biomarkers for epilepsy. Lancet Neurol. 15, 843–856. doi:10.1016/S1474-4422(16)00112-5

Pohlmann-Eden, B., Aldenkamp, A., Baker, G.A., Brandt, C., Cendes, F., Coras, R., Crocker, C.E., Helmstaedter, C., Jones-Gotman, M., Kanner, A.M., Mazarati, A., Mula, M., Smith, M.L., Omisade, A., Tellez-Zenteno, J., Hermann, B.P., 2015. The relevance of neuropsychiatric symptoms and cognitive problems in new-onset epilepsy - Current knowledge and understanding. Epilepsy Behav. EB 51, 199–209. doi:10.1016/j.yebeh.2015.07.005

Porter, R.J., Penry, J.K., 1973. Responsiveness at the onset of spike-wave bursts. Electroencephalogr. Clin. Neurophysiol. 34, 239–245.

Postma, A.V., Denjoy, I., Kamblock, J., Alders, M., Lupoglazoff, J.-M., Vaksmann, G., Dubosq-Bidot, L., Sebillon, P., Mannens, M.M. a. M., Guicheney, P., Wilde, A. a. M., 2005. Catecholaminergic polymorphic ventricular tachycardia: RYR2 mutations, bradycardia, and follow up of the patients. J. Med. Genet. 42, 863–870. doi:10.1136/jmg.2004.028993

Potkin, S.G., Turner, J.A., Fallon, J.A., Lakatos, A., Keator, D.B., Guffanti, G., Macciardi, F., 2009. Gene discovery through imaging genetics: identification of two novel genes associated with schizophrenia. Mol. Psychiatry 14, 416–428. doi:10.1038/mp.2008.127

Proposal for revised classification of epilepsies and epileptic syndromes. Commission on Classification and Terminology of the International League Against Epilepsy, 1989. . Epilepsia 30, 389–399.

Proposal for revised clinical and electroencephalographic classification of epileptic seizures. From the Commission on Classification and Terminology of the International League Against Epilepsy, 1981. . Epilepsia 22, 489–501.

Pulman, J., Jette, N., Dykeman, J., Hemming, K., Hutton, J.L., Marson, A.G., 2014. Topiramate add-on for drug-resistant partial epilepsy. Cochrane Database Syst. Rev. CD001417. doi:10.1002/14651858.CD001417.pub3

Pulsipher, D.T., Seidenberg, M., Guidotti, L., Tuchscherer, V.N., Morton, J., Sheth, R.D., Hermann, B., 2009. Thalamofrontal circuitry and executive dysfunction in recent-onset juvenile myoclonic epilepsy. Epilepsia 50, 1210–1219. doi:10.1111/j.1528-1167.2008.01952.x

Raichle, M.E., MacLeod, A.M., Snyder, A.Z., Powers, W.J., Gusnard, D.A., Shulman, G.L., 2001. A default mode of brain function. Proc. Natl. Acad. Sci. U. S. A. 98, 676–682. doi:10.1073/pnas.98.2.676

Rajapakse, J.C., Giedd, J.N., Rapoport, J.L., 1997. Statistical approach to segmentation of single-channel cerebral MR images. IEEE Trans. Med. Imaging 16, 176–186. doi:10.1109/42.563663

Recommendations for neuroimaging of patients with epilepsy. Commission on Neuroimaging of the International League Against Epilepsy, 1997. . Epilepsia 38, 1255–1256.

Richerson, G.B., Boison, D., Faingold, C.L., Ryvlin, P., 2016. From unwitnessed fatality to witnessed rescue: Pharmacologic intervention in sudden unexpected death in epilepsy. Epilepsia 57 Suppl 1, 35–45. doi:10.1111/epi.13236

Roebling, R., Scheerer, N., Uttner, I., Gruber, O., Kraft, E., Lerche, H., 2009. Evaluation of cognition, structural, and functional MRI in juvenile myoclonic epilepsy. Epilepsia 50, 2456–2465. doi:10.1111/j.1528-1167.2009.02127.x

Rugg-Gunn, F., Duncan, J., Hjalgrim, H., Seyal, M., Bateman, L., 2016. From unwitnessed fatality to witnessed rescue: Nonpharmacologic interventions in sudden unexpected death in epilepsy. Epilepsia 57 Suppl 1, 26–34. doi:10.1111/epi.13231

Ryvlin, P., Cucherat, M., Rheims, S., 2011. Risk of sudden unexpected death in epilepsy in patients given adjunctive antiepileptic treatment for refractory seizures: a meta-analysis of placebo-controlled randomised trials. Lancet Neurol. 10, 961–968. doi:10.1016/S1474-4422(11)70193-4

Ryvlin, P., Nashef, L., Lhatoo, S.D., Bateman, L.M., Bird, J., Bleasel, A., Boon, P., Crespel, A., Dworetzky, B.A., Høgenhaven, H., Lerche, H., Maillard, L., Malter, M.P., Marchal, C., Murthy, J.M.K., Nitsche, M., Pataraia, E., Rabben, T., Rheims, S., Sadzot, B., Schulze-Bonhage, A., Seyal, M., So, E.L., Spitz, M., Szucs, A., Tan, M., Tao, J.X., Tomson, T., 2013. Incidence and mechanisms of cardiorespiratory arrests in epilepsy monitoring units (MORTEMUS): a retrospective study. Lancet Neurol. 12, 966–977. doi:10.1016/S1474-4422(13)70214-X

Saini, J., Kesavadas, C., Thomas, B., Kapilamoorthy, T.R., Gupta, A.K., Radhakrishnan, A., Radhakrishnan, K., 2009. Susceptibility weighted imaging in the diagnostic evaluation of patients with intractable epilepsy. Epilepsia 50, 1462–1473. doi:10.1111/j.1528-1167.2008.01882.x

Sander, J.W., 2003. The epidemiology of epilepsy revisited. Curr. Opin. Neurol. 16, 165–170. doi:10.1097/01.wco.0000063766.15877.8e

Sander, J.W., Shorvon, S.D., 1996. Epidemiology of the epilepsies. J. Neurol. Neurosurg. Psychiatry 61, 433–443.

Savic, I., Lekvall, A., Greitz, D., Helms, G., 2000. MR spectroscopy shows reduced frontal lobe concentrations of N-acetyl aspartate in patients with juvenile myoclonic epilepsy. Epilepsia 41, 290–296.

Savic, I., Osterman, Y., Helms, G., 2004. MRS shows syndrome differentiated metabolite changes in human-generalized epilepsies. NeuroImage 21, 163–172.

Scanlon, C., Ronan, L., Doherty, C.P., Cavalleri, G.L., Tirupati, S., Alhusaini, S., Maguire, S., Delanty, N., Iyer, P.M., Chaila, E., Fitzsimons, M., 2013. MRI-based brain structure volumes in temporal lobe epilepsy patients and their unaffected siblings: a preliminary study. J. Neuroimaging Off.

J. Am. Soc. Neuroimaging 23, 64–70. doi:10.1111/j.1552-6569.2012.00736.x

Schiemann-Delgado, J., Yang, H., Loge, C. de la, Stalvey, T.J., Jones, J., Legoff, D., Mintz, M., 2012. A long-term open-label extension study assessing cognition and behavior, tolerability, safety, and efficacy of adjunctive levetiracetam in children aged 4 to 16 years with partial-onset seizures. J. Child Neurol. 27, 80–89. doi:10.1177/0883073811417183

Schulze-Bonhage, A., 2015. The safety and long-term efficacy of zonisamide as adjunctive therapy for focal epilepsy. Expert Rev. Neurother. 15, 857–865. doi:10.1586/14737175.2015.1065179

Schwartz, P.J., 1998. The autonomic nervous system and sudden death. Eur. Heart J. 19 Suppl F, F72-80.

Seghier, M.L., Price, C.J., 2012. Functional Heterogeneity within the Default Network during Semantic Processing and Speech Production. Front. Psychol. 3, 281. doi:10.3389/fpsyg.2012.00281

Senf, P., Schmitz, B., Holtkamp, M., Janz, D., 2013. Prognosis of juvenile myoclonic epilepsy 45 years after onset: seizure outcome and predictors. Neurology 81, 2128–2133. doi:10.1212/01.wnl.0000437303.36064.f8

Seyal, M., Hardin, K.A., Bateman, L.M., 2012. Postictal generalized EEG suppression is linked to seizure-associated respiratory dysfunction but not postictal apnea. Epilepsia 53, 825–831. doi:10.1111/j.1528-1167.2012.03443.x

Shaw, P., Kabani, N.J., Lerch, J.P., Eckstrand, K., Lenroot, R., Gogtay, N., Greenstein, D., Clasen, L., Evans, A., Rapoport, J.L., Giedd, J.N., Wise, S.P., 2008. Neurodevelopmental trajectories of the human cerebral cortex. J. Neurosci. Off. J. Soc. Neurosci. 28, 3586–3594. doi:10.1523/JNEUROSCI.5309-07.2008

Shen, H.-Y., Li, T., Boison, D., 2010. A novel mouse model for sudden unexpected death in epilepsy (SUDEP): role of impaired adenosine clearance. Epilepsia 51, 465–468. doi:10.1111/j.1528-1167.2009.02248.x

Shoemaker, J.K., Norton, K.N., Baker, J., Luchyshyn, T., 2015. Forebrain organization for autonomic cardiovascular control. Auton. Neurosci. Basic Clin. 188, 5–9. doi:10.1016/j.autneu.2014.10.022

Shoemaker, J.K., Wong, S.W., Cechetto, D.F., 2012. Cortical circuitry associated with reflex cardiovascular control in humans: does the cortical autonomic network “speak” or “listen” during cardiovascular arousal. Anat. Rec. Hoboken NJ 2007 295, 1375–1384. doi:10.1002/ar.22528

Shorvon, S., Tomson, T., 2011. Sudden unexpected death in epilepsy. Lancet Lond. Engl. 378, 2028–2038. doi:10.1016/S0140-6736(11)60176-1

Siniatchkin, M., Koepp, M., 2009. Neuroimaging and neurogenetics of epilepsy in humans. Neuroscience 164, 164–173. doi:10.1016/j.neuroscience.2009.08.056

Smith, S.M., Fox, P.T., Miller, K.L., Glahn, D.C., Fox, P.M., Mackay, C.E., Filippini, N., Watkins, K.E., Toro, R., Laird, A.R., Beckmann, C.F., 2009. Correspondence of the brain’s functional architecture during activation and rest. Proc. Natl. Acad. Sci. U. S. A. 106, 13040–13045. doi:10.1073/pnas.0905267106

Sofroniew, M.V., 2009. Molecular dissection of reactive astrogliosis and glial scar formation. Trends Neurosci. 32, 638–647. doi:10.1016/j.tins.2009.08.002

Sonmez, F., Atakli, D., Sari, H., Atay, T., Arpaci, B., 2004. Cognitive function in juvenile myoclonic epilepsy. Epilepsy Behav. EB 5, 329–336. doi:10.1016/j.yebeh.2004.01.007

Spence, S.A., Hirsch, S.R., Brooks, D.J., Grasby, P.M., 1998. Prefrontal cortex activity in people with schizophrenia and control subjects. Evidence from positron emission tomography for remission of "hypofrontality" with recovery from acute schizophrenia. Br. J. Psychiatry J. Ment. Sci. 172, 316–323.

Spencer, M.D., Holt, R.J., Chura, L.R., Calder, A.J., Suckling, J., Bullmore, E.T., Baron-Cohen, S., 2012. Atypical activation during the Embedded Figures Task as a functional magnetic resonance imaging endophenotype of autism. Brain J. Neurol. 135, 3469–3480. doi:10.1093/brain/aws229

Sperling, M.R., Harris, A., Nei, M., Liporace, J.D., O'Connor, M.J., 2005. Mortality after epilepsy surgery. Epilepsia 46 Suppl 11, 49–53. doi:10.1111/j.1528-1167.2005.00410.x

Stretton, J., Winston, G., Sidhu, M., Centeno, M., Vollmar, C., Bonelli, S., Symms, M., Koepp, M., Duncan, J.S., Thompson, P.J., 2012. Neural correlates of working memory in Temporal Lobe Epilepsy--an fMRI study. NeuroImage 60, 1696–1703. doi:10.1016/j.neuroimage.2012.01.126

Stretton, J., Winston, G.P., Sidhu, M., Bonelli, S., Centeno, M., Vollmar, C., Cleary, R.A., Williams, E., Symms, M.R., Koepp, M.J., Thompson, P.J., Duncan, J.S., 2013. Disrupted segregation of working memory networks in temporal lobe epilepsy. NeuroImage Clin. 2, 273–281. doi:10.1016/j.nicl.2013.01.009

Surges, R., Sander, J.W., 2012. Sudden unexpected death in epilepsy: mechanisms, prevalence, and prevention. Curr. Opin. Neurol. 25, 201–207. doi:10.1097/WCO.0b013e3283506714

Surges, R., Strzelczyk, A., Scott, C.A., Walker, M.C., Sander, J.W., 2011. Postictal generalized electroencephalographic suppression is associated with generalized seizures. Epilepsy Behav. EB 21, 271–274. doi:10.1016/j.yebeh.2011.04.008

Surges, R., Taggart, P., Sander, J.W., Walker, M.C., 2010. Too long or too short? New insights into abnormal cardiac repolarization in people with chronic epilepsy and its potential role in sudden unexpected death. Epilepsia 51, 738–744. doi:10.1111/j.1528-1167.2010.02571.x

Swartz, B.E., Halgren, E., Fuster, J., Mandelkern, M., 1994. An 18FDG-PET study of cortical activation during a short-term visual memory task in humans. Neuroreport 5, 925–928.

Swartz, B.E., Simpkins, F., Halgren, E., Mandelkern, M., Brown, C., Krisdakumtorn, T., Gee, M., 1996. Visual working memory in primary generalized epilepsy: an 18FDG-PET study. Neurology 47, 1203–1212.

Szaflarski, J.P., Allendorfer, J.B., 2012. Topiramate and its effect on fMRI of language in patients with right or left temporal lobe epilepsy. Epilepsy Behav. EB 24, 74–80. doi:10.1016/j.yebeh.2012.02.022

Szaflarski, J.P., Kay, B., Gotman, J., Privitera, M.D., Holland, S.K., 2013. The relationship between the localization of the generalized spike and wave discharge generators and the response to valproate. Epilepsia 54, 471–480. doi:10.1111/epi.12062

Tang, Y., Chen, Q., Yu, X., Xia, W., Luo, C., Huang, X., Tang, H., Gong, Q., Zhou, D., 2014. A resting-state functional connectivity study in patients at high risk for sudden unexpected death in epilepsy. Epilepsy Behav. EB 41, 33–38. doi:10.1016/j.yebeh.2014.08.140

Tang, Y., Xia, W., Yu, X., Zhou, B., Wu, X., Lui, S., Luo, C., Huang, X., Ouyang, L., Chen, Q., Gong, Q., Zhou, D., 2016. Altered cerebral activity associated with topiramate and its withdrawal in patients with epilepsy with language impairment: An fMRI study using the verb generation task. Epilepsy Behav. EB 59, 98–104. doi:10.1016/j.yebeh.2016.03.013

Terreberry, R.R., Neafsey, E.J., 1987. The rat medial frontal cortex projects directly to autonomic regions of the brainstem. Brain Res. Bull. 19, 639–649.

Thom, M., Michalak, Z., Wright, G., Dawson, T., Hilton, D., Joshi, A., Diehl, B., Koepp, M., Lhatoo, S., Sander, J.W., Sisodiya, S.M., 2015. Audit of practice in sudden unexpected death in epilepsy (SUDEP) post mortems and neuropathological findings. Neuropathol. Appl. Neurobiol. doi:10.1111/nan.12265

Thomas, R.H., Walsh, J., Church, C., Sills, G.J., Marson, A.G., Baker, G.A., Rees, M.I., 2014. A comprehensive neuropsychological description of cognition in drug-refractory juvenile myoclonic epilepsy. Epilepsy Behav. EB 36, 124–129. doi:10.1016/j.yebeh.2014.04.027

Thompson, P.J., Baxendale, S.A., Duncan, J.S., Sander, J.W., 2000. Effects of topiramate on cognitive function. J. Neurol. Neurosurg. Psychiatry 69, 636–641.

Thurman, D.J., Hesdorffer, D.C., French, J.A., 2014. Sudden unexpected death in epilepsy: assessing the public health burden. Epilepsia 55, 1479–1485. doi:10.1111/epi.12666

Timmings, P.L., 1993. Sudden unexpected death in epilepsy: a local audit. Seizure 2, 287–290.

Tomson, T., Surges, R., Delamont, R., Haywood, S., Hesdorffer, D.C., 2016. Who to target in sudden unexpected death in epilepsy prevention and how? Risk factors, biomarkers, and intervention study designs. Epilepsia 57 Suppl 1, 4–16. doi:10.1111/epi.13234

Tosun, D., Dabbs, K., Caplan, R., Siddarth, P., Toga, A., Seidenberg, M., Hermann, B., 2011. Deformation-based morphometry of prospective neurodevelopmental changes in new onset paediatric epilepsy. Brain J. Neurol. 134, 1003–1014. doi:10.1093/brain/awr027

Trusheim, M.R., Berndt, E.R., Douglas, F.L., 2007. Stratified medicine: strategic and economic implications of combining drugs and clinical biomarkers. Nat. Rev. Drug Discov. 6, 287–293. doi:10.1038/nrd2251

Tu, E., Bagnall, R.D., Duflou, J., Semsarian, C., 2011. Post-mortem review and genetic analysis of sudden unexpected death in epilepsy (SUDEP) cases. Brain Pathol. Zurich Switz. 21, 201–208. doi:10.1111/j.1750-3639.2010.00438.x

Vadlamudi, L., Andermann, E., Lombroso, C.T., Schachter, S.C., Milne, R.L., Hopper, J.L., Andermann, F., Berkovic, S.F., 2004. Epilepsy in twins: insights from unique historical data of William Lennox. Neurology 62, 1127–1133.

Vijai, J., Cherian, P.J., Stlaja, P.N., Anand, A., Radhakrishnan, K., 2003. Clinical characteristics of a South Indian cohort of juvenile myoclonic epilepsy probands. Seizure 12, 490–496.

Vollmar, C., O'Muircheartaigh, J., Barker, G.J., Symms, M.R., Thompson, P., Kumari, V., Duncan, J.S., Janz, D., Richardson, M.P., Koepp, M.J., 2011. Motor system hyperconnectivity in juvenile myoclonic epilepsy: a cognitive functional magnetic resonance imaging study. Brain J. Neurol. 134, 1710–1719. doi:10.1093/brain/awr098

Vollmar, C., O'Muircheartaigh, J., Symms, M.R., Barker, G.J., Thompson, P., Kumari, V., Stretton, J., Duncan, J.S., Richardson, M.P., Koepp, M.J., 2012. Altered microstructural connectivity in juvenile myoclonic epilepsy:

the missing link. Neurology 78, 1555–1559. doi:10.1212/WNL.0b013e3182563b44
Wandschneider, B., Centeno, M., Vollmar, C., Stretton, J., O'Muircheartaigh, J., Thompson, P.J., Kumari, V., Symms, M., Barker, G.J., Duncan, J.S., Richardson, M.P., Koepp, M.J., 2013. Risk-taking behavior in juvenile myoclonic epilepsy. Epilepsia 54, 2158–2165. doi:10.1111/epi.12413
Wandschneider, B., Kopp, U.A., Kliegel, M., Stephani, U., Kurlemann, G., Janz, D., Schmitz, B., 2010. Prospective memory in patients with juvenile myoclonic epilepsy and their healthy siblings. Neurology 75, 2161–2167. doi:10.1212/WNL.0b013e318202010a
Wandschneider, B., Stretton, J., Sidhu, M., Centeno, M., Kozák, L.R., Symms, M., Thompson, P.J., Duncan, J.S., Koepp, M.J., 2014. Levetiracetam reduces abnormal network activations in temporal lobe epilepsy. Neurology 83, 1508–1512. doi:10.1212/WNL.0000000000000910
Wandschneider, B., Thompson, P.J., Vollmar, C., Koepp, M.J., 2012. Frontal lobe function and structure in juvenile myoclonic epilepsy: a comprehensive review of neuropsychological and imaging data. Epilepsia 53, 2091–2098. doi:10.1111/epi.12003
Watanabe, K., Hara, K., Hakamada, S., Negoro, T., Sugiura, M., Matsumoto, A., Maehara, M., 1982. Seizures with apnea in children. Pediatrics 70, 87–90.
Weinberger, D.R., Berman, K.F., Zec, R.F., 1986. Physiologic dysfunction of dorsolateral prefrontal cortex in schizophrenia. I. Regional cerebral blood flow evidence. Arch. Gen. Psychiatry 43, 114–124.
Wellmer, J., Quesada, C.M., Rothe, L., Elger, C.E., Bien, C.G., Urbach, H., 2013. Proposal for a magnetic resonance imaging protocol for the detection of epileptogenic lesions at early outpatient stages. Epilepsia 54, 1977–1987. doi:10.1111/epi.12375
Wilke, M., Lidzba, K., 2007. LI-tool: a new toolbox to assess lateralization in functional MR-data. J. Neurosci. Methods 163, 128–136. doi:10.1016/j.jneumeth.2007.01.026
Winawer, M.R., Marini, C., Grinton, B.E., Rabinowitz, D., Berkovic, S.F., Scheffer, I.E., Ottman, R., 2005. Familial clustering of seizure types within the idiopathic generalized epilepsies. Neurology 65, 523–528. doi:10.1212/01.wnl.0000172920.34994.63
Winston, G.P., Cardoso, M.J., Williams, E.J., Burdett, J.L., Bartlett, P.A., Espak, M., Behr, C., Duncan, J.S., Ourselin, S., 2013. Automated hippocampal segmentation in patients with epilepsy: available free online. Epilepsia 54, 2166–2173. doi:10.1111/epi.12408
Witt, J.-A., Elger, C.E., Helmstaedter, C., 2015. Adverse cognitive effects of antiepileptic pharmacotherapy: Each additional drug matters. Eur. Neuropsychopharmacol. J. Eur. Coll. Neuropsychopharmacol. 25, 1954–1959. doi:10.1016/j.euroneuro.2015.07.027
Woermann, F.G., Free, S.L., Koepp, M.J., Sisodiya, S.M., Duncan, J.S., 1999. Abnormal cerebral structure in juvenile myoclonic epilepsy demonstrated with voxel-based analysis of MRI. Brain J. Neurol. 122 (Pt 11), 2101–2108.
Woermann, F.G., Jokeit, H., Luerding, R., Freitag, H., Schulz, R., Guertler, S., Okujava, M., Wolf, P., Tuxhorn, I., Ebner, A., 2003. Language lateralization by Wada test and fMRI in 100 patients with epilepsy. Neurology 61, 699–701.
Wolf, P., Yacubian, E.M.T., Avanzini, G., Sander, T., Schmitz, B., Wandschneider, B., Koepp, M., 2015. Juvenile myoclonic epilepsy: A system disorder of the brain. Epilepsy Res. 114, 2–12. doi:10.1016/j.eplepsyres.2015.04.008

Woo, M.A., Macey, P.M., Keens, P.T., Kumar, R., Fonarow, G.C., Hamilton, M.A., Harper, R.M., 2005. Functional abnormalities in brain areas that mediate autonomic nervous system control in advanced heart failure. J. Card. Fail. 11, 437–446. doi:10.1016/j.cardfail.2005.02.003

Yasuda, C.L., Betting, L.E., Cendes, F., 2010. Voxel-based morphometry and epilepsy. Expert Rev. Neurother. 10, 975–984. doi:10.1586/ern.10.63

Yasuda, C.L., Centeno, M., Vollmar, C., Stretton, J., Symms, M., Cendes, F., Mehta, M.A., Thompson, P., Duncan, J.S., Koepp, M.J., 2013. The effect of topiramate on cognitive fMRI. Epilepsy Res. 105, 250–255. doi:10.1016/j.eplepsyres.2012.12.007

Young, N.A., Szabó, C.Á., Phelix, C.F., Flaherty, D.K., Balaram, P., Foust-Yeoman, K.B., Collins, C.E., Kaas, J.H., 2013. Epileptic baboons have lower numbers of neurons in specific areas of cortex. Proc. Natl. Acad. Sci. U. S. A. 110, 19107–19112. doi:10.1073/pnas.1318894110

Zamarian, L., Höfler, J., Kuchukhidze, G., Delazer, M., Bonatti, E., Kemmler, G., Trinka, E., 2013. Decision making in juvenile myoclonic epilepsy. J. Neurol. 260, 839–846. doi:10.1007/s00415-012-6715-z

Zhuo, L., Zhang, Y., Zielke, H.R., Levine, B., Zhang, X., Chang, L., Fowler, D., Li, L., 2012. Sudden unexpected death in epilepsy: Evaluation of forensic autopsy cases. Forensic Sci. Int. 223, 171–175. doi:10.1016/j.forsciint.2012.08.024

Zifkin, B., Andermann, E., Andermann, F., 2005. Mechanisms, genetics, and pathogenesis of juvenile myoclonic epilepsy. Curr. Opin. Neurol. 18, 147–153.